Universidade de Aveiro Departamento de Ciências Médicas

Universidade Católica Portuguesa Faculdade de Medicina Dentária
2021

JOANA COSTA E SILVA

ESTUDO DE ALTERAÇÕES GENÉTICAS NO *NAPRT* E *NAMPT* EM CANCRO

STUDY OF *NAPRT* AND *NAMPT* GENETIC ALTERATIONS IN CANCER

Universidade de Aveiro Departamento de Ciências Médicas

Universidade Católica Portuguesa Faculdade de Medicina Dentária
2021

JOANA COSTA E SILVA

ESTUDO DE ALTERAÇÕES GENÉTICAS NO *NAPRT* E *NAMPT* EM CANCRO

STUDY OF *NAPRT* AND *NAMPT* GENETIC ALTERATIONS IN CANCER

Dissertação apresentada à Universidade de Aveiro para cumprimento dos requisitos necessários à obtenção do grau de Mestre em Biomedicina Molecular, realizada sob a orientação científica da Doutora Raquel Monteiro Marques da Silva, Professora Auxiliar da Faculdade de Medicina Dentária da Universidade Católica Portuguesa, e da Doutora Ana Gabriela da Silva Cavaleiro Henriques, Investigadora Auxiliar do Departamento de Ciências Médicas da Universidade de Aveiro.

o júri

Presidente	Doutora Daniela Maria Oliveira Gandra Ribeiro Equiparada a Investigadora Auxiliar da Universidade de Aveiro
Arguente	Doutora Luísa Cristina da Costa Azevedo Professora Auxiliar Convidada do Departamento de Biologia da Faculdade de Ciências da Universidade do Porto e Investigadora do Instituto de Patologia e Imunologia Molecular da Universidade do Porto e do Instituto de Investigação e Inovação em Saúde da Universidade do Porto
Coorientadora	Doutora Raquel Monteiro Marques da Silva Professora Auxiliar da Faculdade de Medicina Dentária da Universidade Católica Portuguesa

agradecimentos

À Doutora Raquel Silva, por todo o conhecimento transmitido, pela amabilidade, compreensão, disponibilidade e apoio ao longo de toda a dissertação. A Professora Raquel é uma excelente pessoa, é a orientadora que todos queremos e pela qual sentimos admiração e orgulho pela maneira como "faz" ciência.

À Doutora Ana Gabriela Henriques, minha coorientadora, pelo apoio, simpatia e amabilidade que sempre demonstrou. É uma excelente professora e que, acima de tudo, se preocupa com os seus alunos.

Ao Diogo Neves, que me recebeu de braços abertos no laboratório, e à Sara Duarte Pereira, que me ajudou imenso na parte da bioinformática. Obrigada por toda a vossa simpatia, paciência, disponibilidade e ensinamentos. Ambos têm o dom de saber explicar e, se o quiserem, tenho a certeza de que serão excelentes professores e orientadores.

Ao Eduardo e aos professores da UCP-Viseu (Professores Doutores Ana Cristina Esteves, Ana Sofia Duarte, Maria José Correia, Marlene Barros e Nuno Rosa). Obrigada por terem-me recebido tão bem e sempre terem demonstrado disponibilidade para ajudar no que fosse necessário, naquele que era um ambiente totalmente novo para mim. Em especial, ao Eduardo, por também ter-me feito companhia e ajudado na integração.

Aos amigos de Aveiro (Adriana, Carolina, Ricardo e Zé), sem eles esta etapa seria muito mais difícil. Divertimo-nos juntos, partilhámos frustrações e apoiámo-nos uns aos outros. Em especial, obrigada ao Zé por ter sido o melhor colega de casa e por, tal como a Adriana, me ter dado teto quando já não vivia em Aveiro. Obrigada à Carolina pelas boleias e por ser a minha companheira de ginásio em Viseu.

À Carolina, Cristina, Neiva e Zé por serem um grupo de amigos tão incrível, férias sem vocês já não são a mesma coisa. Obrigada pela vossa companhia

significar sempre diversão e momentos bem passados.

À Cristina, Diogo, Inês e Kevin, por ser um grupo tão especial. A nossa amizade é tão bonita, orgulho-me de todos e dos sentimentos que temos uns pelos outros. Obrigada pelo vosso carinho, ainda que a distância dificulte que nos encontremos mais frequentemente. Em especial à Nê, por estar sempre disponível para me ajudar em questões existenciais.

À minha Tininha com quem troco áudios infinitos, obrigada por teres sempre tanta paciência para me ouvir falar de tudo e de nada, por aconselhares-me tão bem e compreenderes como ninguém.

Aos meus amigos de sempre, Bárbara e David, pelo apoio constante. À Bárbara, a pessoa sem a qual não sei como seria a minha vida. Obrigada por todas as conversas, preocupação, ajuda em tudo e mais alguma coisa e por chamares-me à razão sempre que preciso. Ao David, obrigada por seres uma companhia diária, ainda que à distância, obrigada por todos os conselhos e por nunca me julgares.

Ao André, uma amizade mais recente, mas que espero que seja para durar. Obrigada pela companhia aos fins de semana e conversas constantes que me ajudaram imenso e de tantas formas, neste ano que foi tão estranho.

Ao meu tio, que nas suas visitas me faz rir e distrair, no bom sentido. Obrigada por sempre me apoiar, compreender e querer o melhor para mim.

Ao meu pai e à minha irmã, pelo apoio e por acreditarem em mim.

À minha mãe, a pessoa mais importante, por todo o esforço, sacrifício, apoio, confiança, dedicação e carinho, é a ti que devo tudo. Tenho muito orgulho na pessoa e mãe que és e estou-te eternamente grata.

palavras-chave Metabolismo do NAD, *NAPRT*, *NAMPT*, cancro, saliva

resumo

O NAD^+ funciona como coenzima em reações de oxidação-redução e como um substrato para determinadas enzimas e tem, portanto, um papel crítico em muitos processos celulares. Nas células de mamíferos, o NAD^+ intracelular pode ser sintetizado através da síntese *de novo*, a partir do triptofano, ou através das vias de "reciclagem", a partir de outros precursores, como NAM e NA, que são convertidos por NAMPT e NAPRT, respetivamente. Alterações no conteúdo de NAD^+ em células e tecidos estão relacionadas com uma ampla variedade de doenças, incluindo cancro. Uma grande proporção dos casos de tumores ainda é diagnosticada já num estadio avançado e, por isso, são necessários novos biomarcadores economicamente acessíveis, específicos, sensíveis e não invasivos. Os biomarcadores salivares conseguem cumprir esses critérios e são, assim, moléculas promissoras para o rastreio, diagnóstico e prognóstico de cancro. O principal objetivo deste trabalho foi estudar alterações genéticas no *NAMPT* e *NAPRT* em amostras de DNA de dadores saudáveis e em amostras de pacientes com cancro. Para isto, foi otimizada a extração de DNA e RNA a partir de amostras de saliva, como ponto de partida para estudar este biofluido como fonte de biomarcadores de cancro. Os resultados da análise bioinformática mostraram que a frequência de alterações nos genes *NAPRT* e *NAMPT* é baixa nos contextos de cancro investigados. Ainda assim, serão necessários mais estudos para analisar o impacto que estas alterações poderão ter. Há também uma grande necessidade de investigar e otimizar métodos para estudos em saliva, a fim de promovê-la como biópsia líquida de uso generalizado em ambiente clínico.

keywords NAD metabolism, *NAPRT*, *NAMPT*, cancer, saliva

abstract

NAD^+ is both a co-enzyme for oxidation-reduction reactions and a substrate for NAD^+-consuming enzymes and therefore, it is critical for many cellular processes. In mammalian cells, intracellular NAD^+ can be synthesized through either *de novo* synthesis, from tryptophan, or via salvage pathways, from other precursors, such as NAM and NA which are converted by NAMPT and NAPRT, respectively. Changes in the NAD^+ content in cells and tissues are linked with a wide variety of diseases, including cancer. A large proportion of cancer cases is still diagnosed only at an advanced stage and thus, there is a need for new affordable, specific, sensitive and non-invasive biomarkers. Salivary biomarkers can meet these criteria and thus, are promising tools in cancer screening, diagnostic and prognostic. The main objective of this work was to study genetic alterations in *NAMPT* and *NAPRT* in DNA samples from healthy donors and in samples from cancer patients. For this, DNA and RNA extraction from saliva samples was optimized, as a starting point to study this biofluid as a source for cancer biomarkers. The results from the bioinformatics analysis showed that the frequency of alterations in *NAPRT* and *NAMPT* genes is low in the cancer contexts investigated. Nevertheless, it is still necessary to further study the impact that these alterations might have. There is also a great need to investigate and optimize methods for saliva studies, in order to promote it as a liquid biopsy of regular use in clinical settings.

INDEX

FIGURES INDEX

TABLES INDEX

APPENDICES INDEX

LIST OF ABBREVIATIONS AND SYMBOLS

ADPR	adenosine diphosphate ribose/ADP-ribose
ALL	acute lymphoid leukemia
AML	acute myeloid leukemia
Ca^{2+}	calcium
cADPR	cyclic ADP-ribose
CD38/CD157	cADPR synthases
CNA	copy number alteration
DNA	deoxyribonucleic acid
EMT	epithelial-mesenchymal transition
eQTL	expression quantitative trait loci
GTEx	Genotype-Tissue Expression
HNSC	head and neck squamous cell carcinoma
KIRC	kidney renal clear cell carcinoma
KIRP	kidney renal papillary cell carcinoma
LAML	acute myeloid leukemia
LB	loading buffer
MM	multiple myeloma
mRNA	messenger RNA
NA	nicotinic acid
NAAD	nicotinic acid adenine dinucleotide
NAD^+	nicotinamide adenine dinucleotide (oxidized form)
NADH	nicotinamide adenine dinucleotide (reduced form)
$NADP^+$	nicotinamide adenine dinucleotide phosphate (oxidized form)
NADPH	nicotinamide adenine dinucleotide phosphate (reduced form)
NADSYN	NAD^+ synthase
NAM	nicotinamide
NAMN	nicotinic acid mononucleotide
NAMPT	nicotinamide phosphoribosyltransferase
NAPRT	nicotinic acid phosphoribosyltransferase

NMN	nicotinamide mononucleotide
NMNAT	nicotinamide/nicotinic acid mononucleotide adenylyltransferase
NR	nicotinamide riboside
NRH	dihydronicotinamide riboside
NMRK	nicotinamide riboside kinase
PARP	poly-ADP-ribose polymerase
PCR	polymerase chain reaction
rcf	relative centrifugal force
RNA	ribonucleic acid
RPKM	reads per kilobase of transcript per million reads mapped
RT	room temperature
RT-PCR	reverse transcription polymerase chain reaction
SIRT	sirtuin
SNP	single nucleotide polymorphisms
T_a	annealing temperature
TCGA	The Cancer Genome Atlas
TIGD5	tigger transposable element derived 5
TPM	transcripts per million
Trp	tryptophan
WT1	WT1 transcription factor

1. INTRODUCTION

1.1. NAD^+ Metabolism

Nicotinamide adenine dinucleotide (NAD^+) consists of an adenosine diphosphate ribose (ADP-ribose or ADPR) group linked to nicotinamide (NAM). The adenosine monophosphate (AMP) moiety of ADPR derives from adenosine triphosphate (ATP) and NAM is salvaged or synthesized *de novo* (Belenky *et al.*, 2006).

NAD^+ can be converted to its reduced form, NADH, and can be phosphorylated to $NADP^+$ or NADPH (Katsyuba & Auwerx, 2017; Kulikova *et al.*, 2018; Xiao *et al.*, 2018; Ying, 2008). The couples NAD^+/NADH and $NADP^+$/NADPH are essential for redox (oxidation-reduction) reactions, maintaining cellular redox homeostasis and modulating cellular metabolism (Xiao *et al.*, 2018).

The NAD^+/NADH couple participates in several reactions requiring electron exchange, including glycolysis, oxidative phosphorylation, Krebs cycle and fatty acid β-oxidation, and NADH is one of the major electron donors for the electron transport chain (Cantó *et al.*, 2015; Cantó & Auwerx, 2011; Katsyuba & Auwerx, 2017; Xiao *et al.*, 2018; Ying, 2008). $NADP^+$ and its reduced form, NADPH, are involved in cellular defense against oxidative stress and in the biosynthesis of nucleic acids, amino acids, fatty acids and lipids (Katsyuba & Auwerx, 2017; Xiao *et al.*, 2018; Yang & Sauve, 2016).

In redox reactions, NAD^+ and $NADP^+$ are reversibly converted between the oxidized and reduced forms, NADH and NADPH, respectively (Kulikova *et al.*, 2018; Opitz & Heiland, 2015). Therefore, these reactions do not change the overall NAD concentrations in the cell (Opitz & Heiland, 2015; Ying, 2006).

1.1.1. NAD^+-consuming enzymes

NAD^+ is a coenzyme for oxidoreductases and also serves as a substrate for several families of regulatory proteins (Belenky *et al.*, 2006; Houtkooper *et al.*, 2010; Kulikova *et al.*, 2018; Xiao *et al.*, 2018; Ying, 2006). They lead to the conversion of NAD^+ into its precursor, NAM, and release other products containing ADP-ribose as the core structural component (Opitz & Heiland, 2015; Ying, 2008). All NAD^+-consuming enzymes are

inhibited by NAM (Belenky *et al.*, 2006; Magni *et al.*, 2004). These NAD^+-consuming enzymes can be divided into three classes: sirtuins (SIRT1-7), ADP-ribose transferases (ARTs) and poly-ADP-ribose polymerases (PARPs), and cyclic ADP-ribose (cADPR) synthases (CD38 and CD157) (Belenky *et al.*, 2006; Cantó & Auwerx, 2011; Houtkooper *et al.*, 2010; Kulikova *et al.*, 2018; Xiao *et al.*, 2018).

ARTs and PARPs use NAD^+ as a substrate for the ADP-ribosylation of target proteins (Belenky *et al.*, 2006; Ying, 2008). ADP-ribosylation is a NAD^+-dependent post-translational modification of proteins that results in NAD^+ cleavage into NAM and ADPR. One (mono-ADP-ribosylation) or more (poly-ADP-ribosylation) ADPR molecules are transferred by ARTs and PARPs, respectively, onto specific amino acids of the acceptor proteins to modulate their biological activities (Belenky *et al.*, 2006; Kulikova *et al.*, 2018). ADPR can be covalently linked to glutamate, aspartate, lysine, arginine or serine residues (Daniels *et al.*, 2014; Kulikova *et al.*, 2018; Leidecker *et al.*, 2016).

Poly-ADP ribosylation regulates DNA repair, transcription, apoptosis, maintenance of genomic integrity and other fundamental cellular processes (Katsyuba & Auwerx, 2017; Ziegler & Niere, 2004). There are 17 different genes encoding PARP related proteins (Cantó *et al.*, 2015; Houtkooper *et al.*, 2010), but the best studied protein of the PARP family is PARP1, which accounts for more than 85% of PARP activity following DNA damage (Katsyuba & Auwerx, 2017; Kulikova *et al.*, 2018). PARP1 is a sensor of single- and double-strand DNA breaks and participates in the repair of these types of damage (De Vos *et al.*, 2012; Kulikova *et al.*, 2018).

The ARTs family (ART1-5) includes enzymes that carry out mono-ADP-ribosylation in membrane and secreted proteins, including receptors (Seman *et al.*, 2004; Ying, 2008). These enzymes are associated with the regulation of innate immune system responses and cell-cell interactions (Kulikova *et al.*, 2018; Ziegler & Niere, 2004).

Intracellular mono- and poly-ADP-ribosylation are also involved in essential cellular processes, namely, the control of cell cycle, maintenance of telomeres, RNA processing and cell differentiation (Kulikova *et al.*, 2018; Nikiforov *et al.*, 2015).

Sirtuins are type-III histone deacetylases (HDACs), or type-III protein lysine deacetylases, that belong to the conserved family of silent information regulator-2 (Sir2) like proteins. In contrast with other histone deacetylases, sirtuins require NAD^+ as a co-substrate

for their activity (Houtkooper *et al.*, 2010; Katsyuba & Auwerx, 2017; Nikiforov *et al.*, 2015; Opitz & Heiland, 2015). In general, these enzymes reverse acetyl modifications of lysine residues on histones and other proteins including regulatory, structural and catalytically active proteins (Belenky *et al.*, 2006; Katsyuba & Auwerx, 2017; Kulikova *et al.*, 2018; Martínez-Redondo & Vaquero, 2013). Sirtuins bind two substrates, a protein or peptide that contains an acetylated lysine and NAD^+ (Belenky *et al.*, 2006; Imai *et al.*, 2000). Then, they cleave NAD^+ and transfer the acetyl group from the lysine residue of the modified protein to the ADP-ribose, releasing O-acetyl ADP-ribose (OAcADPR), NAM and the deacetylated protein (Belenky *et al.*, 2006; Houtkooper *et al.*, 2010; Kulikova *et al.*, 2018; Tanner *et al.*, 2000).

In mammalian cells, there are seven types of sirtuins (SIRT1-7) that differ in their intracellular localization: SIRT1, 6 and 7 are nuclear, SIRT2 can be found mainly in the cytosol, and SIRT3, 4 and 5 in the mitochondria (Cantó *et al.*, 2015; Houtkooper *et al.*, 2010; Kulikova *et al.*, 2018; Michishita *et al.*, 2005).

NAD^+-dependent deacetylation modulates target protein activity, stability or localization, therefore, regulating many vital processes such as aging, transcription, genome stability, apoptosis, and mitochondrial function (Haigis & Sinclair, 2010; Kulikova *et al.*, 2018; Nikiforov *et al.*, 2015). It is noteworthy the critical impact that sirtuins have in the regulation of cell metabolism (Katsyuba & Auwerx, 2017; Kulikova *et al.*, 2018; Xiao *et al.*, 2018). Sirtuins also participate in the cell response to external signals through the connection of the metabolic status of a cell to its signaling pathways (Kulikova *et al.*, 2018). In addition to deacetylation, sirtuins also display mono ADP-ribosyltransferase activity and other enzymatic activities (reviewed in Cantó *et al.*, 2015; Kulikova *et al.*, 2018).

cADPR is a secondary messenger involved in Ca^{2+} signaling, cell cycle control and insulin signaling, and is produced from NAD^+ by cADPR synthases. The family of cADPR synthases includes a pair of ectoenzymes, CD38 and CD157 (Cantó *et al.*, 2015; Malavasi *et al.*, 2008), which cyclize the ADPR moiety of NAD^+ with production of cADPR and NAM (Belenky *et al.*, 2006) and can also catalyze the hydrolysis of NAD^+ and cADPR to ADPR (Magni *et al.*, 2004). CD38 catalyzes a base exchange reaction between $NADP^+$ and nicotinic acid (NA), producing nicotinic acid adenine dinucleotide phosphate (NAADP) and NAM (Belenky *et al.*, 2006; Magni *et al.*, 2004). All the products of CD38 (cADPR, ADPR and

NAADP) act as second messengers, mediating intracellular calcium mobilization (Belenky *et al.*, 2006; Nikiforov *et al.*, 2015).

Overall, NAD^+ consumption is associated intrinsically with signaling reactions inside and outside cells that can significantly affect vital processes, such as gene expression, DNA repair, apoptosis, mitochondrial function, Ca^{2+} homeostasis and aging (Belenky *et al.*, 2006; Kulikova *et al.*, 2018; Nikiforov *et al.*, 2015; Opitz & Heiland, 2015; Ying, 2008). In these NAD^+-dependent regulatory mechanisms there is cleavage of nicotinamide from NAD^+, so NAD^+ levels must be kept constant in the cell in order for these reactions to occur efficiently (Belenky *et al.*, 2006; Katsyuba & Auwerx, 2017; Kulikova *et al.*, 2018). The major mechanism that maintains NAD^+ levels is its biosynthesis (Dölle *et al.*, 2015; Kulikova *et al.*, 2018).

1.1.2. NAD^+ biosynthesis

In mammalian cells, intracellular NAD^+ can be synthesized through either *de novo* synthesis, from tryptophan (Trp), or via salvage pathways (figure 1) (Houtkooper *et al.*, 2010; Katsyuba & Auwerx, 2017). The latter can be divided into the "amidated" route, which has NAM and nicotinamide riboside (NR) as precursors, and the "deamidated route", that involves the Preiss-Handler pathway through nicotinic acid (NA) (Cantó *et al.*, 2015; Houtkooper *et al.*, 2010; Katsyuba & Auwerx, 2017; Xiao *et al.*, 2018; Yang & Sauve, 2016) and the pathway that has nicotinic acid riboside (NAR), the deamidated form of NR, as precursor (Liu *et al.*, 2018; Shats *et al.*, 2020; Tempel *et al.*, 2007). NAM and NA are collectively referred to as niacin or vitamin B3 (Cantó *et al.*, 2015; Kulikova *et al.*, 2018). All the precursors are provided by the diet (Belenky *et al.*, 2006; Kulikova *et al.*, 2018) and the "amidated" route via NAM is the pathway that predominates in mammals (Garten *et al.*, 2015; Mori *et al.*, 2014).

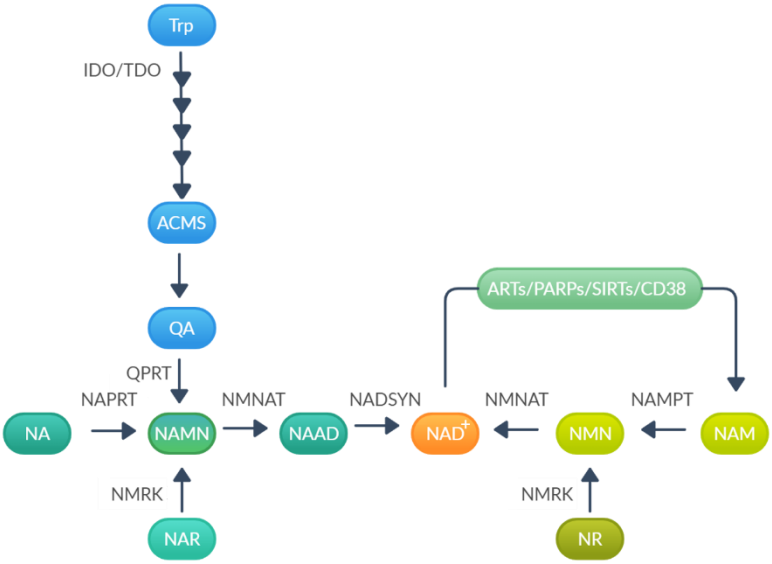

Figure 1 - Schematic overview of NAD^+ biosynthesis and consumption in mammals. Abbreviations: ACMS, α-amino-β-carboxymuconate-ε-semialdehyde; ARTs, ADP-ribose transferases; CD38, cADPR synthase; IDO, indoleamine 2,3-dioxygenase; NA, nicotinic acid; NAAD, nicotinic acid adenine dinucleotide; NAD^+, nicotinamide adenine dinucleotide; NADSYN, NAD^+ synthetase; NAM, nicotinamide; NAMN, nicotinic acid mononucleotide; NAMPT, nicotinamide phosphoribosyltransferase; NAPRT, nicotinic acid phosphoribosyltransferase; NAR, nicotinic acid riboside; NMN, nicotinamide mononucleotide; NMNAT, nicotinamide/nicotinic acid mononucleotide adenylyltransferase; NR, nicotinamide riboside; NMRK, nicotinamide riboside kinases; PARPs, poly-ADP-ribose polymerases; QA, quinolinic acid; QPRT: quinolinate phosphoribosyltransferase; SIRTs, sirtuins; TDO, tryptophan-2,3-dioxygenase; Trp, tryptophan (Adapted from Demareset *et al.*, 2019 and Katsyuba & Auwerx, 2017).

1.1.2.1. *de novo* NAD synthesis

The *de novo* synthesis pathway starts with the amino acid tryptophan (Trp) (Bender, 1983; Houtkooper *et al.*, 2010; Katsyuba & Auwerx, 2017) and consists of eight steps to produce NAD^+ (Bender, 1983; Houtkooper *et al.*, 2010; Katsyuba & Auwerx, 2017), through the enzymes in the kynurenine pathway (Katsyuba & Auwerx, 2017; Xiao *et al.*, 2018; Ying, 2006). In the first and rate-limiting step, Trp is converted by tryptophan-2,3-dioxygenase (TDO) or indoleamine 2,3-dioxygenase (IDO) into N-formylkynurenine (Cantó *et al.*, 2015; Houtkooper *et al.*, 2010; Katsyuba & Auwerx, 2017; Yang & Sauve, 2016). The latter is hydrolyzed to kynurenine by kynurenine formamidase (KFase) (Magni *et al.*, 2004; Xiao *et*

al., 2018). Kynurenine is converted to 3-hidroxykynurenine through a reaction catalyzed by kynurenine 3-hydroxylase (K3H) (Magni *et al.*, 2004; Xiao *et al.*, 2018). Then, 3-hidroxykynurenine is transformed by kynureninase (KYNU) into 3-hydroxyanthranilate, which is converted into α-amino-β-carboxymuconate-ε-semialdehyde (ACMS) by 3-hydroxyanthranilate dioxygenase (3HAO) (Bender, 1983; Houtkooper *et al.*, 2010; Katsyuba & Auwerx, 2017; Xiao *et al.*, 2018). ACMS can undergo spontaneous cyclization forming quinolinic acid (QA). QA is then condensed with 5-phospho-α-D-ribose 1-diphosphate, forming nicotinic acid mononucleotide (NAMN), a reaction catalyzed by the enzyme quinolinate phosphoribosyltransferase (QPRT), which uses phosphoribosyl pyrophosphate (PRPP) as a co-substrate (Houtkooper *et al.*, 2010; Magni *et al.*, 2004; Xiao *et al.*, 2018). This reaction represents another rate-limiting step of the *de novo* synthesis pathway (Houtkooper *et al.*, 2010; Magni *et al.*, 2004; Xiao *et al.*, 2018). From this point, NAMN fuses with the Preiss–Handler pathway, wherein NAMN is adenylated to nicotinic acid adenine dinucleotide (NAAD) by nicotinamide/nicotinic acid mononucleotide adenylyltransferases (NMNATs) (Bender, 1983; Kulikova *et al.*, 2015; Magni *et al.*, 2004; Xiao *et al.*, 2018). Three isoforms of NMNATs have been described in mammals with different subcellular distributions. NMNAT1 is a nuclear enzyme (Emanuelli *et al.*, 2001; Xiao *et al.*, 2018; Yalowitz *et al.*, 2004), NMNAT2 locates in the cytosol and Golgi apparatus (Berger *et al.*, 2005; Xiao *et al.*, 2018; Yalowitz *et al.*, 2004), and NMNAT3 is found in the cytosol and mitochondria (Berger *et al.*, 2005; Xiao *et al.*, 2018; Zhang *et al.*, 2003). The last step in the *de novo* pathway includes the ATP-dependent amidation of NAAD by NAD^+ synthase (NADSYN) (Cantó *et al.*, 2015; Houtkooper *et al.*, 2010; Magni *et al.*, 2004; Xiao *et al.*, 2018). Two NADSYN isoforms, NADSYN1 and 2, have been identified in humans (Hara *et al.*, 2003; Magni *et al.*, 2004; Xiao *et al.*, 2018).

Since all the enzymes catalyzing the different reactions of the *de novo* synthesis pathway are localized in the cytosol, this process most likely takes place there (Houtkooper *et al.*, 2010; Katsyuba & Auwerx, 2017).

1.1.2.2. Salvage pathways

In the mammalian pathway for NAM salvage, NAD^+ synthesis requires only two steps (Katsyuba & Auwerx, 2017; Opitz & Heiland, 2015). The first and rate-limiting step is the conversion of NAM and PRPP into nicotinamide mononucleotide (NMN) and pyrophosphate (PPi), catalyzed by NAMPT (nicotinamide phosphoribosyltransferase) (Dölle *et al.*, 2015; Kulikova *et al.*, 2018; Magni *et al.*, 2004). Then, NMNATs catalyze the reaction between NMN and ATP (adenosine triphosphate) with the formation of NAD^+ (Cantó *et al.*, 2015; Kulikova *et al.*, 2018; Ying, 2008).

In another salvage pathway, Preiss and Handler discovered that NA could be converted into NAD^+ in three steps (Cantó *et al.*, 2015; Preiss & Handler, 1958b, 1958a; Xiao *et al.*, 2018). Nicotinic acid phosphoribosyltransferase (NAPRT) catalyzes the conversion of NA and PRPP to NAMN and PPi (Kulikova *et al.*, 2018; Magni *et al.*, 2004; Xiao *et al.*, 2018). Following this conversion, the Preiss-Handler pathway converges with the *de novo* synthesis pathway (Cantó *et al.*, 2015; Houtkooper *et al.*, 2010; Xiao *et al.*, 2018), wherein NAMN undergoes the same reactions that were previously described for NAD^+ biosynthesis from tryptophan.

The nucleosides NR and NAR are additional NAD^+ precursors in salvage pathways (Yang & Sauve, 2016). NR and NAR are phosphorylated into NMN and NAMN, respectively, by nicotinamide riboside kinases (NMRKs), of which two enzymes have been described in mammals (NMRK1 and NMRK2) (Bieganowski & Brenner, 2004; Tempel *et al.*, 2007; Xiao *et al.*, 2018; Yang & Sauve, 2016). Just like in the aforementioned pathways, NMN and NAMN are converted to the corresponding dinucleotide (NAD^+ and NAAD, respectively) by NMNATs, and NADSYN amidates NAAD to NAD^+ (Cantó *et al.*, 2015; Nikiforov *et al.*, 2015).

More recently, Yang and colleagues investigated dihydronicotinamide riboside (NRH) as a biosynthetic precursor in NAD^+ metabolism, identifying a putative new NAD^+ biosynthetic salvage pathway (Yang *et al.*, 2019). They observed that cell lysates possess an ATP-dependent kinase activity that converts NRH to reduced nicotinamide mononucleotide (NMNH), and that this is independent of NMRKs (Yang *et al.*, 2019). The same group identified that adenosine kinase (AK) is the enzyme that phosphorylates NRH to NMNH and

that AK is required for NRH to be converted to NAD^+ in mammalian cells (Yang *et al.*, 2020). The most likely pathway for NMNH conversion to NAD^+ is adenylation to NADH by NMNATs followed by oxidation to NAD^+ (Yang *et al.*, 2020). Future studies will need to establish if this new NAD^+ biosynthesis pathway has physiological relevance (Ziegler & Nikiforov, 2020).

1.1.3. NAMPT and NAPRT

The *NAMPT* gene (ENSG00000105835) is located in the long arm of chromosome 7 - 7q22.3 (NCBI, July 31, 2020), in the reverse strand, consisting of 38029 bp with 11 exons and 13 alternative transcripts (Ensembl, July 31, 2020). The NAMPT protein has 491 amino acids and a molecular mass of 55,5 kDa (UniProt, July 31, 2020).

NAMPT is ubiquitously expressed (Duarte-Pereira *et al.*, 2016; Garten *et al.*, 2015; Samal *et al.*, 1994), with the highest expression levels detected in liver, skeletal muscle and adipose tissue (Dölle *et al.*, 2015; Samal *et al.*, 1994). NAMPT is abundant in the cytosol and is also present in the nucleus, but its presence in mitochondria remains controversial (Audrito *et al.*, 2020).

In mammals, there is an intracellular (iNAMPT) and an extracellular (eNAMPT) form of NAMPT (Garten *et al.*, 2009; Nikiforov *et al.*, 2015; Xiao *et al.*, 2018). Previously named as pre-B cell colony enhancing factor (PBEF), NAMPT was initially recognized as a secreted cytokine, being a co-factor for B-cell maturation (Garten *et al.*, 2015; Samal *et al.*, 1994), and also as visfatin (Fukuhara *et al.*, 2005). NAMPT was later shown to be an enzyme involved in NAD^+ biosynthesis (Rongvaux *et al.*, 2002; Xiao *et al.*, 2018), thereby modulating the activity of NAD^+-consuming enzymes that regulate cellular metabolism, mitochondrial biogenesis and adaptive responses to inflammatory, oxidative, proteotoxic and genotoxic stress (Garten *et al.*, 2015). NAMPT may also function as a growth factor and adipokine (Audrito *et al.*, 2020).

The *NAPRT* gene (ENSG00000147813) is located in the long arm of chromosome 8 - 8q24.3 (NCBI, July 31, 2020), in the reverse strand, consisting of 4065 bp with 12 exons and 14 alternative transcripts (Ensembl, July 31, 2020). NAPRT protein consists of 538 amino acids and has a molecular mass of 57.6 kDa (UniProt, July 31, 2020).

NAPRT activity was originally described in the context of the Preiss–Handler pathway (Sorci *et al.*, 2010). NAPRT is highly expressed in the liver, kidney and small intestine (Cantó & Auwerx, 2011; Hara *et al.*, 2007). NAPRT is primarily detected in the cytosol and in the nucleus but not in the mitochondria (Audrito *et al.*, 2020; Nikiforov *et al.*, 2011; Piacente *et al.*, 2017).

NAPRT is believed to boost NAD^+ levels when the cells are under stress conditions (Managò *et al.*, 2019), and also participates in energy metabolism (Piacente *et al.*, 2017). Recently, the presence of NAPRT in extracellular fluids (eNAPRT) was discovered, with a role in physiological and inflammatory conditions (Managò *et al.*, 2019).

1.1.4. NAD^+ metabolism and cancer

Alterations of the NAD^+ content in cells and tissues are linked with several diseases, including neurodegenerative disorders, diabetes, obesity, metabolic syndrome, and cancer (Belenky *et al.*, 2006; Katsyuba & Auwerx, 2017; Kulikova *et al.*, 2018).

To promote their rapid proliferation, cancer cells have a high capacity for glucose uptake and an increased rate of anaerobic glycolysis under normal aerobic conditions (Warburg effect) (Garten *et al.*, 2015; Warburg, 1956; Yaku *et al.*, 2018). These metabolic alterations are dependent of higher NAD^+ levels, which functions in cellular processes needed for cancer cell growth, such as progression through the cell-cycle, anti-apoptosis mechanisms, DNA repair, and the regulation of transcription, chromatin dynamics and telomerase activity (Garten *et al.*, 2015).

Intracellular NAD^+ levels can also regulate cancer initiation and progression through the activities of the NAD^+-consuming enzymes, such as PARPs and sirtuins (Yaku *et al.*, 2018). PARP activity increases have been linked to both the suppression and the progression of carcinogenesis, due to their role in DNA repair. As such, PARPs may prevent accumulation of mutations and cancer formation, but may also help cancer cells survive after tumor initiation (Demarest *et al.*, 2019).

Sirtuins might act both in tumor promotion as well as in tumor suppression depending on the tumor context (Alhazzazi *et al.*, 2011; Deng, 2009; Opitz & Heiland, 2015). SIRT1 activity can repress transcription factor signaling, such as Stat3 (signal transducer and activator of transcription 3) and NF-κB (nuclear factor NF-κB), and attenuate inflammatory responses, which suppresses carcinogenesis (Shackelford *et al.*, 2013). However, SIRT1 can

also regulate tumor suppressors such as p53, PTEN (phosphatase and tensin homolog) and retinoblastoma protein, and stabilize oncogenes such as MYCN (MYCN proto-oncogene, bHLH transcription factor), to enhance epithelial-mesenchymal transition (EMT) and metastasis (Demarest *et al.*, 2019; Shackelford *et al.*, 2013). SIRT1 is overexpressed in several malignant tumors such as colorectal cancer, thyroid cancer, hepatocellular carcinoma, leukemia, lung cancer and osteosarcoma (reviewed in Demarest *et al.*, 2019).

NAD^+ is rapidly consumed by NAD^+-dependent enzymes in cancer cells and converted to NAM, therefore NAMPT is essential for the renewal of the intracellular NAD^+ pool (Garten *et al.*, 2015). *NAMPT* overexpression is, thus, associated with the development of many cancers including colorectal, ovarian, breast, gastric, prostate, thyroid, pancreatic, endometrial carcinomas, myeloma, melanoma, gliomas, sarcoma and hematological malignancies (reviewed in Audrito *et al.*, 2020; Garten *et al.*, 2015; Opitz & Heiland, 2015; Yaku *et al.*, 2018). NAMPT, both in its intracellular and extracellular forms, has a direct role on cancer cells increasing cancer aggressiveness, correlating with worse prognosis. This may be due to the regulation of different processes, including metabolic adaptation, DNA repair, gene expression, signaling pathways, cell growth, invasion, stemness, EMT, metastasis, angiogenesis, secretion of both pro-inflammatory and immunosuppressive cytokines, and resistance to genotoxic stress (Audrito *et al.*, 2020).

NAPRT is silenced or downregulated in several tumors (Duarte-Pereira *et al.*, 2014, 2016), and EMT-associated downregulation of NAPRT is observed in different tumor types (Lee *et al.*, 2018). Amplification of the *NAPRT* gene was also detected in prostate, ovarian and pancreatic cancers (Chowdhry *et al.*, 2019; Piacente *et al.*, 2017). In a recent work, the overexpression of *NAPRT* in ovarian cancer correlated with a BRCAness gene expression signature, with defects in homologous recombination DNA repair (Audrito *et al.*, 2020; Piacente *et al.*, 2017). *NAPRT* expression in cancer may be regulated by both transcriptional and post-transcriptional mechanisms, including mutations in transcription factor binding sites, promoter methylation and alternative splicing (Audrito *et al.*, 2020; Duarte-Pereira *et al.*, 2016). eNAPRT was recently identified in sera from patients with a diagnosis of cancer, including solid tumors and hematological malignancies, and the results suggest a possible role of this enzyme in the tumor microenvironment (Audrito *et al.*, 2020; Managò *et al.*, 2019).

The aforementioned NAD^+ metabolism enzymes have been studied as cancer biomarkers and as therapeutic targets for cancer treatment (reviewed in Demarest *et al.*, 2019; Yaku *et al.*, 2018). In particular, NAMPT has received considerable attention and NAMPT inhibitors such as FK866 have been developed as anti-cancer drugs. NAPRT has emerged as a biomarker, primarily because NA could be used as a cytoprotective agent in treatment with NAMPT inhibitors, in NAPRT downregulated tumors (Duarte-Pereira *et al.*, 2016; Shames *et al.*, 2013). However, the therapeutic potential of these enzymes in cancer is not yet fully known and there is still a great need to investigate the mechanisms behind them in different contexts. An optimized anticancer strategy would include patient profiling to identify treatments suitable for the metabolic and genetic status of that particular individual (Demarest *et al.*, 2019).

1.2. Saliva as a cancer biomarker source

Many cancers are still diagnosed at an advanced stage (Rapado-González *et al.*, 2016) because cancer symptoms are frequently not specific and absent until the tumors have metastasized (Wang *et al.*, 2017). The survival rates for some cancers have improved but overall, they are still quite low (Rapado-González *et al.*, 2016). Therefore, there is an urgent need for new cancer screening, early detection, diagnostic, staging and prognostic tools that are fast, affordable, non-invasive and with high sensitivity and specificity (Rapado-González *et al.*, 2016; Wang *et al.*, 2017).

Saliva consists of secretions from the minor and major (parotid, submandibular and sublingual) salivary glands (Bonne & Wong, 2012; Rapado-González *et al.*, 2020). Molecules such as DNA, RNA, proteins and metabolites that are present in the blood can also be found in saliva (Rapado-González *et al.*, 2020; Wang *et al.*, 2017). Saliva composition changes under different pathological conditions (Rapado-González *et al.*, 2016), and detecting these alterations have allowed the detection of oral and systemic diseases (Bonne & Wong, 2012). Multiple molecules present in saliva can potentially be used as biomarkers to detect early-stage cancer and, in addition to diagnosis, can be used for individual risk assessment, prognosis, to monitor the response to treatment and for pharmacogenetic studies (Rapado-González *et al.*, 2016, 2020; Wang *et al.*, 2017).

The scientific community created the term “salivaomics”, due to the ongoing advances in saliva research. “Salivaomics” is a comprehensive approach to explore the different molecules contained in saliva as potential biomarkers. This includes the genome (consisting of both human and microbial DNA), the epigenome, the transcriptome, the metabolome, the proteome and the microbiota (Rapado-González *et al.*, 2020; Wang *et al.*, 2017).

As a diagnostic approach, saliva has several advantages over blood and tissue. It is a non-invasive sample, with easy collection and storage, cost-effective and causes less patient discomfort (Rapado-González *et al.*, 2016, 2020; Wang *et al.*, 2017; Yoshizawa *et al.*, 2013).

Many salivary biomarkers have been described for a wide variety of cancers besides head and neck cancers (Rapado-González *et al.*, 2016, 2020). Several salivary biomarkers can be detected during systemic cancer development, including pancreatic, breast, lung or ovarian cancers (reviewed in Wang *et al.*, 2017). Rapado-González and colleagues stated that salivary biomarkers are sensitive and specific enough to be used for systematic cancer detection (Rapado-González *et al.*, 2020), and many have been identified and validated at the preclinical level (Wang *et al.*, 2017). Yet, further studies are needed in the different “omics” to designate saliva as a liquid biopsy suitable for regular clinical practice (Rapado-González *et al.*, 2016).

2. OBJECTIVES

The main objectives of this work were to study saliva as a source of cancer biomarkers and to investigate *NAPRT* and *NAMPT* in this context. The specific aims were the following:

a) Collection and analysis of saliva samples, namely, optimization of the extraction and amplification of nucleic acids for molecular studies;

b) Search for *NAPRT* and *NAMPT* polymorphisms in saliva from cancer patients;

c) Bioinformatics analyses of the genetic alterations in pediatric leukemia datasets;

d) Bioinformatics analysis of *NAPRT* and *NAMPT* genetic alterations in head and neck cancer and pediatric leukemia datasets.

Due to the COVID-19 pandemic, it was not possible to carry out the objective b), instead bioinformatics analyses were performed (objectives c) and d)).

3. MATERIALS AND METHODS

Saliva samples were collected from two healthy 22-year-old female volunteers. DNA from 8 healthy blood donors over 50 years old (HRC2-A9 and E11, HRC3-A10, B1, B2, B3, C1 and C2) was also tested. These are commercially available samples from the ECACC (European Collection of Cell Cultures) Human Random Control DNA Panel and were purchased from Sigma-Aldrich. Donors have given written, informed consent for their samples to be used for research purposes.

3.1. Saliva sample collection

Subjects were asked to abstain from eating, drinking, smoking or perform oral hygiene procedures at least one hour before sample collection (mouthwash, unstimulated whole saliva (WS), buccal swab and/or cytobrush) that was performed in the morning, until 10 am.

To collect the mouthwash, subjects were given a 50-mL tube with 10 mL of clean water and were asked to rinse the mouth for 30 seconds and expel the water back into the tube. The tubes were immediately placed and maintained on ice until centrifugation at 10000 × g for 10 minutes at 4ºC. The supernatant was discarded, the pellet was resuspended with 1 mL of Milli-Q® water and aliquoted into two 500 µL aliquots. These were centrifuged at 8000 × g for 10 minutes at 4ºC and the supernatant was discarded. The pellet was immediately used for DNA or RNA extraction or stored at -80ºC until further processing. After the mouth rinse, subjects were asked to wait for a minute before buccal swab, cytobrush or saliva collection.

For swab sample collection, the inside of each cheek was rubbed 3, 6 or 30 times with one or two cotton swabs, respectively. The cotton swabs were placed inside 15-mL sterile tubes with a sterile 1000-µL pipette tip in the bottom to facilitate saliva collection by centrifugation at 10000 × g for 10 minutes at 4ºC. The total volume collected was transferred into an eppendorf and the samples were immediately processed.

To collect cytobrush samples, the inside of the right and left cheeks was brushed 30 times each, using one cytobrush for both sides. The brush was separated from the handle, placed in an eppendorf and stored at 4ºC until DNA extraction.

Two methods were used to collect unstimulated WS (protocols adapted from Rosa *et al.*, 2016): passive drooling and sublingual cotton roll. For passive drooling, a 50-mL sterile tube was used to collect passive drooled saliva for 2 minutes. For the sublingual cotton roll method, sublingual saliva was collected with two cotton rolls placed under the tongue for 2 minutes. The cotton rolls were placed inside a 15-mL sterile plastic tube with a sterile 1000-µL pipette tip in the bottom to facilitate saliva collection by centrifugation at 10000 × g for 10 minutes at 4ºC. Then, the cotton rolls were discarded, and the saliva was resuspended by pipetting, followed by vortexing for 5 seconds, and aliquoted into 2 cryovials (one with 200 µL and the other with the remaining volume). Samples were stored at -80ºC until further processing or immediately used for DNA or RNA extraction.

3.2. RNA and DNA extraction

For RNA extraction, two different methods were used: the TRIzol method (adapted protocol from Pandit *et al.*, 2013) and a column-based method, using the RNeasy® Micro Kit (74004, Qiagen) following the manufacturers' instructions.

In the first step of the Qiagen kit protocol, 350 µL of buffer RLT were added, homogenizing for 1 minute. The same volume of 70% ethanol was added and mixed well by pipetting. The samples were transferred to RNeasy MinElute spin columns in 2-mL collection tubes, followed by centrifugation at 8000 × g for 15 seconds at 20ºC. The flow-through was discarded and 350 µL of buffer RW1 were added to the columns, followed by centrifugation at 8000 × g for 15 seconds at 20ºC. The flow-through was discarded and 80 µL of DNase I incubation mix (10 µL of DNase I stock solution and 70 µL of Buffer RDD) were added directly to the membrane columns. The columns were incubated at room temperature (RT) for 30 minutes. Then, 350 µL of buffer RW1 were added to the columns, which were centrifugated at 8000 × g for 30 seconds at 20ºC. The flow-through and the collection tubes were discarded, and the columns were placed in new 2-mL collection tubes. Then, 500 µL of buffer RPE were added to columns, followed by centrifugation at 8000 × g for 30 seconds at 20ºC. The flow-through was discarded and 500 µL of 80% ethanol were added to the columns, followed by centrifugation at 8000 × g for 2 minutes at 20ºC. The flow-through and the collection tubes were discarded, and the columns were placed in new 2-mL collection tubes. With the lid open, the columns were centrifugated at full speed (8000

× g) for 5 minutes at 20ºC. The flow-through and the collection tubes were discarded, and the columns were placed in new 1.5-mL collection tubes. Then, 14 µL of RNase-free water were added directly to the center of the membrane columns and the columns were centrifugated at full speed for 1 minute at 20ºC to elute the RNA. The final elution volume was 12 µL since the dead volume of the column is 2 µL.

For the TRIzol method, 800 µL of TRIzol™ were added to the samples, which were vortexed for 1 minute and incubated for 5 minutes at RT. Then, 200 µL of chloroform were added to the 2-mL eppendorf tube, which was vigorously vortexed for 1 minute and incubated a second time for 5 minutes at RT. The samples were then centrifuged at 10000 × g for 10 minutes at 4°C. The upper aqueous layer (500 µL) was transferred to a new 2-mL eppendorf tube, 200 µL of chloroform were added and the tube was vortexed for 30 seconds. The samples were then centrifuged at 10000 × g for 10 minutes at 4°C. The upper aqueous layer (500 µL) was transferred to a new 2-mL eppendorf tube, an equal volume of isopropyl alcohol was added, and the samples were incubated for 45 minutes at -20ºC. The samples were then centrifuged at 10000 × g for 20 minutes and the supernatant was discarded. The pellet was washed with 1 mL of 70% ethanol and centrifuged at 10000 × g for 5 min at 4°C. The pellet was air-dried, resuspended in 20 µL of RNase-free water and stored at -80°C.

The method used for the DNA extraction was a column-based method, using the NZY Tissue gDNA Isolation Kit (MB13502, NZYTech), according to the manufacturers' instructions. The samples were resuspended with 200 µL of buffer NT1. Then, 25 µL of proteinase K solution (22 mg/mL) and 200 µL of buffer NL were added, and the samples were vortexed for 30 seconds. Samples were incubated for 15 minutes at 56ºC and vortexed for 5 seconds each 3 minutes. Then, 210 µL of 100% ethanol was added to the samples, which were immediately vortexed. This mix was transferred into an NZYSpin Tissue Column placed in a 2-mL collection tube. The tubes were centrifugated at 17700 × g for 1 minute at 15ºC. The flow-through was discarded and the columns were placed in new collection tubes. Then, 500 µL of buffer NW1 were added to each column, followed by centrifugation at 17700 × g for 1 minute at 15ºC. The flow-through was discarded and the columns were placed in new collection tubes. Then, 600 µL of buffer NW2 were added to each column, followed by centrifugation at 17700 × g for 1 minute at 15ºC. The flow-through was discarded and the tubes were centrifugated at 17700 × g for 2 minutes at 15ºC. The columns were placed into clean microcentrifuge tubes and 100 µL of sterile water (preheated

at 56ºC) were added directly to the membrane column. The columns were incubated at room temperature for 1 minute and then, centrifugated at 17700 × g for 2 minutes at 15ºC to elute DNA. The genomic DNA was stored at -20ºC.

In table 1, there is an overview of the different sample collection and nucleic acid extraction protocols. Frozen samples were stored at -80ºC for 24 hours. All frozen samples were thawed on ice before the beginning of the protocols. The samples stored at 4ºC were processed for DNA extraction until 48 hours later. Of note, of the 4 samples obtained by brushing cotton swabs 3 and 30 times, one sample of each was passed through a 25-gauge needle 3 times to ensure complete lysis of cells.

Table 1 – Overview of the samples collected: saliva and mouthwash (fresh, stored at -80ºC and stored at 4ºC), swab (brushing the cotton swab 3, 6 or 30 times) and cytobrush. The initial volume of the sample, the collection method and the protocol of nucleic acids extraction performed are indicated. N.A.: not applicable.

Sample	Sublingual cotton rolls	Drooling	Initial volume	Supernatant	Pellet	RNA (Kit)	RNA (TRIzol)	DNA (Kit)
Fresh saliva	✓	-	200 µL	n.a.	n.a.	✓	✓	✓
Frozen saliva	✓	-	200 µL	n.a.	n.a.	✓	✓	✓
Saliva (4ºC)	-	✓	500 µL	n.a.	n.a.	-	-	✓
Fresh mouthwash	n.a.	n.a.	Pellet	-	✓	✓	✓	✓
Frozen mouthwash	n.a.	n.a.	Pellet	-	✓	✓	✓	✓
Mouthwash (4ºC)	n.a.	n.a.	Pellet	-	✓	-	-	✓
Fresh Swab (3, 6 and 30 times)	n.a.	n.a.	n.a.	n.a.	n.a.	-	-	✓
Buccal cytobrush (4ºC)	n.a.	n.a.	n.a.	n.a.	n.a.	-	-	✓

3.3. Nucleic acid quantification and integrity

The concentration and purity of DNA and RNA were measured by spectrophotometry. For DNA samples from healthy blood donors and the RNA samples, NanoVue Plus™ Spectrophotometer (GE, Healthcare) was used, requiring 1 µL of each sample. For the DNA from saliva samples, a Varian Cary 50 UV-VIS spectrophotometer was used and 50 µL of each sample was diluted in 450 and/or 950 µL of sterile water and resuspended by pipetting. The concentration of DNA and RNA was measured and the purity was estimated with the ratios of absorbance at 260 and 280 nm (A260/A280) and at 260 and 230 nm (A260/A230). To obtain the concentration of the extracted DNA samples from saliva, the A260 nm was multiplied by the DNA extinction coefficient (50 µg/mL) and by the dilution factor. For DNA, a relatively pure sample has an A260/A280 ratio close to 1.8. For RNA, the A260/A280 ratio should be close to 2.0. The ideal A260/A230 ratio values are usually higher than the respective A260/A280 ratio values. For both pure DNA and RNA, an A260/A230 ratio should be around 2 or slightly above.

The integrity of DNA and RNA was also assessed by gel electrophoresis. Samples were separated in 1% agarose gels with TAE (Tris-acetate-EDTA) 1x buffer. The 1% agarose gels were prepared with 60 mL of TAE 1x buffer and 0.6 g of agarose and stained with 2 µL of GreenSafe Premium (NZYTech). The molecular weight marker used was NZYDNA Ladder VII (NZYTech) and 3 µL were loaded into the gel. The samples were loaded with loading buffer (LB; 6x NZYDNA loading dye, NZYTech), as follows: 2 µL of the RNA samples extracted using the RNeasy® Micro Kit were loaded with 8 µL of RNase-free water and 2 µL of LB; 5 µL of the RNA samples extracted with the TRIzol method were loaded with 5 µL of RNase-free water and 2 µL of LB; and 10 µL of the DNA samples extracted using the NZY Tissue gDNA Isolation Kit were loaded with 2 µL of LB. The gels were run at 90 volts (V) for about 30 minutes, until the dye line was approximately at 2/3 of the gel. The gel was placed on ChemiDoc™ MP Imaging System (Bio-Rad) and visualized with Image Lab™ 5.1 Software (Bio-Rad).

After DNA and RNA quality evaluation, DNA and RNA samples were stored at -20ºC and at -80ºC, respectively, until further analysis.

3.4. Polymerase chain reaction (PCR)

PCR was used to amplify exon 4 of the human *NAPRT* gene and exon 7 of the human *NAMPT* gene (previously identified as mutation hotspots). To optimize the PCR reactions, different conditions were tested, such as the annealing temperature, primer concentration and Master Mix volume.

Amplification reactions were performed with 1 μL of DNA in a 20 μL final volume reaction mixture, containing 10 μL of NZYTaq II 2x Green Master Mix (MB35802, NZYTech), 1 μL (2 μM) of primers forward and reverse and 7 μL of water (MB11101, NZYTech). The primers used, regions amplified and product sizes are indicated in table 2. PCR was carried out in the CFX Connect™ Real-Time System (Bio-Rad) thermocycler with an initial denaturing step at 95°C for 15 minutes, followed by 35 cycles of amplification. Each amplification cycle consisted of denaturation at 94°C for 30 seconds, annealing at 62°C for 30 seconds (*NAPRT* primers) or 58ºC for 1 minute (*NAMPT* primers), and extension at 72°C for 1 minute. A final extension step followed, at 72ºC for 10 minutes.

To confirm amplification, 10 μL of each PCR product were loaded into a 1% agarose gel, which was run at 90 V for about 30 minutes, until the dye line was approximately at 2/3 of the gel. To visualize the results, ChemiDoc™ MP Imaging System (Bio-Rad) and Image Lab™ 5.1 Software (Bio-Rad) were used.

Table 2 - Oligonucleotide sequences used for amplification of *NAMPT* and *NAPRT* genes.

Primers	Sequence	Product size (bp)
HsNaprt_ex4_F	CTACAGCGTGTGGAGGTGAG	404
HsNaprt_ex4_R	CACCTGTGCTCACCTTCTGC	
HsNampt_ex7_F	CATAACAGCTTGGGGGAAAG	362
HsNampt_ex7_R	CTCTCTCTGGGCTGCAACT	

3.5. Sequencing

NAMPT amplified products were purified with ExoSAP-IT™ (Applied Biosystems™), by treating 1.5 μL of each sample with 1 μL of ExoSAP-IT™. Reactions

were incubated at 37°C for 15 minutes followed by enzyme inactivation for 15 minutes at 85°C. The resulting *NAMPT* purified fragments were sequenced using the Big Dye® v3.1 Terminator Cycle Sequencing kit (Applied Biosystems™), by adding 1 μL of HsNampt_ex7_F primer (2 μM) and 2 μL of BigDye™ Terminator v3.1 Ready Reaction Mix. The samples were subjected to an initial denaturation step at 94ºC for 5 minutes, 35 cycles of 94ºC for 20 seconds, 58ºC for 10 seconds and 60ºC for 1 minute and 30 seconds, followed by a final extension step at 60ºC for 10 minutes. Sequencing reaction products were purified with Sephadex® (prepared with 20 g Sephadex® in distilled water, added to 300 mL). In clean spin columns, 750 μL of Sephadex® were added, followed by centrifugation at 1840 × g for 4 minutes at 15ºC. The spin columns were transferred to new 1.5 mL-tubes and the products of the previous amplification were added to the center of the resin, followed by centrifugation at 1840 × g for 4 minutes at 4ºC. Then, the tubes were stored at -20ºC until sequencing.

3.6. Bioinformatics analyses

Four types of tumor data were analyzed: Pediatric Acute Lymphoid Leukemia (ALL), Pediatric Acute Myeloid Leukemia (AML), Adult Acute Myeloid Leukemia (LAML) and Head and Neck squamous cell carcinoma (HNSC). The leukemia datasets were selected because NAPRT and NAMPT can have an important role in these types of tumors, and the HNSC dataset was selected with the aim to validate saliva biomarkers.

Information was retrieved from cBioPortal (Cerami *et al.*, 2012; Gao *et al.*, 2013; http://www.cbioportal.org/). Data were generated by the Therapeutically Applicable Research to Generate Effective Treatments (TARGET, https://ocg.cancer.gov/programs/target) initiative, also available on https://portal.gdc.cancer.gov/projects. For ALL (phs000464; 1978 samples) and AML (phs000465; 1025 samples), gene expression (45 samples in AML and 203 samples in ALL), methylation (184 samples in AML and 149 samples in ALL), mutation (150 samples) and copy number alteration (CNA) (240 samples in AML and 764 samples in ALL) data were retrieved. These data were organized as the 10 genes most expressed, with mutations or CNA, and the most and least methylated genes. The median for mRNA expression (RPKM values) and methylation (beta values and M-values) was calculated for each gene and the

median of the RPKM values was $\log_2$ transformed. Ludberg *et al.* defined grouped RPKM values into no expression (<0.1 RPKM), low (0.1–2 RPKM), moderate (2–8 RPKM) and high (> 8 RPKM) expression categories (Lundberg *et al.*, 2010), and these groups were also considered here. In ALL, the M-values of methylation were transformed into beta values, using the following formula (Du *et al.*, 2010):

$$\text{Beta} = \frac{2^M}{2^M+1}$$, where M is the M-value.

Beta values vary between 0 and 1, where a beta value of ≤ 0.3 is considered hypomethylation, and a beta value of ≥0.7 is considered hypermethylation (Gujar *et al.*, 2018).

All genes from the top 10 were searched on the Gene database from NCBI (https://www.ncbi.nlm.nih.gov/gene/), where information about the genes was retrieved (O'Leary *et al.*, 2016).

With the hypermethylated and hypomethylated genes in ALL and AML, a statistical overrepresentation test with the PANTHER GO-Slim Biological Process set was performed on PANTHER (Mi *et al.*, 2019; http://www.pantherdb.org/). The biological processes with a fold enrichment ≥ 2.0 were selected and analyzed.

A specific search for *NAPRT* and *NAMPT* genes was made for HNSC, using two datasets: one of The Cancer Genome Atlas (TCGA, 2015) (Cancer Genome Atlas Network, 2015) and the other of TCGA (2018) from the PanCancer Project, as well as for ALL and AML. Gene expression (515 samples in HNSC), mutations (520 samples in HNSC), CNAs (517 samples in HNSC) and methylation (only for *NAPRT*; 279 samples in HNSC) were retrieved. The HNSC datasets have overlapping data and therefore, the TCGA dataset from 2018, which has more samples (523), was used to assess *NAPRT* and *NAMPT* expression, mutations and CNAs. The TCGA dataset from 2015 was used to assess *NAPRT* methylation, since the other dataset does not have methylation data. For each gene, the median of the beta (methylation) and RPKM (mRNA expression) values of all samples were calculated. The median of the RPKM values was $\log_2$ transformed. All data were retrieved from cBioPortal, except for expression data in HNSC, which was retrieved from UALCAN web-portal (Chandrashekar *et al.*, 2017; http://ualcan.path.uab.edu/). Yusuff *et al.* defined grouped TPM values into no expression (<3 TPM), low (3–10 TPM), moderate (10–25 TPM), high (25–100 TPM) and very high (>100 TPM) expression categories (Yusuff *et al.*, 2020). In the ALL and HNSC (TCGA, 2015) datasets, methylation and expression data for the same

samples in each dataset exists, and through cBioPortal the Pearson correlation between *NAPRT* methylation and expression was calculated. The correlation between CNAs and expression for both *NAPRT* and *NAMPT* in HNSC and *NAMPT* in ALL was also analyzed.

NAPRT cis-eQTL (expression quantitative trait loci), i.e. SNPs that alter *NAPRT* expression, in HNSC and LAML (TCGA) were downloaded from the PancanQTL database (Gong *et al.*, 2018; http://bioinfo.life.hust.edu.cn/PancanQTL/). The localization, number and effect size on gene expression (beta values) of these SNPs were analyzed. The UCSC Genome Browser (Kent *et al.*, 2002; http://genome.ucsc.edu/) was used to localize the eQTL on the human genome (GRCh37/hg19 assembly). In the ClinVar database from NCBI (https://www.ncbi.nlm.nih.gov/clinvar/), each eQTL was searched. In the Genotype-Tissue Expression (GTEx) Portal (https://gtexportal.org/), it was investigated if the eQTL are present in non-pathological tissues. Through Ensembl release 100 (Yates *et al.*, 2020; https://ensembl.org/), allelic frequencies of each SNP were analyzed with data from the 1000 Genomes Project (The 1000 Genomes Project Consortium, 2015). The beta values of the eQTL that have an impact on *NAPRT* expression in HNSC were $\log_2$ transformed and a heatmap was created with all the tumors in which *NAPRT* expression is altered by these SNPs, using the HCE 3.5 (Power Analysis) software.

4. RESULTS

4.1. RNA

RNA was extracted with two different protocols, using the RNeasy® Micro Kit (74004, Qiagen) and the TRIzol method (adapted protocol from Pandit & Punyadeera, 2013). The concentration and purity of RNA were measured by spectrophotometry. RNA samples were also separated by electrophoresis on a 1% agarose gel to assess their integrity.

The RNA concentration was low in all samples extracted with the kit, with a maximum of 9.2 ng/ µl (not shown). The A260/A280 ratio in the fresh and the frozen samples was around 1.6-1.7 and 2.2, respectively. The A260/A230 ratio was very low, close to 0, in all samples. In the agarose gel, no band was observed in all the samples.

The RNA concentration was also low in all samples extracted with TRIzol except in one of the fresh saliva (70.8 ng/µL), frozen saliva (58.4 ng/µL) and frozen mouthwash (76.4 ng/µL) samples. The A260/A280 ratio in all samples was between 1-1.6, except in one of the frozen mouthwash (1.7) and fresh saliva (2.6) samples. The A260/A230 ratio was low, in almost all samples was close to 0, in one of the frozen saliva samples was 0.9 and in one of the frozen mouthwash samples was 1.7. These results are presented in table 3. The sample with the best results was the frozen mouthwash.

Table 3 - Results from quantification of the RNA extracted from saliva using TRIzol. Saliva was collected using sublingual cotton rolls and the frozen samples were stored at -80ºC for 24 hours before RNA extraction. **S:** fresh saliva; **FS:** frozen saliva; **MW:** fresh mouthwash (pellet); **FMW:** frozen mouthwash (pellet); *****: below the detection threshold of the equipment.

	TRIzol		
Sample	**ng/µl**	**A260/A280**	**A260/A230**
S	*	2,579	*
	70,8	1,066	0,062
FS	*	1,472	0,872
	58,4	1,09	0,046
MS	10,2	1,477	0,397
	10,5	1,56	0,034
FMS	76,4	1,705	1,705
	9,3	1,557	0,017

4.2. DNA

DNA extraction was performed with the NZY Tissue gDNA Isolation Kit (MB13502, NZYTech). Fresh samples, stored samples at -80ºC for 24 hours (A) and stored samples at 4ºC for 48 hours (B) before DNA extraction were tested. Fresh and frozen saliva (A) samples were collected with sublingual cotton rolls and saliva (B) samples were collected by drooling. The concentration, purity and integrity of the extracted DNA were determined using spectrophotometry and electrophoresis. Some samples were quantified twice with different dilution factors (DF); DF = 20 (1) and DF = 10 (2), and the results were similar (table 4).

The samples with the best concentration and A260/A280 ratio values were the frozen mouthwash (A) and the samples that were stored at 4ºC for 48 hours (B) (table 4). The remaining samples did not have satisfactory concentration values and A260/A280 ratios. None of the samples had reasonable values of the A260/A230 ratio. These results are shown in table 4. Electrophoretic analysis of the extracted DNA showed detectable levels of high molecular weight genomic DNA in the frozen saliva, frozen mouthwash (A), swab brushed 3 times, swab brushed 3 times (using a needle in the extraction process) and in the saliva (B), mouthwash (B) and buccal cytobrush (B) samples (figure 2). However, a smear was also observed in these samples, suggesting that DNA might be degraded. In the other samples, no band was observed. Thus, the samples with the best results were the frozen mouthwash stored at -80ºC for 24 hours and the saliva, mouthwash and buccal cytobrush stored at 4ºC for 48 hours.

Table 4 - Results from quantification of the DNA extracted from saliva using the NZY Tissue gDNA Isolation Kit. **S:** fresh saliva; **FS:** frozen saliva; **MW:** fresh mouthwash; **FMW:** frozen mouthwash; **SW:** swab (brushed 3 times); **SWN:** swab (brushed 3 times), using a needle in the extraction process; **SW30:** swab brushed 30 times; **SW30N:** swab brushed 30 times, using a needle in the extraction process; **S:** saliva; **MW:** mouthwash; **BC:** buccal cytobrush; **(A):** samples stored at -80ºC for 24 hours; **(B):** samples stored at 4ºC for 48 hours; **(1):** samples quantified with a dilution factor of 20; **(2):** samples quantified with a dilution factor of 10; *****: below the detection threshold of the equipment.

NZY Tissue gDNA Isolation Kit			
Sample	**ng/µl**	**A260/A280**	**A260/A230**
S (1)	4,3	0,98	0,77
FS (A) (1)	5,9	0,74	0,58
MW (1)	18,8	1,98	0,82
FMW (A) (1)	42,6	1,74	1,53
SW (1)	15,9	2,21	1,05
SWN (1)	11,9	2,59	0,70
SW30 (1)	*	1,52	*
SW30N (1)	*	3,50	*
S (B) (1)	49	1,88	0,39
S (B) (2)	34	2	0,52
MW (B) (1)	59	1,90	0,46
MW (B) (2)	58	1,90	0,75
BC (B) (1)	69	1,97	0,52
BC (B) (2)	56	1,90	0,75

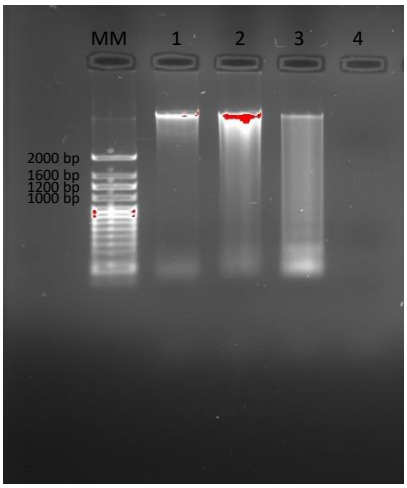

Figure 2 - Agarose gel of the DNA samples extracted from saliva using the NZY Tissue gDNA Isolation Kit. **MM:** Molecular weight marker; **1:** saliva (B); **2:** mouthwash (B); **3:** buccal cytobrush (B); **4:** swab brushed 6 times; **(B):** samples stored at 4ºC for 48 hours. Note: Sample 4 was not quantified because no band was observed in the agarose gel.

The DNA samples from healthy blood donors over 50 years-old (HRC2-E11, HRC3-A10, B1, B2, B3, C1 and C2) were diluted in water and then, quantified before PCR (table 5). In general, all samples have acceptable values of DNA concentration and A260/A280 ratio.

Table 5 - Quantification of DNA from healthy blood donors.

DNA	ng/µl	A260/A280	A260/A230
2-A9 1:10	57,5	1,885	0,646
2-E11 1:100	24,5	1,678	0,521
2-E11 1:10	91,5	1,679	0,691
3-A10 1:10	13,8	1,752	1,375
3-B1 1:10	88,0	1,796	0,680
3-B2 1:10	59,0	1,735	0,656
3-B3 1:10	104,0	1,778	0,748
3-C2 1:10	101,5	1,692	0,698
3-C3 1:10	106,5	1,972	0,786

4.3. PCR

4.3.1. *NAMPT*

The DNA from healthy blood donors was amplified with primers specific for exon 7 of human *NAMPT*. The DNA samples extracted from saliva with the best results (fresh mouthwash, frozen mouthwash stored at -80ºC for 24 hours and the saliva, mouthwash and buccal cytobrush stored at 4ºC for 48 hours) were also used, to test if the low quality and quantity DNA was suitable for amplification and to verify if human DNA was extracted, since saliva is expected to have high amounts of bacterial DNA.

Several conditions were tested. Using a final primer concentration of 2 µM and 30 seconds of annealing temperature, the amplification was successful (figure 3). In all samples, a band of the expected fragment size (362 bp) was visualized in agarose gels.

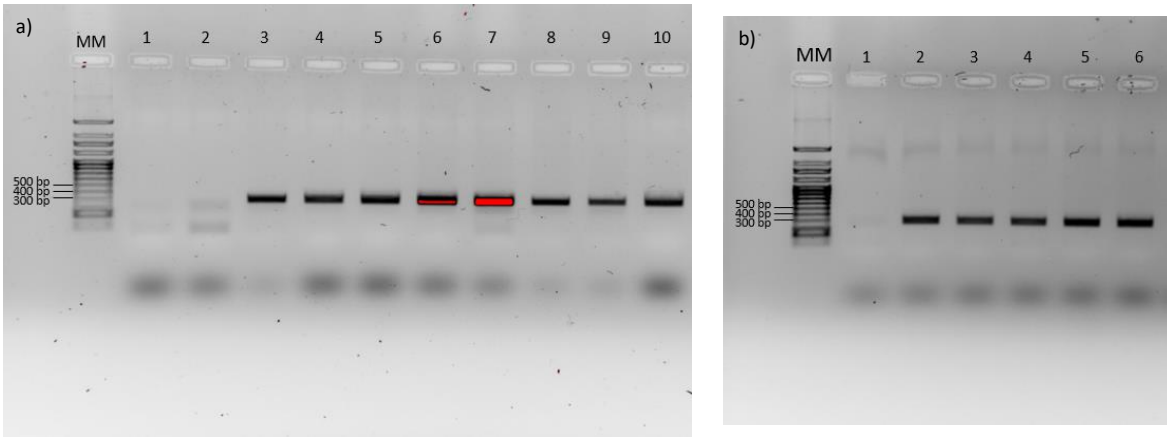

Figure 3 - Agarose gel of the PCR products amplified using human primers for *NAMPT* exon 7. **MM:** molecular weight marker. **a) – 1 and 2:** blank; **3:** 3-A10; **4:** 2-E11; **5:** fresh mouthwash; **6:** frozen mouthwash (-80ºC for 24 hours); **7:** saliva (4ºC for 48 hours); **8:** mouthwash (4ºC for 48 hours); **9:** buccal cytobrush (4ºC for 48 hours); **10:** swab (brushed 3 times). **b) – 1:** blank; **2:** 3-B1; **3:** 3-B2; **4:** 3-B3; **5:** 3-C1; **6:** 3-C2.

4.3.2. *NAPRT*

The same samples that were tested with *NAMPT* primers, were also amplified with primers for exon 4 of human *NAPRT*. To optimize the PCR, different conditions were tested, such as annealing temperature (T_a), primer concentration and Master Mix volume.

As for the Master Mix volume, with 10 µL the band intensity was better (figure 4 - well 3) than with 6.25 µL (figure 4 - well 2). The primers concentration was suspected to be insufficient, so a higher concentration was tested, however, unspecific products were observed, thus several annealing temperatures were tested to try to increase the reaction's specificity.

The best results were observed using 10 µl MasterMix and primers at 2 µM (1 µL), and an annealing temperature of 62ºC for 30 seconds, a band at the expected fragment size (404 bp) was visualized. However, a band in the range of 100 bp was also observed (figure 4b).

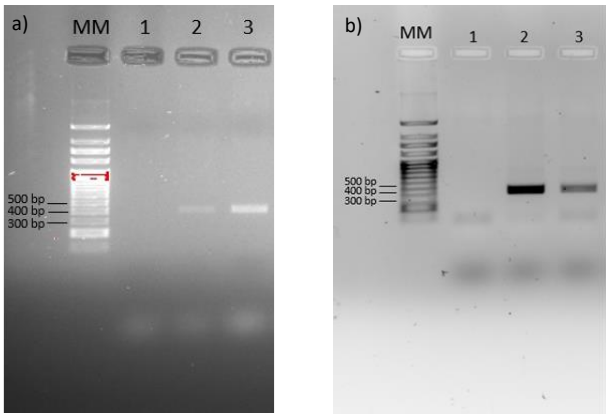

Figure 4 - Agarose gel of the PCR products amplified using human primers for *NAPRT* exon 4 with different PCR conditions. **MM:** molecular weight marker; **1:** blank. **a) - 2:** 6,25 µl MasterMix, primers at 0.2 µM (2 µL), T_a = 60ºC (1 minute), 3-A10; **3:** 10 µl MasterMix, primers at 0.2 µM (2 µL), T_a = 60ºC (1 minute), 3-A10. **b)** T_a = 62ºC (30 seconds); **2:** frozen mouthwash (-80ºC for 24 hours); **3:** 3-B1.

4.4. Bioinformatic analysis

4.4.1. Mutations in AML and ALL

In both types of pediatric leukemia, the most frequently mutated gene is *NRAS* (NRAS proto-oncogene), but the overall gene mutation frequency is not very high (table 6). AML and ALL have 4 commonly mutated genes: *NRAS*, *KRAS* (KRAS proto-oncogene), *FLT3* (fms related receptor tyrosine kinase 3) and *PTPN11* (protein tyrosine phosphatase non-receptor type 11). These genes are involved in growth signaling pathways (Bejar, 2018). *NRAS*, *KRAS* and *PTPN11*, as well as *CCND2*, participate in the Ras pathway and are frequently mutated in juvenile myelomonocytic leukemia (JMML) (Gill *et al.*, 2016; Locatelli *et al.*, 2018; Sakashita *et al.*, 2016; Stieglitz *et al.*, 2016) and in ALL (Tartaglia *et al.*, 2004; Vicente *et al.*, 2015). In fact, somatic *PTPN11* mutations are the most frequent lesion in JMML and they also occur in adult AML and in pediatric AML and ALL, and are associated with a worse prognosis (Alfayez *et al.*, 2020; Tartaglia *et al.*, 2004). *FLT3*, as well as *KIT* (c-Kit or CD117) and *JAK2*, regulate the tyrosine kinase receptor signaling (Gill *et al.*, 2016). These activated growth factor signaling genes are essential in hematopoiesis

and mutations in these genes are associated with AML (Babaei *et al.*, 2016; Duployez *et al.*, 2016; Gill *et al.*, 2016; Larrosa-Garcia & Baer, 2017; Patnaik, 2018).

TET2 (tet methylcytosine dioxygenase 2) and *IDH2* (isocitrate dehydrogenase (NADP(+) 2, which encodes a $NADP^+$-dependent isocitrate dehydrogenase) regulate DNA methylation (Gill *et al.*, 2016; O'Brien *et al.*, 2014). Mutations in these two genes are mutually exclusive in AML, which suggests that they might play a similar role (Gill *et al.*, 2016; O'Brien *et al.*, 2014), and have been found to persist from diagnosis to relapse (O'Brien *et al.*, 2014). However, *TET2* has been identified to be mutated along with other genes such as *FLT3, KRAS, KIT* and *JAK2* (O'Brien *et al.*, 2014; Weissmann *et al.*, 2012).

GATA2 (GATA binding protein 2), *TP53* (tumor protein p53) and *WT1* (WT1 transcription factor) are genes involved in transcription regulation (Gill *et al.*, 2016; Ullmark et al., 2017). *TP53* and *WT1*, both tumor suppressor genes, are frequently mutated in AML (Bejar, 2018; Shin *et al.*, 2016). With a lower incidence, *TP53* mutations have also been identified in pediatric and adult ALL (Comeaux & Mullighan, 2017; Demir *et al.*, 2020; Salmoiraghi *et al.*, 2018; Shin *et al.*, 2016). Additional aberrations with SIRT1 overexpression and subsequent TP53 deacetylation can affect the TP53 pathway (Panuzzo *et al.*, 2020). *WT1* mutations are more common in younger patients and are associated with worse prognosis (reviewed in Panuzzo *et al.*, 2020). Mutations in *GATA2* gene (which encodes for a transcription factor critical in hematopoietic stem cell proliferation and survival) were discovered to be involved in AML (Gill *et al.*, 2016; reviewed in Panuzzo *et al.*, 2020) and other myeloid malignancies (Stieglitz *et al.*, 2016; Wlodarski *et al.*, 2018).

NSD2 (nuclear receptor binding SET domain protein 2), an epigenetic regulator, has a role in hematopoiesis (Swaroop *et al.*, 2019) and it was found to be mutated in pediatric ALL (Jaffe *et al.*, 2013). Mutations in *CREBBP* (CREB binding protein), other epigenetic regulator, are very common in high hyperdiploidy and pediatric ALL relapse cases (Ding *et al.*, 2017; Janczar *et al.*, 2017; Zhang *et al.*, 2020) and co-occur with *KRAS* mutations (Malinowska-Ozdowy *et al.*, 2015; Zhang *et al.*, 2020). The NOTCH pathway was found to be affected in adult and pediatric T-cell acute lymphoblastic leukemia (T-ALL) patients, including mutations in *NOTCH2* (Doerrenber *et al.*, 2017; Neumann *et al.*, 2015).

Table 6 – The ten most mutated genes and respective frequency in Pediatric Acute Myeloid Leukemia (AML, left) and Pediatric Acute Lymphoid Leukemia (ALL, right) (TARGET datasets).

Most mutated genes in AML		**Most mutated genes in ALL**	
Gene	**Frequency (%)**	**Gene**	**Frequency (%)**
NRAS	14.7	NRAS	10.7
KIT	10.0	KRAS	5.3
FLT3	6.7	CREBBP	4.0
KRAS	6.0	PTPN11	4.0
PTPN11	6.0	TP53	4.0
WT1	3.3	FLT3	3.3
TET2	3.3	JAK2	3.3
CCND2	2.7	NSD2	3.3
GATA2	2.7	NOTCH2	2.7
IDH2	2.7	HLA-C	2.0

4.4.2. CNAs in AML and ALL

ALL has a higher frequency of CNAs than AML (table 7), which in both pediatric leukemias is deep deletion (deep loss, possibly a homozygous deletion, according to cBioPortal). Transcription factors and long non-coding RNAs (lncRNAs) that may act as transcriptional regulators for numerous genes, including some genes involved in cancer progression, appear frequently altered. Additionally, in AML there are several HLA (Human Leukocyte Antigen) genes, whereas in ALL, several genes involved in cell cycle regulation have these alterations. Of note, *ELF1* (E74 like ETS transcription factor 1) deletions are more prevalent in pediatric AML than adult AML (Bolouri *et al.*, 2018).

Table 7 - The genes with more CNAs and respective cytoband and frequency in AML (at the left) and ALL (at the right) TARGET datasets.

Most genes with CNAs in AML			Most genes with CNAs in ALL		
Gene	**Cytoband**	**Frequency (%)**	**Gene**	**Cytoband**	**Frequency (%)**
ELF1	13q14.11	15.8	ADAM6	14q32.33	59.6
LINC00102	Xp22.33 and Yp11.2	15.4	LINC00226	14q32.33	46.5
ZEB2	2q22.3	15.0	FAM30A	14q32.33	44.5
MBNL1	3q25.1-q25.2	14.6	LINC00221	14q32.33	40.2
ZEB2-AS1	2q22.3	14.6	CDKN2A	9p21.3	36.1
HLA-DRB6	6p21.32	13.8	CDKN2B	9p21.3	33.6
TMEM14EP	3q25.2	13.8	CDKN2B-AS1	9p21.3	30.9
HLA-DRB5	6p21.32	13.3	MTAP	9p21.3	26.6
HLA-DRB1	6p21.32	12.9	PRSS1	7q34	25.3
NEAT1	11q13.1	12.5	MTRNR2L6	7q34	22.9

4.4.3. Methylation in AML and ALL

In AML, of the 11719 genes analyzed, 23.4% of them are hypermethylated and 65.0% are hypomethylated (table 8). In ALL, of the 14840 genes analyzed, 25.0% of them are hypermethylated and 14.4% are hypomethylated (table 8).

Table 8 - The most (left) and least (right) methylated genes and respective median of the beta values in AML (above) and ALL (below) TARGET datasets.

Most methylated genes				Least methylated genes			
AML		**ALL**		**AML**		**ALL**	
Gene	**Beta value**	**Gene**	**Beta Value**	**Gene**	**Beta value**	**Gene**	**Beta value**
PAQR9	0,98	PTGES	0,97	DAZAP2	0,02	SEC22B	0,02
MYO9B	0,97	AKT1S1	0,97	CLASP2	0,02	OR2A4	0,02
LYPD4	0,97	LMX1B	0,97	C10orf137	0,02	H2AFB3	0,02
NR5A1	0,97	EVI2A	0,97	PHF15	0,02	DFFB	0,02
OR10H1	0,97	SYNGR3	0,96	TPM2	0,02	KIAA0562	0,02

C1orf177	0,97	ABHD2	0,96	SSBP2	0,01	ARFIP2	0,01
TULP2	0,96	PGA5	0,96	NUBP2	0,01	ETV3	0,01
A1BG	0,96	EPHA10	0,96	USP14	0,01	PIAS2	0,01
XAGE2	0,96	LGALS1	0,96	ECE1	0,01	TTTY13	0,01
HOXB1	0,96	ARL4A	0,96	ZFAND2B	0,01	SUDS3	0,01

To understand what biological processes are altered with methylation, a statistical overrepresentation test with the PANTHER GO-Slim Biological Process was performed. The results showed that the hypermethylated genes in AML were mainly related to blood cells differentiation and proliferation and immune response, e.g., hematopoiesis, leukocyte proliferation, lymphocyte differentiation, circulatory system process, immune system development, response to tumor necrosis factor, cell activation involved in immune response and cellular response to chemokine (appendix 1). The results for the hypermethylated genes in ALL were mainly related to development, morphogenesis and differentiation, e.g., embryo development, regulation of cell development, cell morphogenesis involved in differentiation, regulation of cell differentiation and blood circulation (appendix 2).

For the hypomethylated genes, three biological processes had a significant fold enrichment in AML: peroxisome organization, regulation of MAP kinase activity and extrinsic apoptotic signaling pathway. In ALL, DNA repair was the only biologic process with a significant fold enrichment.

4.4.4. Gene expression in AML and ALL

For both leukemias, the most expressed genes were mitochondrial and ribosomal genes, which were not further considered in the analyses. AML and ALL share 7 highly expressed genes: *FTL* (ferritin light chain), *HBB* (hemoglobin subunit beta), *ACTB* (actin beta), *TPT1*, *TMSB10* (thymosin beta 10), *GAPDH* (glyceraldehyde-3-phosphate dehydrogenase) and *CD74* (table 9). *FTL*, frequently overexpressed in AML, encodes the light subunit of ferritin, which is a growth factor for AML cells (Bertoli *et al.*, 2019; Kikyo *et al.*, 1995). *ACTB* encodes beta-actin, a protein with functions in cell motility, division and intercellular signaling. ACTB upregulation is correlated with acute leukemia and associated drug resistance (reviewed in Guo *et al.*, 2013). *TPT1* encodes a protein involved in cellular growth and proliferation that is a key regulator of p53, which in turn represses *TPT1*

transcription. TPT1 also participated in the process of tumor reversion, as low levels of TPT1 are associated with better survival rates than high levels of TPT1 (Amson *et al.*, 2011). *TMSB10* encodes a member of the beta-thymosin family that are actin-binding proteins with physiological roles in inflammatory regulation, tissue development and regeneration (Pan *et al.*, 2020; Zhang *et al.*, 2017). Beta-thymosin is involved in carcinogenesis and tumor progression and TMSB10 is commonly upregulated in many cancers (Pan *et al.*, 2020; Xin Zhang *et al.*, 2017). GAPDH is a metabolic enzyme that also functions in DNA replication and repair, carcinogenesis and cell death (Zhang *et al.*, 2015). A higher gene expression and enzymatic activity of GAPDH is associated with cell proliferation and tumorigenesis (Nicholls *et al.*, 2012). *GAPDH* was found to be upregulated in human precursor B-cell ALL (B-ALL) cells (Martín-Lorenzo *et al.*, 2018) and other cancers, often correlated with reduced survival (Zhang *et al.*, 2015). *CD74* is involved in antigen presentation, and is also a cell surface receptor for macrophage migration inhibitory factor (MIF) (Attar *et al.*, 2013; Su *et al.*, 2016). CD74 expression is associated with various types of cancer (reviewed in Borghese & Clanchy, 2011) and, in AML cells, CD74 is expressed at high levels (Galen *et al.*, 2020; Ruvolo *et al.*, 2019).

Table 9 - The most expressed genes and the respective logarithm of median RPKM in AML (at the left) and ALL (at the right) TARGET datasets.

Most expressed genes in AML		**Most expressed genes in ALL**	
Gene	**Log_2 RPKM**	**Gene**	**Log_2 RPKM**
FTL	11,13	HBB	11,47
HBB	11,03	TMSB10	11,01
ACTB	10,86	CD74	10,98
TPT1	10,56	TPT1	10,88
TMSB10	10,53	HLA-DRA	10,59
GAPDH	10,40	FTL	10,16
CD74	10,29	ACTB	10,13
ACTG1	10,21	LAPTM5	10,10
SRGN	10,08	GAPDH	10,09
LYZ	10,04	HBA2	10,06

4.4.5. Specific analysis of genetic alterations in *NAPRT* and *NAMPT*

The results for *NAPRT* and *NAMPT* expression and *NAPRT* methylation in AML, ALL and HNSC are shown in table 10. *NAPRT* is hypermethylated in AML and methylated in ALL and HNSC. Regarding expression, *NAPRT* and *NAMPT* expression are moderate in both leukemias and are high in HSNC. In ALL, there is no correlation between *NAPRT* methylation and expression (Pearson = -0.05; p-value = 0.620) (appendix 3) and in HSNC, the correlation is negatively moderate (Pearson = -0.49; p-value = $4.47e^{-18}$) (appendix 4).

Table 10 - Maximum, minimum and median values of *NAPRT* and *NAMPT* expression (RPKM and TPM values) and *NAPRT* methylation (beta values) in AML, ALL and HNSC. Data expression in HNSC was provided by UALCAN.

AML	**Median**	**Minimum**	**Maximum**
***NAPRT* methylation**	0,70	0	0,91
***NAPRT* expression (Log_2 RPKM)**	4,11	2,21	5,22
***NAMPT* expression (Log_2 RPKM)**	4,07	1,91	6,96
ALL			
***NAPRT* methylation**	0,56	0,20	0,96
***NAPRT* expression (Log_2 RPKM)**	2,62	-1,17	4,66
***NAMPT* expression (Log_2 RPKM)**	2,06	-0,89	6,45
HNSC			
***NAPRT* methylation**	0,46	0,19	0,86
***NAPRT* expression (TPM)**	85,28	1,19	230,05
***NAMPT* expression (TPM)**	40,04	3,30	126,14

No *NAMPT* mutations were found in the studied datasets. *NAPRT* analysis revealed one missense mutation in AML and four missense and one splice mutations in HNSC (table 11).

Table 11- *NAPRT* mutations with respective protein change and allele frequency in AML and HNSC, provided by cBioPortal.

Dataset	Protein change	Mutation type	Allele frequency
AML	R332C	Missense	0.75
HNSC	R336Q	Missense	0.30
	P228L	Missense	0.08
	G377S	Missense	0.36
	R203Q	Missense	0.22
	X294_splice	Splice	0.17

In general, *NAPRT* and *NAMPT* CNAs frequency in AML, ALL and HNSC is low (figure 5). In HNSC, the predominant alteration is amplification of both *NAMPT* (frequency of 1,34%) and *NAPRT* (frequency of 7,65%). In AML, the only CNA type is a deep deletion in *NAMPT* (frequency of 2,03%). In ALL, for *NAPRT* there is no CNAs and for *NAMPT*, deep deletion and amplification have very low frequencies, 0.24% and 0,12%, respectively. Concerning the correlation between expression and CNAs, in ALL there seems to be no correlation for *NAMPT* (appendix 5). In HNSC, median *NAPRT* expression increases with amplification, and there is also a tendency to expression increase (figure 6). However, these increases are probably not significant. There is a clear tendency to an increase of *NAMPT* expression with amplification (figure 7). However, the number of samples is low.

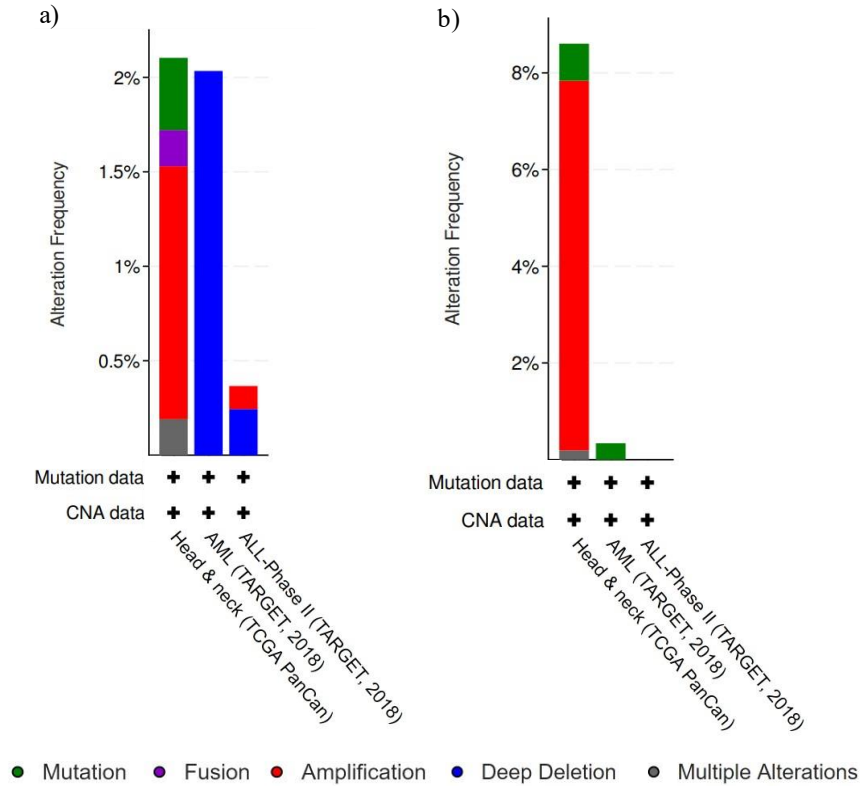

Figure 5 - *NAMPT* (a) and *NAPRT* (b) genomic alterations frequency in the three studied datasets of AML, ALL and HNSC, as provided by cBioPortal.

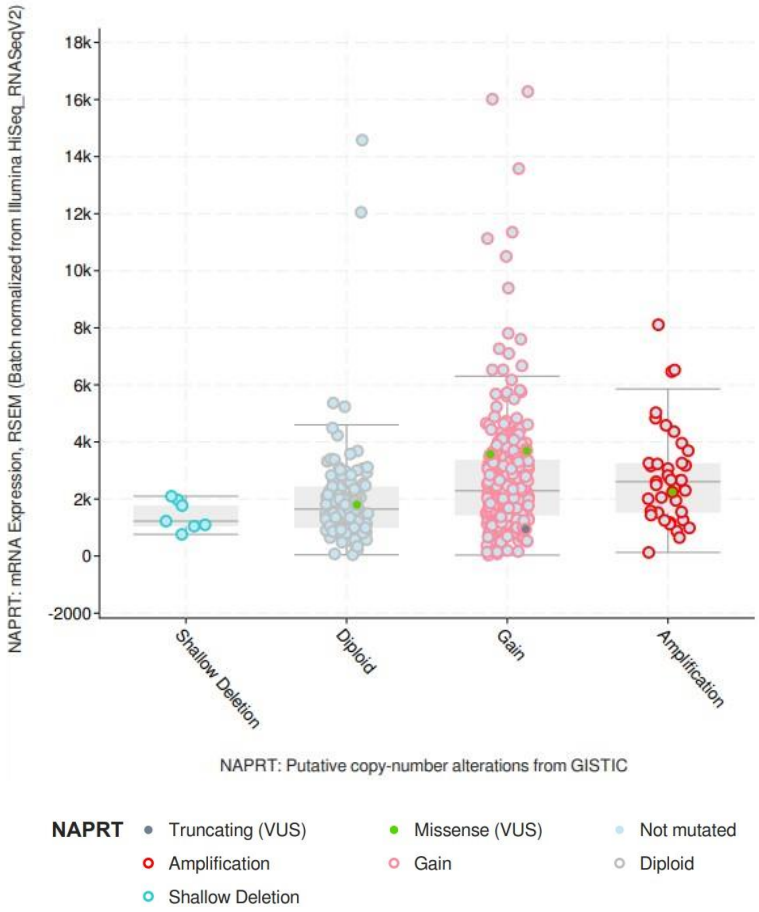

Figure 6 - Plot with *NAPRT* CNAs (horizontal axis) and expression (vertical axis) in HNSC, provided by cBioPortal.

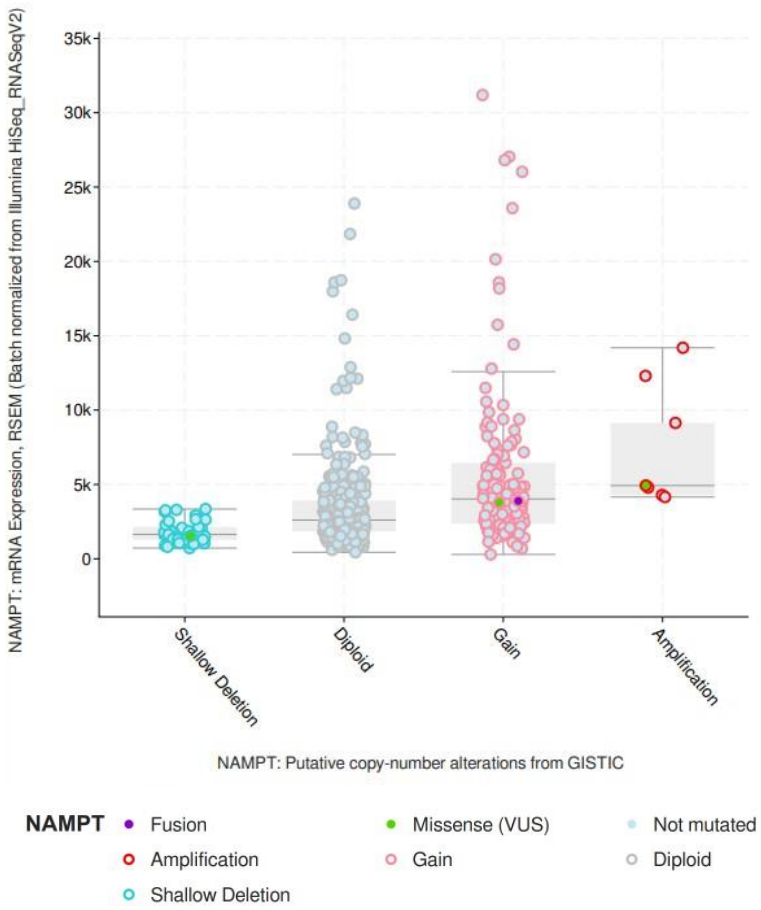

Figure 7 - Plot with *NAMPT* CNAs (horizontal axis) and expression (vertical axis) in HNSC, provided by cBioPortal.

4.4.5.1. *NAPRT* eQTL

In the PancanQTL database, the analysis revealed 101 and 21 SNPs that alter *NAPRT* expression in HNSC and LAML, respectively. Regarding HNSC, 51% of the eQTL have a negative effect on *NAPRT* expression. While in AML, 20 of the 21 eQTL have a positive effect on *NAPRT* expression.

None of the 101 eQTL that alter *NAPRT* expression in HNSC is located in the *NAPRT* gene sequence but in intergenic regions or neighboring genes, such as *EEF1D* (eukaryotic translation elongation factor 1 delta; 51% of the eQTL), *ZC3H3*, *ZNF623* (zinc finger protein 623) and *TIGD5* (tigger transposable element derived 5) (figure 8). Of the 101 SNPs, 18 of them alter the expression of other genes in HNSC (17 alter *ZNF707*, zinc finger protein 707, and 1 alters *GSDMD*, gasdermin D). Their expression is altered in the opposite direction of

NAPRT's gene expression. In other tumors, genes located within the *NAPRT* cytoband, such as *BREA2* (LINC02878, long intergenic non-protein coding RNA 2878) and *C8orf73* (MROH6, maestro heat like repeat family member 6), are also altered by most of these variants. In testicular germ cell tumors (TGCT), *BREA2* expression is altered in the same direction as *NAPRT* in HNSC. *TIGD5* expression is altered in the same way as *NAPRT* and *ZNG707* expression is altered in the opposite way. In all cases in which the eQTL that alter *NAPRT* expression also have an impact on *TSTA3* (*GFUS*, GDP-L-fucose synthase), its expression decreases. Of the 101 SNPs, 15 of them alter *NAPRT* exclusively (11 have an impact only in Lower Grade Glioma, besides HNSC) and are located predominantly within the *ZC3H3* (zinc finger CCCH-type containing 3) gene (appendix 6). Of the 101 eQTL, three alter the *NAPRT* expression only in HSNC and are located in intergenic regions (rs7822731, rs7822746 and rs378433).

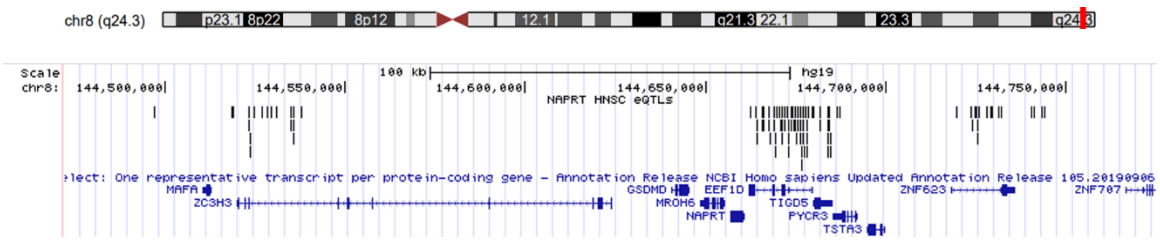

Figure 8 - Localization on the human genome (GRCh37/hg19 assembly) of *NAPRT* eQTL in HNSC. Image produced using UCSC Genome Browser.

Similarly, in LAML, none of the SNPs is located in the *NAPRT* gene sequence, but in neighboring genes (*EEF1D* and *TIGD5*) and in an intergenic region (figure 9). In other tumors, genes located within *NAPRT* cytoband are also altered, such as *BREA2*, *GSDMD* and *C8orf73*. *TIGD5* and *BREA2* expression is altered in the same way as *NAPRT*. In all cases in which the eQTL that alter *NAPRT* expression also have an impact on *BREA2*, its expression increases.

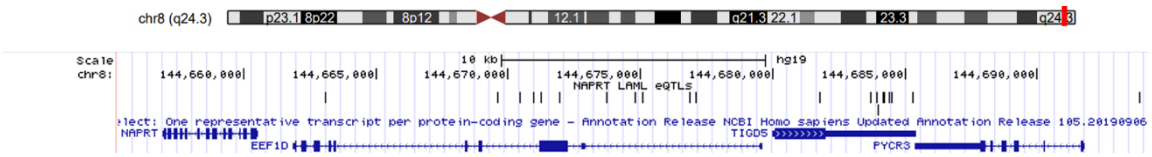

Figure 9 - Localization on the human genome (GRCh37/hg19 assembly) of *NAPRT* eQTL in LAML. Image produced using UCSC Genome Browser.

None of the 122 SNPs (101 eQTL in HNSC and 21 in LAML) were reported in the ClinVar database.

From the 101 *NAPRT* eQTL in HNSC, 4 of them were not present in the GTEx database (rs148839797, rs72024244, rs11778687 and rs113818459), which comprises non-pathological samples. The 3 SNPs that alter *NAPRT* expression only in HNSC (rs7822731, rs7822746 and rs378433), were not present in the only tissue that can be associated with HNSC in GTEx, the minor salivary gland. Of the 15 eQTL that only alter *NAPRT* expression (appendix 6), the 11 that have an impact on HNSC and LGG (lower grade glioma) were not present in the representative tissues in GTEx. The remaining 4 eQTL alter *NAPRT* expression in several tumors. In the corresponding normal tissues of kidney renal papillary cell carcinoma (KIRP), kidney renal clear cell carcinoma (KIRC), TGCT and cervical squamous cell carcinoma and endocervical adenocarcinoma (CESC), these SNPs did not appear in the database.

All 21 *NAPRT* eQTL in LAML were present in GTEx. Besides LAML, these SNPs alter *NAPRT* expression in other tumors and, similar to the *NAPRT* eQTL in HNSC, some of them were not present in the tumor-corresponding normal tissues of KIRP, KIRC, CESC and bladder urothelial carcinoma (BLCA) in GTEx.

It is noteworthy to mention that the absolute values of *NAPRT* eQTL effect size (|β|) in both HNSC and LAML, in general, are not very high (appendix 7 and 8, respectively). In HNSC, the highest absolute beta value is |0,8|, the lowest is |-0,18| and the median is 0,35. In LAML (appendix 8), the highest absolute beta value is |0,75|, the lowest is |0,49| and the median is 0,57.

Concerning allelic frequencies, in LAML, all eQTL were analyzed but in HNSC, a cut-off was used to select the eQTL. The higher beta value for *NAPRT* in all tumors in PancanQTL is 1.16, so 2/3 of that value was subtracted to 1.16 and used as cut-off (beta value = 0.39), to have a considerable number of SNPs. The eQTL that alter only *NAPRT*

expression (appendix 6), the ones that alter *NAPRT* expression only in HNSC (rs7822731, rs7822746 and rs378433) and the ones that were not present on GTEx (rs148839797, rs72024244, rs11778687 and rs113818459) were also included in this analysis. In the majority of the *NAPRT* eQTL in HNSC (appendix 9) and LAML (appendix 10), in most cases, the alternative allele is more frequent than the reference allele in all populations with exception of the African population. The most similar populations are the European and American populations and the East and South Asian populations.

In the heatmap is it clear that the HNSC pattern is very different from the other tumors (figure 10). However, KIRC and KIRP are somewhat similar to HNSC, in which *NAPRT* expression essentially decreases. In the other tumors, these eQTL in most cases increase *NAPRT* expression.

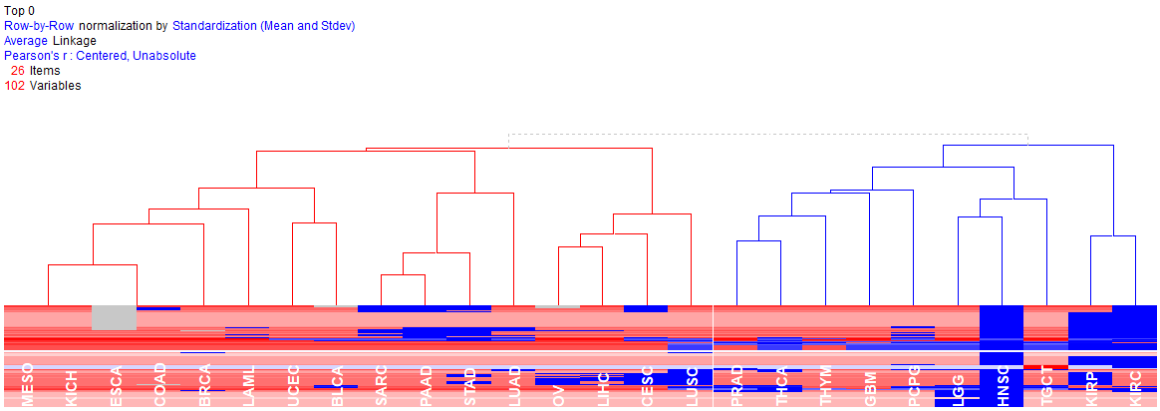

Figure 10 – Heatmap of the eQTL that alter *NAPRT* expression in HNSC and also other tumors (represented). MESO: mesothelioma; KICH: kidney chromophobe; ESCA: esophageal carcinoma; COAD: colon adenocarcinoma; BRCA: breast invasive carcinoma; LAML: acute myeloid leukemia; UCEC: uterine corpus endometrial carcinoma; BLCA: bladder urothelial carcinoma; SARC: sarcoma; PAAD: pancreatic adenocarcinoma; STAD: stomach adenocarcinoma; LUAD: lung adenocarcinoma; OV: ovarian serous cystadenocarcinoma; LIHC: liver hepatocellular carcinoma; CESC: cervical squamous cell carcinoma and endocervical adenocarcinoma; LUSC: lung squamous cell carcinoma; PRAD: prostate adenocarcinoma; THCA: thyroid carcinoma; THYM: thymoma; GBM: glioblastoma multiforme; PCPG: pheochromocytoma and paraganglioma; LGG: lower grade glioma; HNSC: head and neck squamous cell carcinoma; TCGT: testicular germ cell tumors; KIRP: kidney renal papillary cell carcinoma; KIRC: kidney renal clear cell carcinoma.

5. DISCUSSION

Biomarkers with a high degree of sensitivity and specificity, combined with noninvasive and inexpensive modes of sample collection are necessary to improve cancer screening and diagnosis (Rapado-González *et al.*, 2020; Wang *et al.*, 2017; Yoshizawa *et al.*, 2013). Saliva is a body fluid that is potentially rich in diagnostic indicators for both oral and systemic tumors (Rapado-González *et al.*, 2020; Yoshizawa *et al.*, 2013). Thus, the identification and characterization of saliva-based biomarkers could establish saliva as a diagnostic biofluid (Yoshizawa *et al.*, 2013).

Cancer cells require increased levels of NAD^+ to support rapid cell proliferation and to face constant NAD^+ depletion by NAD^+-consuming enzymes, which are involved in DNA repair, cell signaling or prevention of apoptosis (Audrito *et al.*, 2020; Piacente *et al.*, 2017; Yaku *et al.*, 2018). *NAMPT* and *NAPRT* are important enzymes in NAD metabolism, both in normal and in pathological conditions (Duarte-Pereira *et al.*, 2014). NAMPT expression is frequently increased in several types of malignant tumors (reviewed in Demarest *et al.*, 2019). On the other hand, several types of cancer cells lack NAPRT (Duarte-Pereira *et al.*, 2016). In fact, the *NAPRT* promoter region is frequently observed to be hypermethylated in certain types of cancers (Duarte-Pereira *et al.*, 2016; Shames *et al.*, 2013; Yaku *et al.*, 2018). In this study, genetic alterations in *NAPRT* and *NAMPT* were the main target of the analysis.

5.1. DNA and RNA from saliva

The first part of this study was the optimization of RNA and DNA extraction from saliva samples. With the RNeasy® Micro Kit, the RNA concentration was low in all samples and the fresh saliva sample was the one with the highest concentration.

With the TRIzol protocol, the RNA concentration was low in all samples except in one of the fresh saliva, frozen saliva and mouthwash samples. The A260/A280 ratio in all samples was not between the acceptable values for RNA (1.8-2.2), this might be due to contamination of the samples with proteins or other contaminants, like guanidine thiocyanate (Ahlfen & Schlumpberger, 2010; Luebbehusen, 2004), which is present in the lysis reagent of the kit and in TRIzol. As no band was observed in the agarose gels, RNA was not considered adequate for downstream applications. However, the TRIzol protocol did show better results than the RNeasy® Micro Kit in terms of RNA concentration.

The TRIzol protocol was adapted from Pandit *et al.* (Pandit *et al.*, 2013). They developed an in-house method that uses the QIAzol® lysis reagent (Qiagen) to isolate RNA from both the cellular pellet and the cell-free salivary supernatant and compared it with a commercial kit, the NucleoSpin® RNA II kit (Macherey-Nagel). The QIAzol method produced a high yield of total RNA (with A260/A280 ratios between 1.6 and 1.9) from 200 µL of saliva after DNase treatment. With the QIAzol method, they were also able to isolate RNA from archived saliva samples that had been stored without RNase inhibitors at -80°C for more than 2 years (Pandit *et al.*, 2013).

Recently, Gandhi *et al.* compared the yields and quality of RNA extracted from unstimulated whole saliva by their modified TRIzol protocol with that of the RNeasy® Protect Saliva Micro Kit (Gandhi *et al.*, 2020). They did essentially two alterations to the TRIzol protocol: the chloroform step was performed 3 times and the samples were washed twice with 80% of ethanol. A higher RNA concentration and integrity were obtained with the modified TRIzol protocol in comparison with the kit. This might be due to extra chloroform steps in the modified TRIzol protocol, which might have eliminated any potential contaminants (Gandhi *et al.*, 2020).

Anaya and Causado also compared a QIAzol protocol with the RNeasy® Protect Saliva Mini Kit (Qiagen) (Anaya & Causado, 2017). However, they concluded that the method using RNeasy® Protect Saliva Mini Kit showed better RNA concentration and yield characteristics when compared to the method using QIAzol®. This RNeasy® Protect Saliva Mini Kit is similar to the one used in this work, with the difference that at the beginning of the protocol a saliva protection reagent was added. This might explain why they observed higher values of RNA concentration than us. In fact, Fábryová & Celec mentioned that salivary ribonucleases are still active after sampling and therefore need to be inhibited before processing the samples, which can be achieved by adding RNase or commercially available stabilization solutions, like the RNAprotect® Saliva Reagent included in RNeasy® Protect Saliva Mini Kit (Fábryová & Celec, 2014).

With saliva samples from newborns, Maron & Johnson compared RNA yield, quality, stability and RT-qPCR performance for two kits with RNA stabilizing agents, the Qiagen RNeasy Protect Saliva Mini Kit® and the DNA Genotek Oragene•RNA® assay (Maron & Johnson, 2015). However, extracted total salivary RNA was of poor quality and quantity for both assays. These results underline the need for further studies to understand

the differences obtained in RNA extraction from saliva, and it should be pointed out that a possible explanation for these differences might be due to circumstances inherent to each experiment, operator and laboratory (Anaya & Causado, 2017). However, due to the complex nature of this biofluid, it is important to consider the use of an RNA stabilizing agent and additional steps of chloroform and/or ethanol, when using TRIzol, to eliminate potential contaminants.

DNA extraction was tested twice with the NZY Tissue gDNA Isolation Kit. In the first attempt, a good DNA concentration and A260/A280 ratio were obtained but in only one sample (frozen mouthwash). On the other hand, in the second time, all samples (stored at 4ºC) had a good DNA concentration and A260/A280 ratios. These samples were quantified twice with different dilution factors and the results were very similar. In all samples, the values of the A260/A230 ratio were not high enough, possibly indicating the presence of contaminants that absorb at 230 nm (Koetsier & Cantor, 2019; Luebbehusen, 2004; Matlock, 2015). These contaminants include chaotropic salts such as guanidine hydrochloride (Koetsier & Cantor, 2019; Matlock, 2015), which are present in two buffers of the kit used.

Concerning DNA integrity, saliva samples frozen and stored at 4ºC had a high molecular weight band with a moderate smear in the agarose gel. In the frozen mouthwash and the mouthwash and cytobrush samples stored at 4ºC, a high molecular weight band was also observed but with a stronger smear. The two swab samples that presented some DNA concentration, had both a light high molecular weight band and a smear. However, these samples had a high A260/A280 ratio value (2.2-2.6), which is indicative of contamination. In the remaining samples, no band was observed, which probably means that the DNA extraction was not efficient enough. Smears might be an indication of degraded DNA, however, all samples that presented a high molecular weight band and a smear were tested for PCR amplification (except one of the swab samples), and it was successful. Still, further work will be necessary to trace and solve the precise cause(s) involved in DNA degradation.

It is not possible to confirm if the differences between the obtained DNA concentrations can be explained due to the different types of samples used, temperature and/or times of storage since each condition was only tested once. And, despite the need for further optimization with this kit, it was possible to achieve good results in terms of DNA concentration and A260/A280 ratios.

5.2. Genetic analysis

The second part of this study was the bioinformatic analysis. The frequency of the most mutated genes in both AML and ALL TARGET datasets was low, but the gene lists per se were not surprising since many of them have already been linked to cancer, and specifically, leukemias, as already indicated in the Results chapter. Some of the mutated genes have also been associated with enzymes involved in NAD^+ metabolism. The FLT3-ITD (FLT3- internal tandem duplication) mutation is frequently observed in acute myeloid leukemia and is involved in an oncogenic network, in which SIRT1 overexpression is included (Li *et al.,* 2014). *KRAS* was associated with SIRT1 in *KRAS*-driven lung adenocarcinomas (Costa-Machado *et al.,* 2018) and pancreatic cancer (Zhang *et al.*, 2013), and with SIRT2 in *KRAS* mutant colon cancer (Bajpe *et al.,* 2015). p53 has two defined links to NAD^+: SIRT1, which has been shown to modify the p53 response by deacetylation (Hirai *et al.,* 2014; Lee & Gu, 2013; Pan *et al.*, 2014), and interaction with PARP1 (Pan *et al.*, 2014). Very recently, it was demonstrated that mutant p53 induces the expression of SIRT3 (Torrens-Mas *et al.*, 2020). Considering the other genes, Ullmark and colleagues investigated possible gene expression network partners of *WT1* in a large acute myeloid leukemia patient cohort, and one of the genes with the highest correlation to *WT1* was *QPRT* (Ullmark *et al.*, 2017). Mutations in IDH2 have been identified as oncogenic drivers of AML (Sachdeva *et al.,* 2019; Tateishi *et al.*, 2016), and it is known that SIRT5 increases IDH2 activity by deacetylation (Xiao *et al.*, 2018). Recently, Huang *et al.* demonstrated that PARP1 regulates NSD2 via poly ADP-ribosylation upon oxidative stress (Huang *et al.*, 2019).

In the pediatric AML dataset, the deletion of genes *ZEB2* (zinc finger E-box binding homeobox 2), *MBNL1* (muscleblind like splicing regulator 1) and *ELF* stands out. Recurrent focal deletions are characteristic of pediatric AML (Bolouri *et al.*, 2018), specifically impacting *ZEB2*, *MBNL1* and *ELF1* (Bolouri *et al.*, 2018). In ALL, the most altered genes belong to the same loci. 9p21 deletions, especially *CDKN2A/B* deletions, have been shown to frequently occur in pediatric ALL (Chen *et al.*, 2013; Patkar *et al.*, 2017; Salas *et al.*, 2016; Schwab *et al.*, 2013). The pediatric ALL dataset has a higher CNAs frequency than the pediatric AML. In fact, genetic alterations in AML are less than those in other tumors (Vujkovic *et al.*, 2017) and ALL is associated with a high frequency of CNAs (Steeghs *et*

al., 2019). The majority of the these deleted genes are associated with a poor prognosis and drug resistance (Chen *et al.*, 2020; Steeghs *et al.*, 2019; Thakral *et al.*, 2019).

In AML and ALL, the percentage of hypermethylated genes is similar (23 and 25%, respectively) but in AML the percentage of hypomethylated genes is much higher than in ALL (65% in AML and 14% in ALL). However, the significance of these results is yet unclear.

The results from the statistical overrepresentation test with the PANTHER GO-Slim Biological Process set using the hypermethylated genes in AML and ALL were expected, since there was enrichment in biological processes mainly related with hematopoiesis, leukocytes, development and proliferation. Hematopoiesis (formation of blood cellular components) occurs during embryonic development and throughout adulthood to produce and replenish the blood system (Jagannathan-Bogdan & Zon, 2013). Acute leukemias represent a clonal expansion and a block in the differentiation of myeloid or lymphoid hematopoiesis (Lanzkowsky, 2011; Shipley & Butera, 2009). They are characterized by uncontrolled proliferation and accumulation of early hematopoietic cells (known as blast cells) in organs, in particular, bone marrow (Ah-Moye *et al.*, 2014; Cernan *et al.*, 2017). The results with the hypomethylated genes were also not surprising since the identified biological processes are critical for tumor cells.

The most expressed genes in both pediatric leukemias datasets, besides the many mitochondrial and some ribosomal genes, were related with hematopoiesis or with carcinogenesis in general. Mitochondrial gene overexpression in pediatric acute leukemias might be due to the higher need for energy, since acute leukemias are proliferative tumors (Schneider *et al.*, 2001). To gain some insight into this matter, the expression data of the adult AML PanCancer Atlas (TCGA) dataset was analyzed. None of the 12 overexpressed mitochondrial genes in pediatric AML were present in the TCGA dataset, although there were 11 genes in common with pediatric ALL (appendix 11). Very recently, in the first published study with a large pediatric AML cohort analyzing the prognostic impact of mitochondrial gene expression, some of these genes were reported to have an impact on reducing survival (Tyagi *et al.*, 2019), thus, the different expression profile of pediatric leukemias should be further investigated (Gröbner *et al.*, 2018; Ma *et al.*, 2018).

5.2.1. *NAPRT* and *NAMPT*

To date, no papers were found that addressed specifically *NAPRT* and *NAMPT* genetic alterations in pediatric AML and ALL or head and neck tumors. *NAPRT* expression was found to be moderate in AML and ALL datasets and high in the HNSC dataset. Regarding methylation, *NAPRT* was hypermethylated in AML and methylated in ALL and HNSC. In ALL, a correlation between *NAPRT* methylation and mRNA expression was not identified but in HSNC, the correlation was found to be negatively moderate. A negative correlation is in concordance with the general perception that hypermethylated genes are expressed at low levels and therefore are negatively correlated (Chatterjee *et al.*, 2016). In fact, low *NAPRT* expression mediated by *NAPRT* promoter hypermethylation is frequently observed in certain types of cancers (Duarte-Pereira *et al.*, 2016; Shames *et al.*, 2013; Tateishi *et al.*, 2016). Lower levels of *NAPRT* expression were observed in EMT-subtype samples of HNSC in comparison with non-EMT samples (Lee *et al.*, 2018). The median value of circulating eNAPRT was duplicated in sera from patients with cancer, including chronic lymphocytic leukemia (CLL), compared to normal blood donors (Managò *et al.*, 2019). Duarte-Pereira *et al.* observed that in all leukemia cell lines tested, *NAPRT* expression was markedly decreased but it was not associated with *NAPRT* promotor methylation (Duarte-Pereira *et al.*, 2016). In fact, from all the cell lines tested, only one had no NAPRT expression and methylated *NAPRT* promoter (Duarte-Pereira *et al.*, 2016). Of note, *IDH* (isocitrate dehydrogenases) mutations are frequently observed in patients with gliomas and AML and were reported to decrease *NAPRT* expression via increased DNA and histone methylation (Tateishi *et al.*, 2016; Yaku *et al.*, 2018). The divergences of correlation between *NAPRT* promoter methylation and *NAPRT* expression, in this study and others, might be due to tissue/cancer type specificity of expression and regulation mechanisms (Duarte-Pereira *et al.*, 2016). *NAPRT* plays a crucial role in cancer cell metabolism, energy status, protein synthesis, cell size regulation and DNA repair (Piacente *et al.*, 2017). Thus, it is not clear why the loss of *NAPRT* expression would be beneficial to some cancers (Shames *et al.*, 2013) and further studies are needed.

Similarly to *NAPRT*, *NAMPT* expression was found to be moderate in both pediatric leukemias datasets and high in the HNSC dataset. Despite being pediatric leukemias, which might have different expression profiles comparing with adult tumors, the results in pediatric AML and ALL were not expected and differ from what is described by other researchers.

NAMPT has a crucial role in cancer cell metabolism and is frequently overexpressed in several tumors, both in solid tumors and hematological malignancies (reviewed in Dalamaga *et al.*, 2018 and Yaku *et al.*, 2018). Also, Kozako and colleagues, by western blotting, found that NAMPT is highly expressed in peripheral blood mononuclear cells (PBMCs) isolated from patients with acute adult T-cell leukemia/lymphoma (ATL) compared with normal PBMCs (Kozako *et al.*, 2019). Interestingly, in one patient who progressed from chronic to acute ATL, NAMPT was undetectable in the chronic phase but was expressed at high levels in the acute phase (Kozako *et al.*, 2019). In CLL cells, *NAMPT* mRNA levels were significantly higher than those of normal B lymphocytes (Audrito *et al.*, 2015). Pylaeva *et al.* observed that *NAMPT* expression was elevated in tumor-associated neutrophils (TANs) from patients with head-and-neck carcinoma (HNC) compared to healthy donors (Pylaeva *et al.*, 2019). Duarte-Pereira *et al.* observed that NAMPT expression was weaker in leukemia cell lines (NB4, ML2 and HL-60) in comparison with the other tumor types tested (Duarte-Pereira *et al.*, 2016).

In general, CNA frequency in AML, ALL and HNSC datasets was low. *NAPRT* was mainly amplified in HNSC and *NAMPT* was found to be deleted in both pediatric leukemias and amplified in HNSC, and to a smaller extent also amplified in ALL. Concerning the correlation between expression and CNA, no significant correlation was observed. *NAMPT* is frequently amplified in some cancers (reviewed in Pramono *et al.*, 2020). The most common alteration in *NAPRT* was amplification and no correlation was found between *NAPRT* amplification and increased expression (Duarte-Pereira *et al.*, 2019). *NAPRT* was found to be amplified and subsequently overexpressed in some cancers, such as head and neck, ovarian, pancreatic and prostate cancers (Chowdhry *et al.*, 2019; Piacente *et al.*, 2017).

In the three analyzed datasets, *NAMPT* mutations were not found. In *NAPRT*, most of the identified mutations were missense but with very low frequencies. Duarte-Pereira *et al.* observed that, in public databases, *NAMPT* is shown to be less diverse than *NAPRT* (Duarte-Pereira *et al.*, 2014). Indeed, *NAPRT* is more permissive to mutations and, thus, much more polymorphic than *NAMPT* (Duarte-Pereira *et al.*, 2014). In a larger analysis of 216 cancer studies, *NAPRT* and *NAMPT* were mutated in less than 1% of the tumors (Chowdhry *et al.*, 2019).

In HNSC, 51% (51/101) of the eQTL that impacted *NAPRT* expression, influenced it negatively. While in AML, 20/21 *NAPRT* eQTL had a positive effect on *NAPRT* expression. Curiously, none of the eQTL were located in the *NAPRT* gene sequence but in intergenic regions or neighboring genes. Some eQTL were common to different tumors and genes, others exclusively influenced *NAPRT* and only a few had an impact on *NAPRT* in HNSC.

All 21 *NAPRT* eQTL in LAML were present in GTEx, but some were not present in the tumor-corresponding normal tissues of the altered cancers. A few *NAPRT* eQTL in HNSC were not present in any of the normal tissues represented in GTEx, some were not present in the only tissue that can be associated with HNSC in GTEx (minor salivary gland) and others were not present in the tumor-corresponding normal tissues of the altered tumors. However, it is not possible to affirm that the eQTL which were not in GTEx, are cancer-specific variants. HNSC involves other tissues besides the minor salivary gland and, since tissues are not homogenous and in GTEx the cellular subtypes are not discriminated, in the other tumors the same association cannot be made directly.

Regarding allelic frequencies, in the majority of the *NAPRT* eQTL in HNSC and LAML, the most similar populations are the European and American populations and the East and South Asian populations. In most cases, the alternative allele was found to be more frequent than the reference allele in all populations with exception of the African population. Thus, although these SNPs are present in tumors, they are also frequent in the general population.

The heatmap resulting from *NAPRT* eQTL in HNSC with the effect sizes in all 26 impacted tumors (TCGA), showed that these eQTL essentially increase *NAPRT* expression. On the other hand, in HNSC the effect is the total opposite. KIRC and KIRP are the only exceptions, showing a similar pattern to HNSC, in which most SNPs decrease *NAPRT* expression. In a molecular clustering of the complete set of tumors in TCGA, primarily organized by histology, tissue type, or anatomic origin, KIRC and KIRP clustered together while KICH (kidney chromophobe) was in a different cluster (Hoadley *et al.*, 2018), supporting that these tumors have a different signature. Further studies are needed to understand these patterns. For this, a more detailed analysis of the 33 tumors in the TCGA PanCancer Project was carried out, focusing on *NAPRT* alterations (eQTL, SNPs, DNA methylation and CNAs), and the results are being prepared for publication.

6. CONCLUSIONS AND FUTURE PERSPECTIVES

The results obtained for the extraction of nucleic acids from saliva were not ideal. The number of samples and replicates tested was low, due to the pandemic, and in the future it is necessary to repeat the protocols described and perhaps test different ones, as mentioned in the discussion chapter. Due to the low number of replicates, it was not possible to conclude which is the best saliva collection method neither the best temperatures and times of storage, thus, these variables must also be further analyzed. Concerning RNA, it will be important to test the use of DNase and perform RT-PCR to assure that downstream applications can be successfully conducted.

Sequencing of *NAMPT* and *NAPRT* fragments in non-pathological samples should be compared with the sequencing results, for the same regions, in pediatric leukemias and head and neck tumor samples. Since *NAPRT* is frequently hypermethylated, bisulfite conversions could also be performed.

Considering *NAPRT* and *NAMPT* variants, the frequencies were low but further studies are required to clarify if these variants are correlated with gene and protein expression, in both pathological and non-pathological conditions.

Overall, a complete analysis of NAMPT and NAPRT expression and regulation should be made to design a better therapeutic strategy for each patient.

NAD metabolism holds great potential for the development of cancer treatments and there is some expectation that saliva can be routinely used in clinal practice. Nevertheless, there is no doubt that many questions remain to be answered and that further studies will be greatly needed.

7. BIBLIOGRAPHY

Ah-Moye, D., Davies, C., Goody, J., Hayward, P., & Frewin, R. (2014). Introduction to haematology and transfusion science. In *Clinical Biochemistry: Metabolic and Clinical Aspects* (Third Edit, pp. 497–514). Elsevier Ltd. https://doi.org/10.1016/B978-0-7020-5140-1.00026-2

Ahlfen, S. von, & Schlumpberger, M. (2010). Effects of low A260 /A230 ratios in RNA preparations on downstream applications. *QIAGEN Gene Expression Newsletter*, *15*, 7–8.

Alfayez, M., Issa, G. C., Patel, K. P., Wang, F., Wang, X., Short, N. J., Cortes, J. E., Kadia, T., Ravandi, F., Pierce, S., Assi, R., Garcia-manero, G., Dinardo, C. D., Daver, N., Pemmaraju, N., Kantarjian, H., & Borthakur, G. (2020). The Clinical impact of PTPN11 mutations in adults with acute myeloid leukemia. *Leukemia*. https://doi.org/10.1038/s41375-020-0920-z

Alhazzazi, T. Y., Kamarajan, P., Verdin, E., & Kapila, Y. L. (2011). SIRT3 and Cancer: Tumor Promoter or Suppressor? *Biochimica et Biophysica Acta*, *1816*(1), 80–88. https://doi.org/10.1016/j.bbcan.2011.04.004.SIRT3

Amson, R., Pece, S., Lespagnol, A., Vyas, R., Mazzarol, G., Tosoni, D., Colaluca, I., Viale, G., Rodrigues-ferreira, S., Wynendaele, J., Chaloin, O., Hoebeke, J., Marine, J., Paolo, P., Fiore, D., & Telerman, A. (2011). Reciprocal repression between P53 and TCTP. *Nature Medicine*, *18*(1), 91–99. https://doi.org/10.1038/nm.2546

Anaya, M. V. M., & Causado, A. S. (2017). Evaluation of two RNA extraction methods in children's saliva. *Revista Odontológica Mexicana*, *21*(4), 237–243. https://doi.org/10.1016/j.rodmex.2018.01.014

Attar, E. C., Johnson, J. L., Amrein, P. C., Lozanski, G., Wadleigh, M., Deangelo, D. J., Kolitz, J. E., Powell, B. L., Voorhees, P., Wang, E. S., Blum, W., Stone, R. M., Marcucci, G., Bloomfield, C. D., Moser, B., & Larson, R. A. (2013). Bortezomib Added to Daunorubicin and Cytarabine During Induction Therapy and to Intermediate-Dose Cytarabine for Consolidation in Patients With Previously Untreated Acute Myeloid Leukemia Age 60 to 75 Years: CALGB (Alliance) Study 10502. *Journal of Clinical Oncology*, *31*(7), 923–929. https://doi.org/10.1200/JCO.2012.45.2177

Audrito, V., Messana, V. G., & Deaglio, S. (2020). NAMPT and NAPRT: Two Metabolic

Enzymes With Key Roles in Inflammation. *Frontiers in Oncology*, *10*(358), 1–17. https://doi.org/10.3389/fonc.2020.00358

Audrito, V., Serra, S., Brusa, D., Mazzola, F., Arruga, F., Vaisitti, T., Coscia, M., Maffei, R., Rossi, D., Wang, T., Inghirami, G., Rizzi, M., Gaidano, G., Garcia, J. G. N., Wolberger, C., Raffaelli, N., & Deaglio, S. (2015). Extracellular nicotinamide phosphoribosyltransferase (NAMPT) promotes M2 macrophage polarization in chronic lymphocytic leukemia. *Blood*, *125*(1), 111–123. https://doi.org/10.1182/blood-2014-07-589069

Babaei, M. A., Kamalidehghan, B., Saleem, M., Huri, H. Z., & Ahmadipour, F. (2016). Receptor tyrosine kinase (c-Kit) inhibitors: a potential therapeutic target in cancer cells. *Drug Design, Development and Therapy*, *10*, 2443–2459. https://doi.org/10.2147/DDDT.S89114

Bajpe, P. K., Prahallad, A., Horlings, H., Nagtegaal, I., Beijersbergen, R., & Bernards, R. (2015). A chromatin modifier genetic screen identifies SIRT2 as a modulator of response to targeted therapies through the regulation of MEK kinase activity. *Oncogene*, *34*(4), 531–536. https://doi.org/10.1038/onc.2013.588

Bejar, R. (2018). What biologic factors predict for transformation to AML? *Best Practice & Research Clinical Haematology*, *31*(4), 341–345. https://doi.org/10.1016/j.beha.2018.10.002

Belenky, P., Bogan, K. L., & Brenner, C. (2006). NAD+ metabolism in health and disease. *Trends in Biochemical Sciences*, *32*(1), 12–19. https://doi.org/10.1016/j.tibs.2006.11.006

Bender, D. A. (1983). Biochemistry of tryptophan in health and disease. *Molecular Aspects of Medicine*, *6*(2), 101–197. https://doi.org/10.1016/0098-2997(83)90005-5

Berger, F., Lau, C., Dahlmann, M., & Ziegler, M. (2005). Subcellular compartmentation and differential catalytic properties of the three human nicotinamide mononucleotide adenylyltransferase isoforms. *Journal of Biological Chemistry*, *280*(43), 36334–36341. https://doi.org/10.1074/jbc.M508660200

Bertoli, S., Paubelle, E., Bérard, E., Saland, E., Thomas, X., Tavitian, S., Virginie, M., François, L., Delabesse, E., Sarry, A., Huguet, F., Larrue, C., Bosc, C., Farge, T., Emmanuel, J., Mauricette, S., & Récher, C. (2019). Ferritin heavy/light chain (FTH1/FTL) expression, serum ferritin levels, and their functional as well as prognostic

roles in acute myeloid leukemia. *European Journal of Haematology*, *102*(2), 131–142. https://doi.org/10.1111/ejh.13183

Bieganowski, P., & Brenner, C. (2004). Discoveries of Nicotinamide Riboside as a Nutrient and Conserved NRK Genes Establish a Preiss-Handler Independent Route to NAD+ in Fungi and Humans. *Cell*, *117*(4), 495–502. https://doi.org/10.1016/s0092-8674(04)00416-7

Bogan, K. L., & Brenner, C. (2008). Nicotinic Acid, Nicotinamide, and Nicotinamide Riboside: A Molecular Evaluation of NAD+ Precursor Vitamins in Human Nutrition. *Annual Review of Nutrition*, *28*(1), 115–130. https://doi.org/10.1146/annurev.nutr.28.061807.155443

Bolouri, H., Farrar, J. E., Jr, T. T., Ries, R. E., Lim, E. L., Alonzo, T. A., Ma, Y., Moore, R., Mungall, A. J., Marra, M. A., Zhang, J., Ma, X., Liu, Y., Liu, Y., Auvil, J. M. G., Davidsen, T. M., Gesuwan, P., Hermida, L. C., Salhia, B., … Meshinchi, S. (2018). The molecular landscape of pediatric acute myeloid leukemia reveals recurrent structural alterations and age-specific mutational interactions. *Nature Medicine*, *24*(1), 103–112. https://doi.org/10.1038/nm.4439.The

Bonne, N. J., & Wong, D. T. W. (2012). Salivary biomarker development using genomic, proteomic and metabolomic approaches. *Genome Medicine*, *4*(82), 1–12. https://doi.org/10.1186/gm383

Borghese, F., & Clanchy, F. I. L. (2011). CD74: an emerging opportunity as a therapeutic target in cancer and autoimmune disease. *Expert Opinion on Therapeutic Targets*, *15*(3), 237–251. https://doi.org/10.1517/14728222.2011.550879

Cantó, C., & Auwerx, J. (2011). NAD+ as a signaling molecule modulating metabolism. *Critical Reviews in Biochemistry and Molecular Biology*, *76*, 291–298. https://doi.org/10.1101/sqb.2012.76.010439.NAD

Cantó, C., Menzies, K., & Auwerx, J. (2015). NAD+ metabolism and the control of energy homeostasis - a balancing act between mitochondria and the nucleus. *Cell Metabolism*, *22*(1), 31–53. https://doi.org/10.1016/j.physbeh.2017.03.040

Cerami, E., Gao, J., Dogrusoz, U., Gross, B. E., Sumer, S. O., Aksoy, B. A., Jacobsen, A., Byrne, C. J., Heuer, M. L., Larsson, E., Antipin, Y., Reva, B., Goldberg, A. P., Sander, C., & Schultz, N. (2012). The CBio Cancer Genomics Portal: An Open Platform for Exploring Multidimensional Cancer Genomics Data. *Cancer Discovery*, *2*(5), 401–404.

https://doi.org/10.1371/journal.pone.0178059

Cernan, M., Szotkowski, T., & Pikalova, Z. (2017). Mixed-phenotype acute leukemia: state-of-the-art of the diagnosis, classification and treatment. *Biomed Pap Med Fac Univ Palacky Olomouc Czech Repub.*, *161*(3), 234–241. https://doi.org/10.5507/bp.2017.013

Chandrashekar, D. S., Bashel, B., Balasubramanya, S. A. H., Creighton, C. J., Ponce-Rodriguez, I., Chakravarthi, B. V. S. K., & Varambally, S. (2017). UALCAN: A Portal for Facilitating Tumor Subgroup Gene Expression and Survival Analyses. *Neoplasia (United States)*, *19*(8), 649–658. https://doi.org/10.1016/j.neo.2017.05.002

Chatterjee, A., Stockwell, P. A., Rodger, E. J., Parry, M. F., & Eccles, M. R. (2016). Scan-tcga tools for integrated epigenomic and transcriptomic analysis of tumor subgroups. *Epigenomics*, *8*(10), 1315–1330. https://doi.org/10.2217/epi-2016-0063

Chen, C., Bartenhagen, C., Gombert, M., Okpanyi, V., Binder, V., Ro, S., Bradtke, J., Teigler-schlegel, A., Harbott, J., Ginzel, S., & Thiele, R. (2013). Next-Generation-Sequencing-Based Risk Stratification and Identification of New Genes Involved in Structural and Sequence Variations in Near Haploid Lymphoblastic Leukemia. *Genes, Choromosomes & Cancer*, *52*(6), 564–579. https://doi.org/10.1002/gcc

Chen, L., Shi, Y., Li, J., Yang, X., Li, R., Zhou, X., & Zhu, L. (2020). LncRNA CDKN2B-AS1 contributes to tumorigenesis and chemoresistance in pediatric T-cell acute lymphoblastic leukemia through miR-335-3p/TRAF5 axis. *Anti-Cancer Drugs*, 1–13. https://doi.org/10.1097/CAD.0000000000001001

Chiarugi, A., Dölle, C., Felici, R., & Ziegler, M. (2012). The NAD metabolome - a key determinant of cancer cell biology. *Nature Reviews Cancer*, *12*(11), 741–752. https://doi.org/10.1038/nrc3340

Chowdhry, S., Zanca, C., Rajkumar, U., Koga, T., Diao, Y., Liu, F., Turner, K., Yang, H., Brunk, E., Bi, J., Bafna, V., Ren, B., & Mischel, P. S. (2019). NAD metabolic dependency in cancer is shaped by gene amplification and enhancer remodeling. *Nature*, *569*(7757), 570–575. https://doi.org/10.1038/s41586-019-1150-2.NAD

Comeaux, E. Q., & Mullighan, C. G. (2017). TP53 Mutations in Hypodiploid Acute Lymphoblastic Leukemia. *Cold Spring Harbor Perspectives in Medicine*, *7*(3), a026286. https://doi.org/10.1101/cshperspect.a026286

Costa-Machado, L. F., Martín-hernández, R., Sanchez-luengo, M. Á., Vales-villamarin, C.,

Barradas, M., Lynch, C., Nava, D. De, Cabo, R. De, Cañamero, M., Martinez, L., & Sanchez-carbayo, M. (2018). Sirt1 protects from K-Ras-driven lung carcinogenesis. *EMBO Reports*, *19*(9), e43879. https://doi.org/10.15252/embr.201643879

Dalamaga, M., Christodoulatos, G. S., & Mantzoros, C. S. (2018). The role of extracellular and intracellular nicotinamide phosphoribosyl-transferase in cancer: diagnostic and therapeutic perspectives and challenges. *Metabolism: Clinical and Experimental*, *82*, 72–87. https://doi.org/10.1016/j.metabol.2018.01.001

Daniels, C. M., Ong, S. E., & Leung, A. K. L. (2014). Phosphoproteomic approach to characterize protein mono- and poly(ADP-ribosyl)ation sites from cells. *Journal of Proteome Research*, *13*(8), 3510–3522. https://doi.org/10.1021/pr401032q

De Vos, M., Schreiber, V., & Dantzer, F. (2012). The diverse roles and clinical relevance of PARPs in DNA damage repair: Current state of the art. *Biochemical Pharmacology*, *84*(2), 137–146. https://doi.org/10.1016/j.bcp.2012.03.018

Demarest, T. G., Babbar, M., Okur, M. N., Dan, X., Croteau, D. L., Fakouri, N. B., Mattson, M. P., & Bohr, V. A. (2019). NAD+ Metabolism in Aging and Cancer. *Annual Review of Cancer Biology*, *3*, 105–130. https://doi.org/10.1146/annurev-cancerbio-030518-055905

Demir, S., Boldrin, E., Sun, Q., Hampp, S., Tausch, E., Eckert, C., Ebinger, M., Handgretinger, R., te Kronnie, G., Wiesmüller, L., Stilgenbauer, S., Selivanova, G., Debatin, K. M., & Meyer, L. H. (2020). Therapeutic targeting of mutant p53 in pediatric acute lymphoblastic leukemia. *Haematologica*, *105*(1), 170–181. https://doi.org/10.3324/haematol.2018.199364

Deng, C. (2009). SIRT1, Is It a Tumor Promoter or Tumor Suppressor? *International Journal of Biological Sciences*, *5*(2), 147–152. https://doi.org/10.7150/ijbs.5.147

Ding, L.-W., Sun, Q.-Y., Tan, K.-T., Chien, W., Mayakonda, A., Yeoh, A. E. J., Kawamata, N., Nagata, Y., Xiao, J.-F., Loh, X.-Y., Lin, D.-C., Garg, M., Jiang, Y.-Y., Xu, L., Lim, S.-L., Liu, L.-Z., Madan, V., Sanada, M., Fernández, L. T., … Koeffler, H. P. (2017). Mutational landscape of pediatric acute lymphoblastic leukemia. *Cancer Research*, *77*(2), 390–400. https://doi.org/10.1158/0008-5472.CAN-16-1303.Mutational

Doerrenber, M., Kloetgen, A., Hezaveh, K., Wossmann, W., Bleckmann, K., Stanulla, M., Schrappe, M., McHardy, A. C., Borkhardt, A., & Hoell, J. I. (2017). T-Cell Acute Lymphoblastic Leukemia in Infants has Distinct Genetic and Epigenetic Features

Compared to Childhood Cases. *Genes, Choromosomes & Cancer*, *56*(2), 159–167. https://doi.org/10.1002/gcc

Dölle, C., Skoge, R., VanLinden, M., & Ziegler, M. (2015). NAD Biosynthesis in Humans - Enzymes, Metabolites and Therapeutic Aspects. *Current Topics in Medicinal Chemistry*, *13*(23), 2907–2917. https://doi.org/10.2174/1568026613136660206

Du, P., Zhang, X., Huang, C. C., Jafari, N., Kibbe, W. A., Hou, L., & Lin, S. M. (2010). Comparison of Beta-value and M-value methods for quantifying methylation levels by microarray analysis. *BMC Bioinformatics*, *11*(584), 1–9. https://doi.org/10.1186/1471-2105-11-587

Duarte-Pereira, S., Matos, S., Oliveira, J. L., & Silva, R. M. (2019). *Analysis of NAPRT Genetic Variants AND Gene Expression in Tumors*. https://doi.org/10.1097/MD.0000000000015772

Duarte-Pereira, S., Pereira-Castro, I., Silva, S. S., Correia, M. G., Neto, C., da Costa, L. T., Amorim, A., & Silva, R. M. (2016). Extensive regulation of nicotinate phosphoribosyltransferase (NAPRT) expression in human tissues and tumors. *Oncotarget*, *7*(2), 1973–1983. https://doi.org/10.18632/oncotarget.6538

Duarte-Pereira, S., Silva, S. S., Azevedo, L., Castro, L., Amorim, A., & Silva, R. M. (2014). Nampt and Naprt1: Novel polymorphisms and distribution of variants between normal tissues and tumor samples. *Scientific Reports*, *4*(6311), 1–7. https://doi.org/10.1038/srep06311

Duployez, N., Marceau-renaut, A., Boissel, N., Petit, A., Bucci, M., Geffroy, S., Renneville, A., Ragu, C., Figeac, M., Celli-lebras, K., Lacombe, C., Micol, J., Abdel-wahab, O., Cornillet, P., Ifrah, N., Leverger, G., Jourdan, E., & Preudhomme, C. (2016). Comprehensive mutational profiling of core binding factor acute myeloid leukemia. *Blood*, *127*(20), 2451–2459. https://doi.org/10.1182/blood-2015-12-688705.

Emanuelli, M., Carnevali, F., Saccucci, F., Pierella, F., Amici, A., Raffaelli, N., & Magni, G. (2001). Molecular cloning, chromosomal localization, tissue mRNA levels, bacterial expression, and enzymatic properties of human NMN adenylyltransferase. *Journal of Biological Chemistry*, *276*(1), 406–412. https://doi.org/10.1074/jbc.M008700200

Fábryová, H., & Celec, P. (2014). On the origin and diagnostic use of salivary RNA. *Oral Diseases*, *20*(2), 146–152. https://doi.org/10.1111/odi.12098

Fukuhara, A., Matsuda, M., Nishizawa, M., Segawa, K., Tanaka, M., Kishimoto, K.,

Matsuki, Y., Murakami, M., Ichisaka, T., Murakami, H., Watanabe, E., Takagi, T., Akiyoshi, M., Ohtsubo, T., Kihara, S., Yamashita, S., Makishima, M., Funahashi, T., Yamanaka, S., … Shimomura, I. (2005). Visfatin: A protein secreted by visceral fat that Mimics the effects of insulin. *Science*, *307*(5708), 426–430. https://doi.org/10.1126/science.1097243

Galen, P. van, Hovestadt, V., II, M. W., Hughes, T., Griffin, G. K., Battaglia, S., Verga, J. A., Stephansky, J., Pastika, T. J., Story, J. L., Pinkus, G. S., Pozdnyakova, O., Galinsky, I., Stone, R. M., Graubert, T. A., Shalek, A. K., Aster, J. C., Lane, A. A., & Bernstein, B. E. (2020). Single-cell RNA-seq reveals AML hierarchies relevant to disease progression and immunity. *Cell*, *176*(6), 1265–1281. https://doi.org/10.1016/j.cell.2019.01.031.

Gandhi, V., O'Brien, M. H., & Yadav, S. (2020). High-Quality and High-Yield RNA Extraction Method From Whole Human Saliva. *Biomarker Insights*, *15*, 1–9. https://doi.org/10.1177/1177271920929705

Gao, J., Aksoy, B. A., Dogrusoz, U., Dresdner, G., Gross, B., Sumer, S. O., Sun, Y., Jacobsen, A., Sinha, R., Larsson, E., Cerami, E., Sander, C., & Schult, N. (2013). Integrative Analysis of Complex Cancer Genomics and Clinical Profiles Using the cBioPortal. *Science Signaling*, *6*(269), p11. https://doi.org/10.1126/scisignal.2004088.Integrative

Garten, A., Petzold, S., Körner, A., Imai, S., & Kiess, W. (2009). Nampt: Linking NAD biology, metabolism, and cancer. *Trends in Endocrinology and Metabolism*, *20*(3), 130–138. https://doi.org/10.1016/j.tem.2008.10.004.

Garten, A., Schuster, S., Penke, M., Gorski, T., De Giorgis, T., & Kiess, W. (2015). Physiological and pathophysiological roles of NAMPT and NAD metabolism. *Nature Reviews Endocrinology*, *11*(9), 535–546. https://doi.org/10.1038/nrendo.2015.117

Gill, H., Leung, A. Y. H., & Kwong, Y. (2016). Molecular and Cellular Mechanisms of Myelodysplastic Syndrome: Implications on Targeted Therapy. *International Journal of Molecular Sciences*, *17*(4), 440. https://doi.org/10.3390/ijms17040440

Gong, J., Mei, S., Liu, C., Xiang, Y., Ye, Y., Zhang, Z., Feng, J., Liu, R., Diao, L., Guo, A. Y., Miao, X., & Han, L. (2018). PancanQTL: Systematic identification of cis-eQTLs and trans-eQTLs in 33 cancer types. *Nucleic Acids Research*, *46*(D1), D971–D976. https://doi.org/10.1093/nar/gkx861

Gröbner, S. N., Worst, B. C., Weischenfeldt, J., Buchhalter, I., Kleinheinz, K., Rudneva, V. A., Johann, P. D., Balasubramanian, G. P., Segura-Wang, M., Brabetz, S., Bender, S., Hutter, B., Sturm, D., Pfaff, E., Hübschmann, D., Zipprich, G., Heinold, M., Eils, J., Lawerenz, C., … Pfister, S. M. (2018). The landscape of genomic alterations across childhood cancers. *Nature*, *555*(7696), 321–327. https://doi.org/10.1038/nature25480

Gujar, H., Liang, J. W., Wong, N. C., & Mozhui, K. (2018). Profiling DNA methylation differences between inbred mouse strains on the Illumina Human Infinium MethylationEPIC microarray. *PLoS ONE*, *13*(3), e0193496. https://doi.org/10.1371/journal.pone.0193496

Guo, C., Liu, S., Wang, J., Sun, M., & Greenaway, F. T. (2013). ACTB in cancer. *Clinica Chimica Acta*, *417*, 39–44. https://doi.org/10.1016/j.cca.2012.12.012

Haigis, M. C., & Sinclair, D. A. (2010). Mammalian Sirtuins: Biological Insights and Disease Relevance. *Annual Review of Phatologylogy*, *5*, 253–295. https://doi.org/10.1146/annurev.pathol.4.110807.092250.Mammalian

Hara, N., Yamada, K., Shibata, T., Osago, H., Hashimoto, T., & Tsuchiya, M. (2007). Elevation of Cellular NAD Levels by Nicotinic Acid and Involvement of Nicotinic Acid Phosphoribosyltransferase in Human Cells. *The Jour*, *282*(34), 24574–24582. https://doi.org/10.1074/jbc.M610357200

Hara, N., Yamada, K., Terashima, M., Osago, H., Shimoyama, M., & Tsuchiya, M. (2003). Molecular Identification of Human Glutamine- and Ammonia-dependent NAD Synthetases. *The Journal of Biological Chemistry*, *278*(13), 10914–10921. https://doi.org/10.1074/jbc.M209203200

Hirai, S., Endo, S., Saito, R., Hirose, M., Ueno, T., Suzuki, H., & Yamato, K. (2014). Antitumor Effects of a Sirtuin Inhibitor, Tenovin-6, against Gastric Cancer Cells via Death Receptor 5 Up-Regulation. *PLoS One*, *9*(7), e102831. https://doi.org/10.1371/journal.pone.0102831

Hoadley, K. A., Yau, C., Hinoue, T., Wolf, D. M., Lazar, A. J., Drill, E., Shen, R., Taylor, A. M., Andrew, D., Akbani, R., Bowlby, R., Wong, C. K., Wiznerowicz, M., Sanchez-vega, F., Robertson, G., Schneider, B. G., Lawrence, M. S., Cancer, T., Atlas, G., … Medical, H. (2018). Cell-of-Origin Patterns Dominate the Molecular Classification of 10,000 Tumors from 33 Types of Cancer. *Cell*, *173*(2), 291–304. https://doi.org/10.1016/j.cell.2018.03.022.

Houtkooper, R. H., Cantó, C., Wanders, R. J., & Auwerx, J. (2010). The secret life of NAD+: An old metabolite controlling new metabolic signaling pathways. *Endocrine Reviews*, *31*(2), 194–223. https://doi.org/10.1210/er.2009-0026

Huang, X. X., Leduc, X. R. D., Fornelli, X. L., Schunter, A. J., Bennett, R. L., Kelleher, X. N. L., & Licht, X. J. D. (2019). Defining the NSD2 interactome: PARP1 PARylation reduces NSD2 histone methyltransferase activity and impedes chromatin binding. *The Journal of Biological Chemistry*, *294*(33), 12459–12471. https://doi.org/10.1074/jbc.RA118.006159

Imai, S., Armstrong, C. M., Kaeberlein, M., & Guarente, L. (2000). Transcriptional silencing and longevity protein Sir2 is an NAD-dependent histone deacetylase. *Nature*, *6771*(403), 795–800. https://doi.org/10.1038/35001622

Jaffe, J. D., Wang, Y., Chan, H. M., Zhang, J., Huether, R., Yu, Z., Gibaja, V., Venkatesan, K., Schlegel, R., Sellers, W. R., Keen, N., Liu, J., Caponigro, G., Barretina, J., Cooke, V. G., Mullighan, C., Carr, S. A., & James, R. (2013). Global chromatin profiling reveals NSD2 mutations in pediatric acute lymphoblastic leukemia. *Nature Genetics*, *45*(11), 1386–1391. https://doi.org/10.1038/ng.2777.

Jagannathan-Bogdan, M., & Zon, L. I. (2013). Hematopoiesis. *Development (Cambridge, England)*, *140*(12), 2463–2467. https://doi.org/10.1242/dev.083147

Janczar, S., Janczar, K., Pastorczak, A., Harb, H., Paige, A. J. W., Zalewska-szewczyk, B., Danilewicz, M., & Mlynarski, W. (2017). The Role of Histone Protein Modifications and Mutations in Histone Modifiers in Pediatric B-Cell Progenitor Acute Lymphoblastic Leukemia. *Cancers*, *9*(1), 2. https://doi.org/10.3390/cancers9010002

Katsyuba, E., & Auwerx, J. (2017). Modulating NAD+ metabolism, from bench to bedside. *The EMBO Journal*, *36*(18), 2670–2683. https://doi.org/10.15252/embj.201797135

Kent, W. J., Sugnet, C. W., Furey, T. S., Roskin, K. M., Pringle, T. H., Zahler, A. M., & Haussler, D. (2002). The Human Genome Browser at UCSC. *Genome Research*, *12*(6), 996–1006. https://doi.org/10.1101/gr.229102.

Kikyo, N., Hagiwara, K., Yazaki, Y., & Okabe, T. (1995). Growth stimulation of ferritin of human leukemia cells in vitro. *J Cancer Res Clin Oncol*, *121*, 76–78. https://doi.org/10.1007/BF01202216

Koetsier, G., & Cantor, E. (2019). A Practical Guide to Analyzing Nucleic Acid Concentration and Purity with Microvolume Spectrophotometers. In *New England*

Biolabs. https://www.neb.com/-/media/catalog/application-notes/mvs_analysis_of_na_concentration_and_purity.pdf?rev=be7c8e19f4d34e558527496ea51623dc

Kozako, T., Aikawa, A., Ohsugi, T., Uchida, Y. ichiro, Kato, N., Sato, K., Ishitsuka, K., Yoshimitsu, M., & Honda, S. ichiro. (2019). High expression of NAMPT in adult T-cell leukemia/lymphoma and anti-tumor activity of a NAMPT inhibitor. *European Journal of Pharmacology*, *865*, 172738. https://doi.org/10.1016/j.ejphar.2019.172738

Kulikova, V. A., Gromyko, D. V., & Nikiforov, A. A. (2018). The Regulatory Role of NAD in Human and Animal Cells. *Biochemistry (Moscow)*, *83*(7), 800–812. https://doi.org/10.1134/S0006297918070040

Kulikova, V., Shabalin, K., Nerinovski, K., Dölle, C., Niere, M., Yakimov, A., Redpath, P., Khodorkovskiy, M., Migaud, M. E., Ziegler, M., & Nikiforov, A. (2015). Generation, release, and uptake of the NAD precursor nicotinic acid riboside by human cells. *Journal of Biological Chemistry*, *290*(45), 27124–27137. https://doi.org/10.1074/jbc.M115.664458

Lanzkowsky, P. (2011). Leukemias. In *Leukemias. Manual of Pediatric Hematology and Oncology* (pp. 518–566). https://doi.org/10.1016/B978-0-12-375154-6.00017-3

Larrosa-Garcia, M., & Baer, M. R. (2017). FLT3 inhibitors in acute myeloid leukemia: Current status and future directions. *Molecular Cancer Therapeutics*, *16*(6), 991–1001. https://doi.org/10.1158/1535-7163.MCT-16-0876.

Lee, J., Kim, H., Lee, J. E., Shin, S. J., Oh, S., Kwon, G., Kim, H., Choi, Y. Y., White, M. A., Paik, S., Cheong, J. H., & Kim, H. S. (2018). Selective Cytotoxicity of the NAMPT Inhibitor FK866 Toward Gastric Cancer Cells With Markers of the Epithelial-Mesenchymal Transition, Due to Loss of NAPRT. *Gastroenterology*, *155*(3), 799–814. https://doi.org/10.1053/j.gastro.2018.05.024

Lee, J. T., & Gu, W. (2013). SIRT1: Regulator of p53 Deacetylation. *Genes & Cancer*, *4*(3–4), 112–117. https://doi.org/10.1177/1947601913484496

Leidecker, O., Bonfiglio, J. J., Colby, T., Zhang, Q., Atanassov, I., Zaja, R., Palazzo, L., Stockum, A., Ahel, I., & Matic, I. (2016). Serine is a new target residue for endogenous ADP-ribosylation on histones. *Nature Chemical Biology*, *12*(12), 998–1000. https://doi.org/10.1038/nchembio.2180

Li, L., Osdal, T., Ho, Y., Chun, S., Mcdonald, T., Agarwal, P., Lin, A., Chu, S., Qi, J., Li,

L., Hsieh, Y., Santos, C. Dos, Ha, T., Popa, M., Hovland, R., Bruserud, Ø., Tore, B., Kuo, Y., Chen, W., … Mccormack, E. (2014). SIRT1 Activation by a c-MYC Oncogenic Network Promotes the Maintenance and Drug Resistance of Human FLT3-ITD Acute Myeloid Leukemia Stem Cells. *Cell Stem Cell*, *15*(4), 431–446. https://doi.org/10.1016/j.stem.2014.08.001.

Liu, H. W., Smith, C. B., Schmidt, M. S., Cambronne, X. A., Cohen, M. S., Migaud, M. E., Brenner, C., & Goodman, R. H. (2018). Pharmacological bypass of NAD+ salvage pathway protects neurons from chemotherapyinduced degeneration. *Proceedings of the National Academy of Sciences of the United States of America*, *115*(42), 10654–10659. https://doi.org/10.1073/pnas.1809392115

Locatelli, F., Algeri, M., Merli, P., & Strocchio, L. (2018). Novel approaches to diagnosis and treatment of Juvenile Myelomonocytic Leukemia. *Expert Review of Hematology*, *11*(2), 129–143. https://doi.org/10.1080/17474086.2018.1421937

Luebbehusen, H. (2004). *The Significance of the 260/230 Ratio in Determining Nucleic Acid Purity*.

Lundberg, E., Fagerberg, L., Klevebring, D., Matic, I., Geiger, T., Cox, J., Älgenäs, C., Lundeberg, J., Mann, M., & Uhlen, M. (2010). Defining the transcriptome and proteome in three functionally different human cell lines. *Molecular Systems Biology*, *6*(450), 1–9. https://doi.org/10.1038/msb.2010.106

Ma, X., Liu, Y., Liu, Y., Alexandrov, L. B., Edmonson, M. N., Gawad, C., Zhou, X., Li, Y., Rusch, M. C., John, E., Huether, R., Gonzalez-Pena, V., Wilkinson, M. R., Hermida, L. C., Davis, S., Sioson, E., Pounds, S., Cao, X., Ries, R. E., … Zhang, J. (2018). Pan-cancer genome and transcriptome analyses of 1,699 paediatric leukaemias and solid tumours. *Nature*, *555*(7696), 371–376. https://doi.org/10.1038/nature25795

Magni, G., Amici, A., Emanuelli, M., Orsomando, G., Raffaelli, N., & Ruggieri, S. (2004). Enzymology of NAD+ homeostasis in man. *Cellular and Molecular Life Sciences*, *61*(1), 19–34. https://doi.org/10.1007/s00018-003-3161-1

Malavasi, F., Deaglio, S., Funaro, A., Ferrero, E., Horenstein, A. L., Ortolan, E., Vaisitti, T., & Aydin, S. (2008). Evolution and function of the ADP ribosyl cyclase/CD38 gene family in physiology and pathology. *Physiological Reviews*, *88*(3), 841–886. https://doi.org/10.1152/physrev.00035.2007

Malinowska-Ozdowy, K., Frech, C., Schönegger, Eckert, C., Cazzaniga, G., Stanulla, M.,

Stadt, U. zur, Mecklenbräuker, A., Schuster, M., Kneidinger, D., Stackelberg, A. von, Locatelli, F., Schrappe, M., Horstmann, M., Attarbaschi, A., Bock, C., Mann, G., Haas, O., & Panzer-Grümayer, R. (2015). KRAS and CREBBP mutations: a relapse-linked malicious liaison in childhood high hyperdiploid acute lymphoblastic leukemia. *Leukemia*, *29*(8), 1656–1667. https://doi.org/10.1038/leu.2015.107

Managò, A., Audrito, V., Mazzola, F., Sorci, L., Gaudino, F., Gizzi, K., Vitale, N., Incarnato, D., Minazzato, G., Ianniello, A., Varriale, A., D'Auria, S., Mengozzi, G., Politano, G., Oliviero, S., Raffaelli, N., & Deaglio, S. (2019). Extracellular nicotinate phosphoribosyltransferase binds Toll like receptor 4 and mediates inflammation. *Nature Communications*, *10*(1), 1–14. https://doi.org/10.1038/s41467-019-12055-2

Maron, J., & Johnson, K. (2015). Comparative performance analyses of commercially available products for salivary collection and nucleic acid processing in the newborn. *Biotechnic & Histochemistry*, *90*(8), 581–586. https://doi.org/10.3109/10520295.2015.1048289.

Martín-Lorenzo, A., Auer, F., Chan, L. N., García-Ramírez, I., González-Herrero, I., Rodríguez-Hernández, G., Bartenhagen, C., Dugas, M., Gombert, M., Ginzel, S., Blanco, O., Orfao, A., Alonso-López, D., Rivas, J. D. Las, García-Cenador, M. B., Criado, F. J. G.-, Müschen, M., Sánchez-García, I., Borkhardt, A., … Hauer, J. (2018). Loss of Pax5 exploits Sca1-BCR-ABLp190 susceptibility to confer the metabolic shift essential for pB-ALL. *Cancer Research*, *78*(10), 2669–2679. https://doi.org/10.1158/0008-5472.CAN-17-3262.

Martínez-Redondo, P., & Vaquero, A. (2013). The Diversity of Histone Versus Nonhistone Sirtuin Substrates. *Genes and Cancer*, *4*(3–4), 148–163. https://doi.org/10.1177/1947601913483767

Matlock, B. (2015). Assessment of Nucleic Acid Purity. In *Technical Note 52646 (Thermo Scientific).*

Mi, H., Muruganujan, A., Ebert, D., Huang, X., & Thomas, D. (2019). PANTHER version 14: more genomes, a new PANTHER GO-slim and improvements in enrichment analysis tools. *Nucleic Acids Research*, *47*(D1), D419–D426. https://doi.org/10.1093/nar/gky1038

Michishita, E., Park, J. Y., Burneskis, J. M., Barrett, J. C., & Horikawa, I. (2005). Evolutionarily Conserved and Nonconserved Cellular Localizations and Functions of

Human SIRT Proteins. *Molecular Biology of the Cell*, *16*(10), 4623–4635. https://doi.org/10.1091/mbc.E05

Mori, V., Amici, A., Mazzola, F., & Stefano, M. Di. (2014). Metabolic Profiling of Alternative NAD Biosynthetic Routes in Mouse Tissues. *PLoS ONE*, *9*(11), 1–27. https://doi.org/10.1371/journal.pone.0113939

Neumann, M., Vosberg, S., Schlee, C., Heesch, S., Gökbuget, N., Hoelzer, D., Graf, A., Krebs, S., Bartram, I., Blum, H., Brüggemann, M., Hecht, J., & Stefan, K. (2015). Mutational spectrum of adult T-ALL. *Oncotarget*, *6*(5), 2754–2766. https://doi.org/10.18632/oncotarget.2218

Nicholls, C., Li, H., & Liu, J. (2012). GAPDH: A common enzyme with uncommon functions. *Clinical and Experimental Pharmacology and Physiology*, *39*(8), 674–679. https://doi.org/10.1111/j.1440-1681.2011.05599.x

Nikiforov, A., Do, C., Niere, M., & Ziegler, M. (2011). Pathways and Subcellular Compartmentation of NAD Biosynthesis in Human Cells. *The Journal of Biological Chemistry*, *286*(24), 21767–21778. https://doi.org/10.1074/jbc.M110.213298

Nikiforov, A., Kulikova, V., & Ziegler, M. (2015). The human NAD metabolome: Functions, metabolism and compartmentalization. *Critical Reviews in Biochemistry and Molecular Biology*, *50*(4), 284–297. https://doi.org/10.3109/10409238.2015.1028612

O'Brien, E. C., Prideaux, S., & Chevassut, T. (2014). The epigenetic landscape of acute myeloid leukemia. *Advances in Hematology*, *2014:10317*, 1–14. https://doi.org/10.1155/2014/103175

O'Leary, N. A., Wright, M. W., Brister, J. R., Ciufo, S., Haddad, D., McVeigh, R., Rajput, B., Robbertse, B., Smith-White, B., Ako-Adjei, D., Astashyn, A., Badretdin, A., Bao, Y., Blinkova, O., Brover, V., Chetvernin, V., Choi, J., Cox, E., Ermolaeva, O., … Pruitt, K. D. (2016). Reference sequence (RefSeq) database at NCBI: Current status, taxonomic expansion, and functional annotation. *Nucleic Acids Research*, *44*(D1), D733–D745. https://doi.org/10.1093/nar/gkv1189

Opitz, C. A., & Heiland, I. (2015). Dynamics of NAD-metabolism: everything but constant. *Biochemical Society Transactions*, *43*(6), 1127–1132. https://doi.org/10.1042/BST20150133

Pan, L., Ahn, D., Sharif, T., Clements, D., Gujar, S. A., & Lee, P. W. K. (2014). The NAD+

synthesizing enzyme nicotinamide is a p53 downstream target. *Cell Cycle*, *13*(6), 1041–1048. https://doi.org/10.4161/cc.28128

Pan, Q., Cheng, G., Liu, Y., Xu, T., Zhang, H. A. O., & Li, B. (2020). TMSB10 acts as a biomarker and promotes progression of clear cell renal cell carcinoma. *International Journal of Oncology*, *56*(5), 1101–1114. https://doi.org/10.3892/ijo.2020.4991

Pandit, P., Cooper-White, J., & Punyadeera, C. (2013). High-Yield RNA-Extraction Method for Saliva. *Clinical Chemistry*, *59*(7), 1118–1122. https://doi.org/10.1373/clinchem.2012.197863

Panuzzo, C., Signorino, E., Calabrese, C., Ali, M. S., Petiti, J., Bracco, E., & Cilloni, D. (2020). Landscape of Tumor Suppressor Mutations in Acute Myeloid Leukemia. *Journal of Clinical Medicine*, *9*(3), 802. https://doi.org/10.3390/jcm9030802

Patkar, N., Subramanian, P. G., Tembhare, P., Mandalia, S., & Chaterjee, G. (2017). An integrated genomic profile that includes copy number alterations is highly predictive of minimal residual disease status in childhood precursor B-lineage acute lymphoblastic leukemia. *Indian Journal Pathology and Microbiology*, *60*(2), 209–2013. https://doi.org/10.4103/IJPM.IJPM_466_16

Patnaik, M. M. (2018). The importance of FLT3 mutational analysis in acute myeloid leukemia. *Leukemia & Lymphoma*, *59*(10), 2273–2286. https://doi.org/10.1080/10428194.2017.1399312

Piacente, F., Caffa, I., Ravera, S., Sociali, G., Passalacqua, M., Vellone, V. G., Becherini, P., Reverberi, D., Monacelli, F., Ballestrero, A., Odetti, P., Cagnetta, A., Cea, M., Nahimana, A., Duchosal, M., & Bruzzone, S. (2017). Nicotinic Acid Phosphoribosyltransferase Regulates Cancer Cell Metabolism, Susceptibility to NAMPT Inhibitors, and DNA Repair. *Cancer Research*, *77*(14), 3857–3869. https://doi.org/10.1158/0008-5472.CAN-16-3079

Pramono, A. A., Rather, G. M., Herman, H., Lestari, K., & Bertino, J. R. (2020). NAD- and NADPH-Contributing Enzymes as Therapeutic Targets in Cancer: An Overview. *Biomolecules*, *10*(3), 358. https://doi.org/10.3390/biom10030358

Preiss, J., & Handler, P. (1958a). Biosynthesis of Diphosphopyridine Nucleotide. I. Identification of Intermediates. *The Journal of Biological Chemistry*, *233*(2), 488–492.

Preiss, J., & Handler, P. (1958b). Biosynthesis of Diphosphopyridine Nucleotide. II. Enzymatic Aspects. *The Journal of Biological Chemistry*, *233*(2), 493–500.

Pylaeva, E., Harati, M. D., Spyra, I., Bordbari, S., Strachan, S., Thakur, B. K., Höing, B., Franklin, C., Skokowa, J., Welte, K., Schadendorf, D., Bankfalvi, A., Brandau, S., Lang, S., & Jablonska, J. (2019). NAMPT signaling is critical for the proangiogenic activity of tumor-associated neutrophils. *International Journal of Cancer*, *144*(1), 136–149. https://doi.org/10.1002/ijc.31808

Rapado-González, Ó., Majem, B., Muinelo-Romay, L., López-lópez, R., & Suarez-cunqueiro Mercedes, M. (2016). Cancer Salivary Biomarkers for Tumours Distant to the Oral Cavity. *International Journal of Molecular Sciences*, *17*(9), 1531. https://doi.org/10.3390/ijms17091531

Rapado-González, Ó., Martínez-Reglero, C., Salgado-Barreira, Á., Takkouche, B., López-López, R., Suárez-Cunqueiro Mercedes, M., & Muinelo-Romay, L. (2020). Salivary biomarkers for cancer diagnosis: a meta-analysis. *Annals of Medicine*, *52*(3–4), 131–144. https://doi.org/10.1080/07853890.2020.1730431

Rongvaux, A., Shea, R. J., Mulks, M. H., Gigot, D., Leo, O., & Andris, F. (2002). Pre-B-cell colony-enhancing factor , whose expression is up-regulated in activated lymphocytes, is a nicotinamide phosphoribosyltransferase, a cytosolic enzyme involved in NAD biosynthesis. *European Journal of Immunology*, *32*(11), 3225–3234. https://doi.org/10.1002/1521-4141(200211)32:11<3225::AID-IMMU3225>3.0.CO;2-L

Rosa, N., Marques, J., Esteves, E., Fernandes, M., Mendes, V. M., Afonso, Â., Dias, S., Pereira, J. P., Manadas, B., Correia, M. J., & Barros, M. (2016). Protein Quality Assessment on Saliva Samples for Biobanking Purposes. *Biopreservation and Biobanking*, *14*(4), 289–297. https://doi.org/10.1089/bio.2015.0054

Ruvolo, P. P., Hu, C. W., Qiu, Y., Ruvolo, V. R., Go, R. L., Hubner, S. E., Coombes, K. R., Andreeff, M., Qutub, A. A., & Kornblau, S. M. (2019). LGALS3 is connected to CD74 in a previously unknown protein network that is associated with poor survival in patients with AML. *EBioMedicine*, *44*, 126–137. https://doi.org/10.1016/j.ebiom.2019.05.025

Sachdeva, A., Rajguru, J. P., Sohi, K., Sachdeva, S. S., Kaur, K., Devi, R., & Rana, V. (2019). Association of leukemia and mitochondrial diseases - A review. *Journal of Family Medicine and Primary Care*, *8*(10), 3120–3124. https://doi.org/10.4103/jfmpc.jfmpc_679_19

Sakashita, K., Matsuda, K., & Koike, K. (2016). Diagnosis and treatment of juvenile myelomonocytic leukemia. *Pediatrics International*, *58*(8), 681–690. https://doi.org/10.1111/ped.13068

Salas, P. C., Fernández, L., Vela, M., Bueno, D., González, B., & Valentín, J. (2016). The role of CDKN2A/B deletions in pediatric acute lymphoblastic leukemia. *Pediatric Hematology and Oncology*, *33*(7–8), 415–422. https://doi.org/10.1080/08880018.2016.1251518

Salmoiraghi, S., Rambaldi, A., & Spinelli, O. (2018). TP53 in adult acute lymphoblastic leukemia. *Leukemia and Lymphoma*, *59*(4), 778–789. https://doi.org/10.1080/10428194.2017.1344839

Samal, B., Sun, Y., Stearns, G., Suggs, S., & Mcniece, I. A. N. (1994). Cloning and Characterization of the cDNA Encoding a Novel Human Pre-B-Cell Colony-Enhancing Factor. *Molecular and Cellular Biology*, *14*(2), 1431–1437. https://doi.org/10.1128/mcb.14.2.1431

Schneider, P., Vasse, M., Sbaa-Ketata, E., Lenormand, B., Hong, L., Soria, C., & Vannier, J. P. (2001). The growth of highly proliferative acute lymphoblastic leukemia may be independent of stroma and/or angiogenesis. *Leukemia*, *15*(7), 1143–1145. https://doi.org/10.1038/sj.leu.2402141

Schwab, C. J., Chilton, L., Morrison, H., Jones, L., Al-shehhi, H., Erhorn, A., Russell, L. J., Moorman, A. V, & Harrison, C. J. (2013). Genes commonly deleted in childhood B-cell precursor acute lymphoblastic leukemia: association with cytogenetics and clinical features. *Haematologica*, *98*(7), 1081–1088. https://doi.org/10.3324/haematol.2013.085175

Seman, M., Adriouch, S., Haag, F., & Koch-Nolte, F. (2004). Ecto-ADP-Ribosyltransferases (ARTs): Emerging Actors in Cell Communication and Signaling. *Current Medicinal Chemistry*, *11*(7), 857–872. https://doi.org/10.2174/0929867043455611

Shackelford, R. E., Mayhall, K., Maxwell, N. M., Kandil, E., & Coppola, D. (2013). Nicotinamide Phosphoribosyltransferase in Malignancy: A Review. *Genes & Cancer*, *4*(11–12), 447–456. https://doi.org/10.1177/1947601913507576

Shames, D. S., Elkins, K., Walter, K., Holcomb, T., Du, P., Mohl, D., Xiao, Y., Pham, T., Haverty, P. M., Liederer, B., Liang, X., Yauch, R. L., Brien, T. O., Bourgon, R., Koeppen, H., & Belmont, L. D. (2013). Loss of NAPRT1 Expression by Tumor-

Specific Promoter Methylation Provides a Novel Predictive Biomarker for NAMPT Inhibitors. *American Association for Cancer Research*, *19*(24), 6912–6923. https://doi.org/10.1158/1078-0432.CCR-13-1186

Shats, I., Williams, J. G., Liu, J., Makarov, M. V, Wu, X., Lih, F. B., Deterding, L. J., Lim, C., Xu, X., Randall, T. A., Lee, E., Li, W., Fan, W., Li, J.-L., Sokolsky, M., Kabanov, A. V, Li, L., Migaud, M. E., Locasale, J. W., & Li, X. (2020). Bacteria Boost Mammalian Host NAD Metabolism by Engaging the Deamidated Biosynthesis Pathway. *Cell Metabolism*, *31*(3), 564-579.E7. https://doi.org/10.1016/j.cmet.2020.02.001

Shin, S. Y., Lee, S. T., Kim, H. J., Cho, E. H., Kim, J. W., Park, S., Jung, C. W., & Kim, S. H. (2016). Mutation profiling of 19 candidate genes in acute myeloid leukemia suggests significance of DNMT3A mutations. *Oncotarget*, *7*(34), 54825–54837. https://doi.org/10.18632/oncotarget.10240

Shipley, J. L., & Butera, J. N. (2009). Acute myelogenous leukemia. *Experimental Hematology*, *37*(6), 649–658. https://doi.org/10.1016/j.exphem.2009.04.002

Sorci, L., Kurnasov, O., Rodionov, D. A., & Osterman, A. L. (2010). Genomics and Enzymology of NAD Biosynthesis. In *Comprehensive Natural Products II: Chemistry and Biology* (Vol. 7, pp. 213–257). https://doi.org/10.1016/b978-008045382-8.00138-6

Steeghs, E. M. P., Boer, J. M., Hoogkamer, A. Q., Boeree, A., Haas, V. De, Groot-kruseman, H. A. De, Horstmann, M. A., Escherich, G., Pieters, R., & Boer, M. L. Den. (2019). Copy number alterations in B-cell development genes, drug resistance, and clinical outcome in pediatric B-cell precursor acute lymphoblastic leukemia. *Scientific Reports*, *9*(1), 1–11. https://doi.org/10.1038/s41598-019-41078-4

Stieglitz, E., Taylor-weiner, A. N., Chang, T. Y., Gelston, L. C., Archambeault, S. L., Abusin, G., Beckman, K., & Brown, P. A. (2016). The Genomic Landscape of Juvenile Myelomonocytic Leukemia. *Nature Genetics*, *47*(11), 1326–1333. https://doi.org/10.1038/ng.3400.

Su, H., Na, N., Zhang, X., & Zhao, Y. (2016). The biological function and significance of CD74 in immune diseases. *Inflammation Research*, *66*(3), 209–216. https://doi.org/10.1007/s00011-016-0995-1

Swaroop, A., Oyer, J. A., Will, C. M., Huang, X., Yu, W., Troche, C., Bulic, M., Durham,

B. H., Wen, Q. J., Crispino, J. D., Jr, A. D. M., Bennett, R. L., Kelleher, N. L., & Licht, J. D. (2019). An Activating Mutation of the NSD2 Histone Methyltransferase Drives Oncogenic Reprogramming in Acute Lymphocytic Leukemia. *Oncogene*, *38*(5), 671–686. https://doi.org/10.1038/s41388-018-0474-y.

Tanner, K. G., Landry, J., Sternglanz, R., & Denu, J. M. (2000). Silent information regulator 2 family of NAD-dependent histoneprotein deacetylases generates a unique product, 1-O-acetyl-ADP-ribose. *Proceedings of the National Academy of Sciences of the United States of America*, *97*(26), 14178–14182. https://doi.org/10.1073/pnas.250422697

Tartaglia, M., Martinelli, S., Cazzaniga, G., Cordeddu, V., Iavarone, I., Spinelli, M., Palmi, C., Carta, C., Pession, A., Aricò, M., Masera, G., Basso, G., Sorcini, M., Gelb, B. D., & Biondi, A. (2004). Genetic evidence for lineage-related and differentiation stage-related contribution of somatic PTPN11 mutations to leukemogenesis in childhood acute leukemia. *Blood*, *104*(2), 307–313. https://doi.org/10.1182/blood-2003-11-3876

Tateishi, K., Wakimoto, H., Iafrate, A. J., Tanaka, S., Loebel, F., Lelic, N., Wiederschain, D., Bedel, O., Deng, G., Zhang, B., He, T., Shi, X., Gerszten, R. E., Zhang, Y., Yeh, J., Curry, W. T., Zhao, D., Sundaram, S., Koerner, M. V. A., … Hospital, G. (2016). Extreme vulnerability of IDH1 mutant cancers to NAD+ depletion. *Cancer Cell*, *28*(6), 773–784. https://doi.org/10.1016/j.ccell.2015.11.006.

Tempel, W., Rabeh, W. M., Bogan, K. L., Belenky, P., Wojcik, M., Seidle, H. F., Nedyalkova, L., Yang, T., Sauve, A. A., Park, H. W., & Brenner, C. (2007). Nicotinamide riboside kinase structures reveal new pathways to NAD+. *PLoS Biology*, *5*(10), e263. https://doi.org/10.1371/journal.pbio.0050263

Thakral, D., Kaur, G., Gupta, R., Benard-slagter, A., & Savola, S. (2019). Rapid Identification of Key Copy Number Alterations in B- and T-Cell Acute Lymphoblastic Leukemia by Digital Multiplex Ligation-Dependent Probe Amplification. *Frontiers in Oncology*, *9*, 871. https://doi.org/10.3389/fonc.2019.00871

The 1000 Genomes Project Consortium (2015). A global reference for human genetic variation. *Nature*, *526*(7571), 68–74. https://doi.org/10.1038/nature15393

The Cancer Genome Atlas Network (2015). Comprehensive genomic characterization of head and neck squamous cell carcinomas. *Nature*, *517*(7536), 576–582. https://doi.org/10.1038/nature14129.

Torrens-Mas, M., Cordani, M., Mullappilly, N., Riganti, C., Palmieri, M., Pons, D. G., Roca,

P., Oliver, J., & Donadelli, M. (2020). Mutant p53 induces SIRT3/MnSOD axis to moderate ROS production in melanoma cells. *Archives of Biochemistry and Biophysics*, *679*, 1–8. https://doi.org/10.1016/j.abb.2019.108219

Tyagi, A., Pramanik, R., Bakhshi, R., Singh, A., Vishnubhatla, S., & Bakhshi, S. (2019). Expression of mitochondrial genes predicts survival in pediatric acute myeloid leukemia. *International Journal of Hematology*, *110*(2), 205–212. https://doi.org/10.1007/s12185-019-02666-2

Ullmark, T., Montano, G., Järvstråt, L., Jernmark Nilsson, H., Håkansson, E., Drott, K., Nilsson, B., Vidovic, K., & Gullberg, U. (2017). Anti-apoptotic quinolinate phosphoribosyltransferase (QPRT) is a target gene of Wilms' tumor gene 1 (WT1) protein in leukemic cells. *Biochemical and Biophysical Research Communications*, *482*(4), 802–807. https://doi.org/10.1016/j.bbrc.2016.11.114

Vicente, C., Schwab, C., Broux, M., Geerdens, E., Degryse, S., Demeyer, S., Lahortiga, I., Elliott, A., Chilton, L., Starza, R. La, Mecucci, C., Vandenberghe, P., Goulden, N., Vora, A., Moorman, A. V, Soulier, J., Harrison, C. J., & Clappier, E. (2015). Targeted sequencing identifies associations between IL7R-JAK mutations and epigenetic modulators in T-cell acute lymphoblastic leukemia. *Haematologica*, *100*(10), 1301–1310. https://doi.org/10.3324/haematol.2015.130179

Vujkovic, M., Attiyeh, E. F., Ries, R. E., Goodman, E. K., Ding, Y., Kavcic, M., Alonzo, T. A., Wang, Y., Gerbing, R. B., Sung, L., Hirsch, B., Raimondi, S., Gamis, A. S., Meshinchi, S., & Aplenc, R. (2017). Genomic architecture and treatment outcome in pediatric acute myeloid leukemia: a Children' s Oncology Group report. *Blood*, *129*(23), 3051–3058. https://doi.org/10.1182/blood-2017-03-772384.

Wang, X., Kaczor-Urbanowicz, K. E., & Wong, D. T. W. (2017). Salivary biomarkers in cancer detection. *Medical Oncology (Northwood, London, England)*, *34*(1), 7. https://doi.org/10.1007/s12032-016-0863-4

Warburg, O. (1956). On the Origin of Cancer Cells. *Science*, *123*(3191), 309–314. https://doi.org/10.1126/science.123.3191.309

Weissmann, S., Alpermann, T., Grossmann, V., Kowarsch, A., Nadarajah, N., Eder, C., Dicker, F., Fasan, A., Haferlach, C., Haferlach, T., Kern, W., Schnittger, S., & Kohlmann, A. (2012). Landscape of TET2 mutations in acute myeloid leukemia. *Leukemia*, *26*(5), 934–942. https://doi.org/10.1038/leu.2011.326

Wlodarski, M. W., Collin, M., Horwitz, M. S., Cancer, G., Kingdom, U., Trust, F., & Kingdom, U. (2018). GATA2 deficiency and related myeloid neoplasms Marcin. *Seminars in Hematology*, *54*(2), 81–86. https://doi.org/10.1053/j.seminhematol.2017.05.002.

Xiao, W., Wang, R. S., Handy, D. E., & Loscalzo, J. (2018). NAD(H) and NADP(H) Redox Couples and Cellular Energy Metabolism. *Antioxidants and Redox Signaling*, *28*(3), 251–272. https://doi.org/10.1089/ars.2017.7216

Yaku, K., Okabe, K., Hikosaka, K., & Nakagawa, T. (2018). NAD metabolism in Cancer Therapeutics. *Frontiers in Oncology*, *8*(622), 1–9. https://doi.org/10.3389/fonc.2018.00622

Yalowitz, J. A., Xiao, S., Biju, M. P., Antony, A. C., Cummings, O. W., Deeg, M. A., & Jayaram, H. N. (2004). Characterization of human brain nicotinamide 5′-mononucleotide adenylyltransferase-2 and expression in human pancreas. *Biochemical Journal*, *377*(2), 317–326. https://doi.org/10.1042/BJ20030518

Yang, Y., Mohammed, F. S., Zhang, N., & Sauve, A. A. (2019). Dihydronicotinamide riboside is a potent NAD+ concentration enhancer in vitro and in vivo. *Journal of Biological Chemistry*, *294*, 9295–9307. https://doi.org/10.1074/jbc.RA118.005772

Yang, Y., & Sauve, A. A. (2016). NAD+ metabolism: Bioenergetics, signaling and manipulation for therapy. *Biochimica et Biophysica Acta*, *1864*(12), 1787–1800. https://doi.org/10.1016/j.bbapap.2016.06.014.NAD

Yang, Y., Zhang, N., Zhang, G., & Sauve, A. A. (2020). NRH salvage and conversion to NAD+ requires NRH kinase activity by adenosine kinase. *Nature Metabolism*, *2*(4), 364–379. https://doi.org/10.1038/s42255-020-0194-9

Yates, A. D., Achuthan, P., Akanni, W., Allen, J., Allen, J., Alvarez-jarreta, J., Amode, M. R., Armean, I. M., Azov, A. G., Bennett, R., Marug, C., Cummins, C., Bhai, J., Billis, K., Boddu, S., Davidson, C., Dodiya, K., Fatima, R., Gall, A., … Flicek, P. (2020). Ensembl 2020. *Nucleic Acids Research*, *48*(D1), D682–D688. https://doi.org/10.1093/nar/gkz966

Ying, W. (2006). NAD+ and NADH in cellular functions and cell death. *Frontiers in Bioscience*, *11*(SUPPL. 3), 3129–3148. https://doi.org/10.2741/2038

Ying, W. (2008). NAD+/NADH and NADP+/NADPH in Cellular Functions and cell death: Regulation and Biological consequences. *Antioxidants and Redox Signaling*, *10*(2),

179–206. https://doi.org/10.1089/ars.2007.1672

Yoshizawa, J. M., Schafer, C. A., Schafer, J. J., Farrell, J. J., Paster, B. J., & Wong, T. W. (2013). Salivary Biomarkers: Toward Future Clinical and Diagnostic Utilities. *Clinical Microbiology Reviews*, *26*(4), 781–791. https://doi.org/10.1128/CMR.00021-13

Yusuff, T., Jensen, M., & Pizzo, S. Y. (2020). Drosophila models of pathogenic copy-number variant genes show global and non- neuronal defects during development. *PLoS Genetics*, *16*(6), e1008792. https://doi.org/10.1371/journal.pgen.1008792

Zhang, H., Wang, H., Qian, X., Zhu, X., Miao, H., Yu, Y., Meng, J., Le, J., Jiang, J., Cao, P., Jiang, W., Wang, P., Fu, Y., Li, J., Qian, M., & Zhai, X. (2020). Ras pathway mutation feature in the same individuals at diagnosis and relapse of childhood acute lymphoblastic leukemia. *Translational Pediatrics*, *9*(1), 4–12. https://doi.org/10.21037/tp.2020.01.07

Zhang, Jin-ying, Zhang, F., Hong, C., Giuliano, A. E., Cui, X., & Zhou, G. (2015). Critical protein GAPDH and its regulatory mechanisms in cancer cells. *Cancer Biology & Medicine*, *12*(1), 10–22. https://doi.org/10.7497/j.issn.2095-3941.2014.0019

Zhang, Jun-gang, Zhao, G., Qin, Q., Wang, B., Liu, L., Liu, Y., Deng, S., Tian, K., & Wang, C. (2013). Nicotinamide prohibits proliferation and enhances chemosensitivity of pancreatic cancer cells through deregulating SIRT1 and Ras/Akt pathways. *Pancreatology*, *13*(2), 140–146. https://doi.org/10.1016/j.pan.2013.01.001

Zhang, Xin, Ren, D., Guo, L., Wang, L., Wu, S., Lin, C., Ye, L., Zhu, J., Li, J., Song, L., Lin, H., & He, Z. (2017). Thymosin beta 10 is a key regulator of tumorigenesis and metastasis and a novel serum marker in breast cancer. *Breast Cancer Research*, *19*(1), 1–15. https://doi.org/10.1186/s13058-016-0785-2

Zhang, Xuejun, Kurnasov, O. V., Karthikeyan, S., Grishin, N. V., Osterman, A. L., & Zhang, H. (2003). Structural characterization of a human cytosolic NMN/NaMN adenylyltransferase and implication in human NAD biosynthesis. *Journal of Biological Chemistry*, *278*(15), 13503–13511. https://doi.org/10.1074/jbc.M300073200

Ziegler, M., & Niere, M. (2004). NAD+ surfaces again. *Biochemical Journal*, *382*(3), e5–e6. https://doi.org/10.1042/BJ20041217

Ziegler, M., & Nikiforov, A. A. (2020). NAD on the rise again. *Nature Metabolism*, *2*(4), 291–292. https://doi.org/10.1038/s42255-020-0197-6

8. APPENDICES

Appendix 1 - Results from the statistical overrepresentation test with the PANTHER GO-Slim Biological Process set and the hypermethylated genes in AML. GO: Gene Ontology; FDR: False Discovery Rate.

Biological Process	GO	Fold Enrichment	Raw p-value	FDR
Peptide hormone secretion	0030072	5,57	$3{,}56e^{-3}$	$3{,}45e^{-2}$
Regulation of hormone secretion	0046883	4.95	$5.35e^{-3}$	$4.80e^{-2}$
Cholesterol transport	0030301	4.95	$5.35e^{-3}$	$4.78e^{-2}$
Skeletal muscle contraction	0003009	4.33	4.52e-^{3}	$4.18e^{-2}$
B cell differentiation	0030183	4.30	$4.05e^{-4}$	$8.03e^{-3}$
T cell activation involved in immune response	0002286	4.30	$4.05e^{-4}$	$7.95e^{-3}$
B cell proliferation	0042100	4.20	$1.46e^{-4}$	$4.87e^{-3}$
Cardiac muscle contraction	0060048	4.13	$9.39e^{-4}$	$1.36e^{-2}$
Heart process	0003015	4.03	$2.01e^{-4}$	$5.32e^{-3}$
Cell activation involved in immune response	0002263	3.98	$7.28e^{-5}$	$2.95e^{-3}$
Cholesterol homeostasis	0042632	3.93	$2.16e^{-3}$	$2.37e^{-2}$
Lymphocyte activation involved in immune response	0002285	3.89	$7.63e^{-4}$	$1.23e^{-2}$
Heart contraction	0060047	3.88	$4.56e^{-4}$	$8.55e^{-3}$
Leukocyte activation involved in immune response	0002366	3.85	$1.64e^{-4}$	$5.04e^{-3}$
Sensory perception of light stimulus	0050953	3.72	$2.91e^{-3}$	$2.93e^{-2}$
Defense response to Gram-negative bacterium	0050829	3.72	$2.91e^{-3}$	$2.91e^{-2}$
Striated muscle contraction	0006941	3.72	$3.65e^{-4}$	$7.69e^{-3}$
Response to interleukin-1	0070555	3.60	$1.05e^{-4}$	$3.79e^{-3}$
Defense response to Gram-positive bacterium	0050830	3.54	$2.27e^{-3}$	$2.42e^{-2}$
Spermatid development	0007286	3.52	$3.84e^{-3}$	$3.67e^{-2}$
Sensory perception of taste	0050909	3.47	$3.79e^{-4}$	$7.66e^{-3}$
Mononuclear cell proliferation	0032943	3.46	$2.39e^{-5}$	$1.49e^{-3}$
Lymphocyte proliferation	0046651	3.46	$2.39e^{-5}$	$1.45e^{-3}$
Leukocyte proliferation	0070661	3.46	$2.39e^{-5}$	$1.41e^{-3}$
Regulation of hormone levels	0010817	3.40	$1.78e^{-4}$	$5.11e^{-3}$

Negative regulation of leukocyte activation	0002695	3.38	$2.96e^{-3}$	$2.95e^{-2}$
Lymphocyte differentiation	0030098	3.38	$2.95e^{-4}$	$6.62e^{-3}$
Negative regulation of cell activation	0050866	3.38	$2.96e^{-3}$	$2.94e^{-2}$
Leukocyte differentiation	0002521	3.36	$5.09e^{-5}$	$2.44e^{-3}$
Detection of chemical stimulus involved in sensory perception of taste	0050912	3.33	$8.15e^{-4}$	$1.28e^{-2}$
Detection of chemical stimulus involved in sensory perception	0050907	3.33	$8.15e^{-4}$	$1.27e^{-2}$
Detection of stimulus involved in sensory perception	0050906	3.33	$8.15e^{-4}$	$1.26e^{-2}$
Detection of chemical stimulus involved in sensory perception of bitter taste	0001580	3.33	$8.15e^{-4}$	$1.25e^{-2}$
Lymphocyte migration	0072676	3.28	$3.79e^{-4}$	$7.60e^{-3}$
Negative regulation of peptidase activity	0010466	3.27	$3.31e^{-6}$	$3.60e^{-4}$
Antimicrobial humoral immune response mediated by antimicrobial peptide	0061844	3.27	$2.27e^{-3}$	$2.44e^{-2}$
Cellular component assembly involved in morphogenesis	0010927	3.27	$2.27e^{-3}$	$2.43e^{-2}$
Regulation of receptor signaling pathway via JAK-STAT	0046425	3.22	$1.04e^{-3}$	$1.47e^{-2}$
Negative regulation of proteolysis	0045861	3.22	$4.22e^{-6}$	$3.96e^{-4}$
Regulation of receptor signaling pathway via STAT	1904892	3.22	$1.04e^{-3}$	$1.46e^{-2}$
Negative regulation of endopeptidase activity	0010951	3.18	$1.13e^{-5}$	$8.32e^{-4}$
Chemokine-mediated signaling pathway	0070098	3.16	$2.25e^{-4}$	$5.53e^{-3}$
Muscle tissue development	0060537	3.14	$2.89e^{-3}$	$2.92e^{-2}$
Leukocyte chemotaxis	0030595	3.14	$3.02e^{-5}$	$1.64e^{-3}$
Granulocyte chemotaxis	0071621	3.11	$1.73e^{-4}$	$5.09e^{-3}$
Cell chemotaxis	0060326	3.10	$4.42e^{-7}$	$7.60e^{-5}$
Cellular response to chemokine	1990869	3.08	$2.83e^{-4}$	$6.57e^{-3}$
Response to chemokine	1990868	3.08	$2.83e^{-4}$	$6.50e^{-3}$

Negative regulation of immune system process	0002683	3.03	$3.64e^{-3}$	$3.49e^{-2}$
Spermatogenesis	0007283	2.97	$5.81e^{-4}$	$1.02e^{-2}$
Male gamete generation	0048232	2.94	$4.41e^{-4}$	$8.35e^{-3}$
Negative regulation of hydrolase activity	0051346	2.89	$1.27e^{-5}$	$9.01e^{-4}$
Hemopoiesis	0030097	2.89	1.95e-4	$5.29e^{-3}$
Hematopoietic or lymphoid organ development	0048534	2.89	$1.95e^{-4}$	$5.22e^{-3}$
Cellular response to tumor necrosis factor	0071356	2.86	$1.17e^{-3}$	$1.51e^{-2}$
Detection of chemical stimulus	0009593	2.84	$2.55e^{-3}$	$2.63e^{-2}$
Steroid metabolic process	0008202	2.83	$8.86e^{-4}$	$1.31e^{-2}$
Immune system development	0002520	2.82	$1.51e^{-4}$	$4.87e^{-3}$
Circulatory system process	0003013	2.81	$1.06e^{-3}$	$1.42e^{-2}$
Response to tumor necrosis factor	0034612	2.81	$1.06e^{-3}$	$1.41e^{-2}$
T cell activation	0042110	2.79	$2.37e^{-4}$	$5.77e^{-3}$
Positive regulation of ERK1 and ERK2 cascade	0070374	2.79	$2.40e^{-3}$	$2.50e^{-2}$
Detection of stimulus	0051606	2.77	$1.71e^{-4}$	$5.18e^{-3}$
Muscle contraction	0006936	2.76	$1.66e^{-3}$	$1.99e^{-2}$

Appendix 2 - Results from the statistical overrepresentation test with the PANTHER GO-Slim Biological Process set and the hypermethylated genes in ALL. GO: Gene Ontology; FDR: False Discovery Rate.

Biological Process	**GO**	**Fold Enrichment**	**Raw p-value**	**FDR**
Embryo development ending in birth or egg hatching	0009792	3.48	$3.30e^{-4}$	$3.95e^{-3}$
Chordate embryonic development	0043009	3.48	$3.30e^{-4}$	$3.93e^{-3}$
Embryonic organ development	0048568	3.44	$6.12e^{-5}$	$9.36e^{-4}$
Embryonic morphogenesis	0048598	3.43	$3.09e^{-6}$	$7.88e^{-5}$
Morphogenesis of an epithelium	0002009	3.16	$2.35e^{-3}$	$2.06e^{-2}$
Negative regulation of MAP kinase activity	0043407	3.05	$6.43e^{-3}$	$4.76e^{-2}$
Anterior/posterior pattern specification	0009952	3.02	$4.88e^{-5}$	$7.58e^{-4}$

Neural crest cell differentiation	0014033	2.90	$5.81e^{-3}$	$4.38e^{-2}$
Non-canonical Wnt signaling pathway	0035567	2.90	$5.81e^{-3}$	$4.36e^{-2}$
Embryo development	0009790	2.75	1.39^{-6}	$4.22e^{-5}$
Regionalization	0003002	2.73	$1.27e^{-4}$	$1.77e^{-3}$
Head development	0060322	2.71	$4.10e^{-3}$	$3.25e^{-2}$
Brain development	0007420	2.71	$4.10e^{-3}$	$3.23e^{-2}$
Negative regulation of neuron differentiation	0045665	2.69	$6.04e^{-3}$	$4.52e^{-2}$
Developmental growth involved in morphogenesis	0060560	2.69	$6.04e^{-3}$	$4.50e^{-2}$
Skeletal system development	0001501	2.68	$1.57e^{-4}$	$2.08e^{-3}$
Cell growth	0016049	2.62	$4.80e^{-3}$	$3.71e^{-2}$
Pattern specification process	0007389	2.52	$8.05e^{-5}$	$1.19e^{-3}$
Blood circulation	0008015	2.50	$1.85e^{-3}$	$1.72e^{-2}$
Circulatory system process	0003013	2.45	$2.08e^{-3}$	$1.92e^{-2}$
Regulation of axonogenesis	0050770	2.43	$3.00e^{-3}$	$2.49e^{-2}$
Regulation of neuron differentiation	0045664	2.38	$2.56e^{-5}$	$4.67e^{-4}$
Regulation of neuron projection development	0010975	2.35	$4.28e^{-4}$	$4.91e^{-3}$
Tissue morphogenesis	0048729	2.34	$2.76e^{-3}$	$2.38e^{-2}$
Cell fate commitment	0045165	2.34	$1.23e^{-3}$	$1.24e^{-2}$
Regulation of plasma membrane bounded cell projection organization	0120035	2.33	$1.00e^{-4}$	$1.45e^{-3}$
Regulation of cell projection organization	0031344	2.30	$1.74e^{-4}$	$2.27e^{-3}$
Tube development	0035295	2.30	$1.38e^{-3}$	$1.36e^{-2}$
Axon guidance	0007411	2.30	$3.55e^{-5}$	$5.81e^{-4}$
Neuron projection guidance	0097485	2.30	$3.55e^{-5}$	$5.77e^{-4}$
Positive regulation of nervous system development	005196	2.29	$5.59e^{-3}$	$4.22e^{-2}$
Positive regulation of cell differentiation	0045597	2.28	$1.11e^{-3}$	$1.13e^{-2}$
Canonical Wnt signaling pathway	0060070	2.27	$3.94e^{-4}$	$4.62e^{-3}$
Regulation of neurogenesis	0050767	2.25	$2.35e^{-5}$	$4.41e^{-4}$
Regulation of nervous system development	0051960	2.25	$8.58e^{-6}$	$1.87e^{-4}$
Animal organ morphogenesis	0009887	2.23	$2.65e^{-5}$	$4.72e^{-4}$
Central nervous system development	0007417	2.23	$1.41e^{-3}$	$1.38e^{-2}$
Tube morphogenesis	0035239	2.21	$3.11e^{-3}$	$2.54e^{-2}$

Regulation of cell migration	0030334	2.19	$4.36e^{-4}$	$4.97e^{-3}$
Regulation of MAP kinase activity	0043405	2.17	$2.17e^{-3}$	$1.97e^{-2}$
Neuron differentiation	0030182	2.17	$3.61e^{-10}$	$2.19e^{-8}$
Regulation of cell development	0060284	2.16	$4.64e^{-5}$	$7.25e^{-4}$
Regulation of cell differentiation	0045595	2.16	$2.33e^{-6}$	$6.49e^{-5}$
Axonogenesis	0007409	2.14	$2.57e^{-5}$	$4.66e^{-4}$
Generation of neurons	0048699	2.12	$3.29e^{-10}$	2.06^{-8}
Axon development	0061564	2.11	$2.92e^{-5}$	$5.06e^{-4}$
Wnt signaling pathway	0016055	2.10	$1.31e^{-4}$	$1.80e^{-3}$
Regulation of locomotion	0040012	2.10	$4.09e^{-4}$	$4.77e^{-3}$
Regulation of multicellular organismal development	2000026	2.10	$1.48e^{-6}$	$4.36e^{-5}$
Regulation of anatomical structure morphogenesis	0022603	2.09	$3.18e^{-5}$	$5.33e^{-4}$
Cell surface receptor signaling pathway involved in cell-cell signaling	1905114	2.09	$6.41e^{-5}$	$9.65e^{-4}$
Cell-cell signaling by wnt	0198738	2.08	$1.40e^{-4}$	$1.90e^{-3}$
Regulation of cell motility	2000145	2.08	$7.06e^{-4}$	$7.67e^{-3}$
Epithelium development	0060429	2.08	$4.20e^{-3}$	$3.27e^{-2}$
Neurogenesis	0022008	2.08	$3.77e^{-10}$	$2.23e^{-8}$
Positive regulation of developmental process	0051094	2.07	$1.25e^{-3}$	$1.24e^{-2}$
Cell morphogenesis involved in neuron differentiation	0048667	2.06	$3.27e^{-5}$	$5.44e^{-4}$
Cell projection morphogenesis	0048858	2.05	$1.04e^{-5}$	$2.15e^{-4}$
Neuron projection morphogenesis	0048812	2.05	$1.04e^{-5}$	$2.13e^{-4}$
Plasma membrane bounded cell projection morphogenesis	0120039	2.05	$1.04e^{-5}$	$2.11e^{-4}$
Regulation of cellular component movement	0051270	2.05	$6.73e^{-4}$	$7.35e^{-3}$
Regulation of developmental process	0050793	2.04	$5.46e^{-8}$	$2.21e^{-6}$
Cell part morphogenesis	0032990	2.04	$1.61e^{-5}$	$3.10e^{-4}$
Tissue development	0009888	2.03	$4.78e^{-6}$	$1.11e^{-4}$
Neuron projection development	0031175	2.00	$2.90e^{-6}$	$7.67e^{-5}$
Cell morphogenesis involved in differentiation	0000904	2.00	$7.24e^{-6}$	$1.59e^{-4}$

Appendix 3 - Plot with *NAPRT* methylation (horizontal axis) and expression (vertical axis) in ALL, provided by cBioPortal.

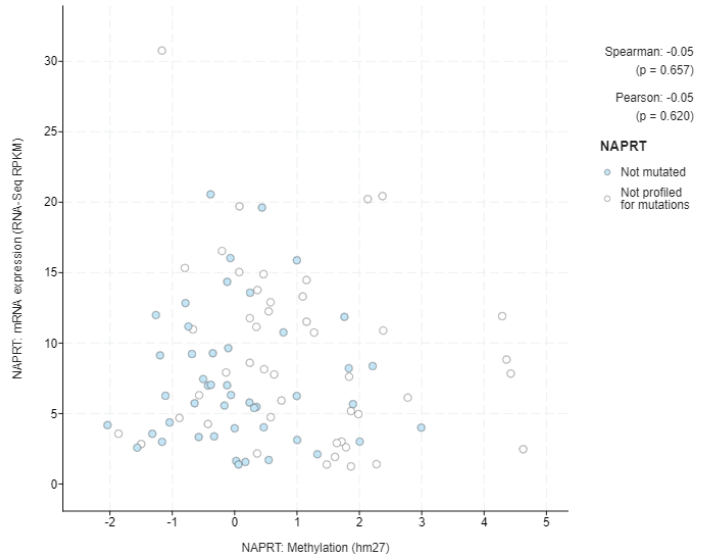

Appendix 4 - Plot with *NAPRT* methylation (horizontal axis) and expression (vertical axis) in HNSC, provided by cBioPortal.

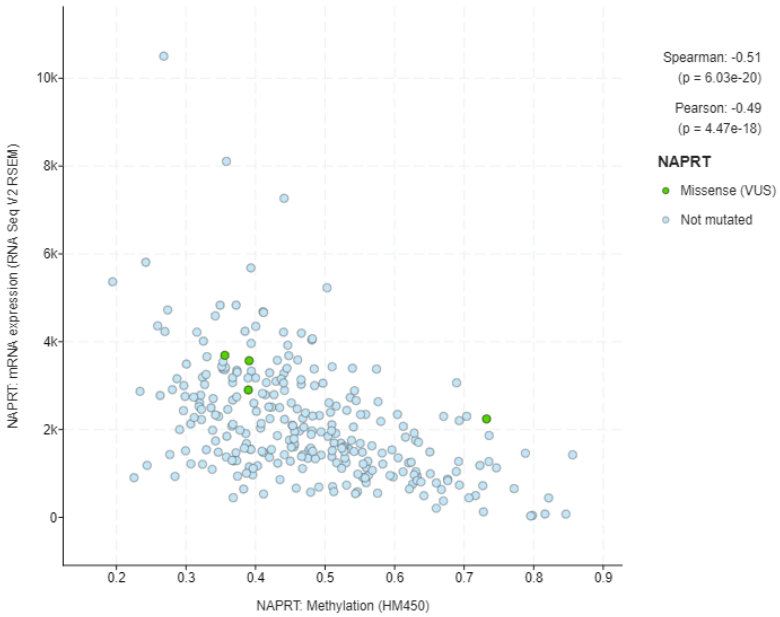

Appendix 5 - Plot with *NAMPT* CNAs (horizontal axis) and expression (vertical axis) in HNSC, provided by cBioPortal.

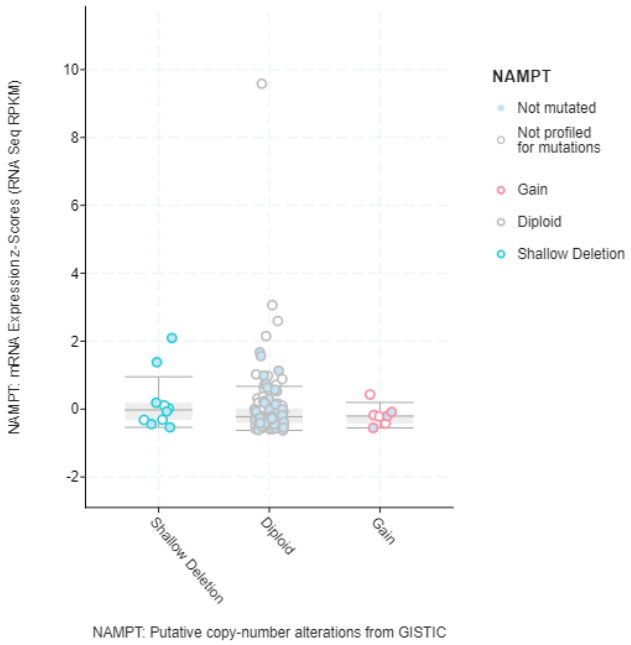

Appendix 6 – SNPs that alter exclusively *NAPRT* expression in HNSC (beta values showed) and other tumors. HNSC: head and neck squamous cell carcinoma; LGG: lower grade glioma; PRAD: prostate adenocarcinoma; LUAD: lung adenocarcinoma; SARC: sarcoma; PCPG: pheochromocytoma and paraganglioma; KIRP: kidney renal papillary cell carcinoma; OV: ovarian serous cystadenocarcinoma; TCGT: testicular germ cell tumors; KIRC: kidney renal clear cell carcinoma; CESC: cervical squamous cell carcinoma and endocervical adenocarcinoma.

SNP	Gene	Beta value (HNSC)	Tumors
rs10464952	ZC3H3	0,2	LGG
rs11777600	ZC3H3	0,2	LGG
rs11776571	ZC3H3	0,19	LGG
rs2294115	ZC3H3	-0,18	LGG
rs2294114	ZC3H3	-0,18	LGG
rs11773918	intergenic	-0,19	LGG
rs2294116	ZC3H3	-0,19	LGG
rs2294112	ZC3H3	-0,19	LGG
rs4874122	intergenic	-0,19	LGG
rs530881	ZC3H3	-0,19	LGG
rs13252596	ZC3H3	-0,2	LGG

rs112147940	EEF1D	-0,54	PRAD, LUAD, HNSC, SARC, PCPG, THCA, KIRP, OV, TGCT
rs58016285	EEF1D	-0,57	PRAD, HNSC, SARC, PCPG, KIRP, OV, TGCT, KIRC
rs79185314	EEF1D	-0,57	PRAD, LUAD, HNSC, SARC, PCPG, KIRP, OV, TGCT KIRC
rs115791742	TIGD5	-0,63	PRAD, LUAD, HNSC, SARC, PCPG, KIRP, TGCT, KIRC, LGG, CESC

Appendix 7 – All *NAPRT* eQTL in HNSC and respective effect sizes from the highest to the lowest absolute beta value.

SNP	Beta value	SNP	Beta value	SNP	Beta value	SNP	Beta value
rs10866913	0,8	**rs10110174**	0,4	**rs3793371**	-0,34	**rs11777600**	0,20
rs112147940	-0,54	**rs4874163**	0,39	**rs78170940**	-0,32	**rs13252596**	-0,20
rs58016285	-0,57	**rs7830957**	0,39	**rs72499135**	-0,31	**rs10100594**	-0,20
rs79185314	-0,57	**rs751932**	0,38	**rs4874440**	-0,29	**rs113818459**	-0,20
rs115791742	-0,63	**rs7821226**	0,38	**rs2123758**	0,28	**rs4874130**	-0,20
rs9657360	0,49	**rs1057556**	0,38	**rs1563148**	0,28	**rs4874131**	-0,20
rs10282929	0,49	**rs4874165**	0,38	**rs1062391**	0,28	**rs11776571**	0,19
rs34979030	0,49	**rs10650180**	0,38	**rs7822731**	0,27	**rs11773918**	-0,19
rs10094377	0,49	**rs9314410**	0,38	**rs7822746**	0,26	**rs2294116**	-0,19
rs10093709	0,49	**rs10097491**	0,38	**rs12679471**	-0,26	**rs2294112**	-0,19
rs10112966	0,48	**rs7844940**	0,38	**rs378433**	-0,26	**rs13272031**	-0,19
rs10090650	0,48	**rs7814045**	0,38	**rs62522224**	-0,25	**rs4874122**	-0,19
rs73718108	-0,44	**rs2010898**	0,38	**rs4873815**	-0,24	**rs530881**	-0,19
rs4874157	-0,46	**rs11136303**	-0,38	**rs896962**	-0,24	**rs2294115**	-0,18
rs7841183	-0,46	**rs6995338**	0,37	**rs755217**	-0,24	**rs2294114**	-0,18
rs113122933	-0,46	**rs3793366**	0,36	**rs11784456**	0,24	**rs4874164**	0,4
rs75547282	-0,46	**rs2382962**	-0,36	**rs148839797**	0,24	**rs33967841**	0,4
rs34037472	-0,46	**rs3812447**	-0,35	**rs72024244**	0,24	**rs2085019**	0,4
rs4495441	-0,47	**rs62522165**	-0,35	**rs9650468**	0,23	**rs62522168**	-0,35
rs4874167	0,42	**rs76108894**	-0,35	**rs3750203**	0,23	**rs58573550**	-0,35
rs1466219	0,41	**rs59742520**	-0,35	**rs6997021**	0,23	**rs62523607**	-0,35
rs10109931	0,41	**rs76225457**	-0,35	**rs7003244**	0,23	**rs7821027**	-0,21
rs4874159	0,41	**rs58274382**	-0,35	**rs10107353**	0,23	**rs11785686**	-0,21
rs4874160	0,41	**rs58477175**	-0,35	**rs896937**	0,23	**rs10464952**	0,20
rs3812448	0,41	**rs61652493**	-0,35	**rs11778687**	-0,22		
rs4874160	0,41	**rs62522167**	-0,35	**rs4875043**	0,22		

Appendix 8 - All *NAPRT* eQTL in LAML and respective effect sizes from the highest to the lowest absolute beta value.

SNP	Beta value	SNP	Beta value	SNP	Beta value
rs1809148	-0,75	**rs10090650**	0,57	**rs4874160**	0,54
rs9657360	0,61	**rs33967841**	0,57	**rs10866913**	0,53
rs10282929	0,66	**rs2085019**	0,59	**rs1466219**	0,5
rs10112966	0,6	**rs4874164**	0,55	**rs4874163**	0,5
rs10094377	0,6	**rs3816477**	0,58	**rs3812448**	0,51
rs34979030	0,6	**rs10109931**	0,54	**rs4874167**	0,5
rs10093709	0,59	**rs4874159**	0,54	**rs4873808**	0,49

Appendix 9 - Allelic frequencies of the selected *NAPRT* eQTL in HNSC in all (ALL) populations (African, American, East Asian, European and South Asian) from the 1000 Genomes Project. Ref: reference; Alt: alternative; AFR: African; AMR: American; EAS: East Asian; EUR: European; SAS: South Asian; *: TATTTATTTATTTATTTATTT/TATTTATTTATTTATTTATTTATTTATTTA/TATTTATTTATTTATTTATTTATTTATTT; **: TTTTTTTGTTTTTTTTTTT/TTTTTTT; ***: TCTTCT/TCT.

eQTL	Gene	Ref/Alt alleles	ALL	AFR	AMR	EAS	EUR	SAS
rs148839797	intergenic	G/C	68/32	95/5	53/47	85/15	35/65	57/43
rs72024244	intergenic	*	33/66/1	6/92/2	46/53/1	20/79/1	65/35	39/61
rs11778687	ZNF623	C/T	33/67	7/93	47/53	15/85	66/34	43/57
rs113818459 (merged into rs55708095)	ZC3H3	**	45/55	37/63	45/55	51/49	37/63	58/42
rs7822731	intergenic	A/G	74/26	83/17	87/13	44/56	87/13	71/29
rs7822746	intergenic	A/G	74/26	83/17	87/13	44/56	87/13	71/29
rs378433	intergenic	C/T	27/73	20/80	13/87	56/44	14/86	30/70
rs10464952	ZC3H3	C/T	57/43	72/28	55/45	49/51	63/37	42/58
rs11777600	ZC3H3	C/T	57/43	72/28	55/45	49/51	63/37	42/58
rs11776571	ZC3H3	G/A	57/43	72/28	55/45	49/51	63/37	42/58
rs2294115	ZC3H3	G/A	45/55	37/63	45/55	51/49	37/63	58/42
rs2294114	ZC3H3	G/A	45/55	37/63	45/55	51/49	37/63	58/42
rs11773918	intergenic	C/T	45/55	37/63	45/55	50/50	37/63	58/42
rs2294116	ZC3H3	A/T	45/55	37/63	45/55	51/49	37/63	58/42
rs2294112	ZC3H3	G/C	45/55	36/64	45/55	51/49	37/63	58/42
rs4874122	intergenic	A/G	45/55	36/64	44/56	50/50	37/63	58/42
rs530881	ZC3H3	G/A	46/54	35/65	46/54	56/44	37/63	58/42
rs13252596	ZC3H3	G/A	45/55	37/63	45/55	52/48	37/63	58/42
rs112147940	EEF1D	G/A	94/6	86/14	96/4	100/0	95/5	96/2
rs58016285	EEF1D	G/A	96/4	90/10	96/4	100/0	95/5	96/2

rs79185314	EEF1D	C/A	96/4	91/9	96/4	100/0	95/5	98/2
rs115791742	TIGD5	G/A	97/3	93/7	97/3	100/0	95/5	98/2
rs10866913	TIGD5	T/C	34/66	46/54	24/76	49/51	15/85	31/69
rs9657360	EEF1D	C/T	41/59	64/36	29/71	48/52	20/80	32/68
rs10282929	TIGD5	G/T	40/60	60/40	28/72	49/51	20/80	33/67
rs34979030	TIGD5	***	39/61	56/44	28/72	50/50	20/80	33/67
rs10094377	TIGD5	T/C	39/61	56/44	28/72	50/50	20/80	33/67
rs10093709	TIGD5	A/G	38/62	54/46	27/73	50/50	20/80	33/67
rs10112966	TIGD5	C/T	39/61	56/44	28/72	49/51	20/80	33/67
rs10090650	TIGD5	A/G	40/60	60/40	28/72	49/51	20/80	33/67
rs4874167	TIGD5	T/C	22/78	43/57	11/89	15/85	12/88	17/83
rs1466219	EEF1D	C/A	36/64	53/47	25/75	48/52	15/85	31/69
rs10109931	EEF1D	C/T	35/65	50/50	24/76	49/51	15/85	31/69
rs4874159	EEF1D	C/T	36/64	51/49	25/75	49/51	15/85	31/69
rs4874160	EEF1D	C/A/G	26/64/10	46/49/5	19/75/6	34/51/15	8/85/7	15/69/16
rs3812448	EEF1D	G/A	36/64	52/48	25/75	49/51	15/85	31/69
rs4874164	EEF1D	G/A	36/64	51/49	25/75	48/52	15/85	31/69
rs33967841	EEF1D	GT/G	36/64	51/49	25/75	48/52	15/85	31/69
rs2085019	EEF1D	C/T	36/64	51/49	25/75	49/51	15/85	31/69
rs10110174	EEF1D	C/T	26/74	47/53	19/81	34/66	8/92	15/85
rs4874163	EEF1D	G/A	36/64	53/47	25/75	48/52	15/85	31/69
rs7830957	EEF1D	G/T	26/74	46/54	19/81	34/66	8/92	15/85
rs73718108	EEF1D	T/C	20/80	25/75	17/83	34/66	8/92	15/85
rs4874157	EEF1D	G/A	80/20	76/24	83/17	65/35	92/8	84/16
rs7841183	EEF1D	G/A	80/20	76/24	83/17	65/35	92/8	84/16
rs113122933	EEF1D	G/A	80/20	76/24	83/17	67/33	92/8	85/15
rs75547282	EEF1D	C/T	80/20	76/24	83/17	67/33	92/8	85/15
rs34037472	EEF1D	/AA	80/20	76/24	83/17	67/33	92/8	85/15
rs4495441	EEF1D	G/A	80/20	76/24	83/17	67/33	92/8	85/15

Appendix 10- Allelic frequencies *NAPRT* eQTL in LAML in all (ALL) populations (African, American, East Asian, European and South Asian) from the 1000 Genomes Project. Ref: reference; Alt: alternative; AFR: African; AMR: American; EAS: East Asian; EUR: European; SAS: South Asian.

eQTL	**Gene**	**Ref/Alt alleles**	**ALL**	**AFR**	**AMR**	**EAS**	**EUR**	**SAS**
rs9657360	EEF1D	C/T	41/59	64/36	29/71	48/52	20/80	32/68
rs10282929	TIGD5	C/T	40/60	60/40	28/72	49/51	20/80	33/67
rs10112966	TIGD5	C/T	39/61	56/44	28/72	49/51	20/80	33/67
rs10094377	TIGD5	T/C	39/61	56/44	28/72	50/50	20/80	33/67

rs34979030	TIGD5	TCTTCT/TCT	39/61	56/44	28/72	50/50	20/80	33/67
rs10093709	TIGD5	A/G	38/62	54/46	27/73	50/50	20/80	33/67
rs10090650	TIGD5	A/G	40/60	60/40	28/72	49/51	20/80	33/67
rs1809148	EEF1D	G/A	76/24	68/32	80/20	65/35	87/13	83/17
rs33967841	EEF1D	GT/G	36/64	51/49	25/75	48/52	15/85	31/69
rs2085019	EEF1D	C/T	36/64	51/49	25/75	49/51	15/85	31/69
rs4874164	EEF1D	G/A	36/64	51/49	25/75	48/52	15/85	31/69
rs3816477	TIGD5	T/C	23/77	50/50	11/89	15/85	12/88	17/83
rs10109931	EEF1D	C/T	35/65	50/50	24/76	49/51	15/85	31/69
rs4874159	EEF1D	C/T	36/64	51/49	25/75	49/51	15/85	31/69
rs4874160	EEF1D	C/A/G	26/64/10	46/49/5	19/75/6	34/51/15	8/85/7	15/69/16
rs10866913	TIGD5	T/C	34/66	46/54	24/76	49/51	15/85	31/69
rs1466219	EEF1D	C/A	36/64	53/47	25/75	48/52	15/85	31/69
rs4874163	EEF1D	G/A	36/64	53/47	25/75	48/52	15/85	31/69
rs3812448	EEF1D	G/A	36/64	52/48	25/75	49/51	15/85	31/69
rs4874167	TIGD5	T/C	22/78	43/57	11/89	15/85	12/88	17/83
rs4873808	intergenic	C/T	72/28	84/15	78/22	37/63	84/16	72/28

Appendix 11 - Overexpressed mitochondrial genes and the respective logarithm of median RPKM in AML (at the left) and ALL (at the right) TARGET datasets.

AML		**ALL**	
Gene	**Log_2 RPKM**	**Gene**	**Log_2 RPKM**
MT-CO3	15,35	MT-CO3	14,98
MT-CO1	14,75	MT-ND4	14,90
MT-ND4	14,65	MT-CO2	14,40
MT-ND1	14,36	MT-ATP6	14,39
MT-ATP8	14,23	MT-CO1	14,30
MT-ATP6	14,17	MT-CYB	14,24
MT-CO2	14,17	MT-ND1	14,11
MT-CYB	14,15	MT-ATP8	14,10
MT-ND4L	13,74	MT-ND2	14,09
MT-ND2	13,68	MT-ND4L	13,64
MT-ND5	12,98	MT-RNR2	13,32
MT-ND3	12,55	MT-ND5	12,38